Characterization of the zinc-sensitive metal-regulatory transcription factor 1 in hippocampal epileptic network formation using an animal model of Temporal Lobe Epilepsy

Doctoral thesis

to obtain a doctorate (PhD)

from the Faculty of Medicine

of the University of Bonn

Annachiara Meconi

Fermo, Italy

2023

Written with authorization of

the Faculty of Medicine of the University of Bonn

First reviewer: Prof. Dr. Albert Becker

Second reviewer: Dr. Philippe Lory

Day of oral examination: 25th September 2023

From the Institute of Neuropathology

Director: Prof. Dr. med. Torsten Pietsch

Table of contents

List of abbreviations

a.a	Amino acid
Bdnf	Brain-Derived Neurotrophic Factor
BSA	Bovine Serum Albumin
BME	Basal Medium Eagle
Ca^{2+}	Calcium
Cd^{2+}	Cadmium
ChIP	Chromatin-ImmunoPrecipitation
Cl^-	Chloride
CNS	Central Nervous System
Creb1	cAMP responsive element binding protein 1
Crm1	Chromosomal Maintenance 1
Cu^{2+}	Copper
DE	Differentially Expressed
DG	Dentate gyrus
DMEM	Dulbecco's Modified Eagle Medium
dnMtf1	Dominant-negative Metal-regulatory Transcription Factor 1
dNTP	Deoxyribonucleotides
Drd2	Dopamine Receptor D2
Erg1	Early Growth Response 1
FACS	Fluorescence-activated cells sorting
FCS	Fetal Calf Serum

GABA	Gamma-AminoButyric Acid
GFP	Green Fluorescence Protein
GluR2	Glutamate AMPA receptor subunit 2
GO	Gene Ontology
h	Hours
HBBS	Hanks' Balanced Salt Solution
HEK293	Human Embryonic Kidney 293
H_2O_2	Hydrogen peroxide
HS	Hippocampal Sclerosis
Htr2a	Serotonin 5-HT-2A Receptor
HVA	High Voltage Activated
i.p.	Intraperitoneal
I_{CaT}	low-voltage activated Ca^{2+} current
Ighg1	Immunoglobulin Heavy constant Gamma 1
ILAE	International League Against Epilepsy
IMDM	Iscove’s Modified Dulbecco’s Medium
iRFP	InfraRed Fluorescent Protein
K^+	Potassium
Ko	Knock-out
LTD	Long-Term Depression
LTP	Long-Term Potentiation
LVA	Low Voltage Activated
MFS	Mossy-Fiber Sprouting

Mg^{2+}	Magnesium
mGluR1	Metabotropic Glutamate Receptor 1
min	Minutes
MREs	Metal Responsive Elements
mRNA	Messenger Ribonucleic Acid
Mtf1	Metal-regulatory Transcription Factor 1
mTLE	Mesial Temporal Lobe Epilepsy
Na^{+}	Sodium
NES	Nuclear Export Signal
Nf-κB	Nuclear factor-kB
Ni^{2+}	Nickel
NLS	Nuclear Localization Signal
NRSF	Neuron-Restrictive Silencer Factor
nTLE	Neocortical Temporal Lobe Epilepsy
OE	Overexpression
PBS	Phosphate Buffer Saline
PBMC	Peripheral Blood Mononuclear Cells
PCA	Principal Component Analysis
PCs	Pyramidal cells
PCR	Polymerase Chain reaction
pCREB1	phosphorylated CREB1
PFA	Paraformaldehyde
PTZ	Pentylenetetrazol

rAAV	Adeno-Associated virus
REST1	Repressor Element 1-Silencing Transcription factor
RNA-seq	RNA-sequencing
ROIs	Regions of Interest
RT	Room temperature
RT-PCR	Real Time-Polymerase Chain Reaction
s.c.	Subcutaneous
SE	Status Epilepticus
SEM	Standard Error Mean
TF	Transcription Factor
TLE	Temporal Lobe Epilepsy
TSS	Transcriptional Start Site
Zn^{2+}	Zinc

1. Introduction

1.1 Epilepsy and Temporal Lobe Epilepsy: incidence and definition

Epilepsy is a chronic brain disorder characterized by an enduring predisposition to develop epileptic seizures due to an abnormal neuronal network activity (Fisher et al., 2014; Fischer, 2015). It is estimated that approximately 70 million people worldwide are affected by some form of epilepsy, resulting in the second most common cause of mental disability with a global disease impact similar to the one of breast cancer in woman or lung cancer in men (Ngugi et al., 2010; Kale, 1997). Since the beginning of the 20th century, the International League Against Epilepsy (ILAE) aims to advance and disseminate the knowledge about epilepsy, leading to constant and more accurate revisions of the classification of epilepsy and seizure types over the years. In the last update, epilepsies and seizure types have been classified taking into consideration 1) the types of seizures, 2) the epilepsy types, 3) the syndromic diagnosis and 4) the etiology (Scheffer et al., 2017; Fisher et al., 2017). With regard to the epileptic locus, epilepsy can be classified as *i*) generalized, when seizures affect both cerebral hemispheres; *ii*) focal, if seizures develop in a specific area of the brain; or *iii*) with unknown onset, when the origin of seizures is not detectable (Fisher et al., 2017). Etiology-wise, it is nowadays accepted that epilepsy can be cause by genetic as well as environmental factors. Epilepsies with an unclear promoting cause are addressed as *genetic* or *idiopathic*, while epilepsies provoked by external stimuli like stroke, brain tumors, brain infection or status epilepticus (SE) are defined as *acquired* or *symptomatic* (Shorvon, 2011; Engel, 1996; Bien and Elger, 2007; Bien et al. 2007; Liu et al., 2016; Pitkänen et al., 2016; Vezzani et al. 2016). Sometimes, genetic mutations do not cause the occurrence of epilepsy but a predisposition to it by lowering the threshold for seizures occurrence when in concomitance with external stimuli (Speca et al., 2014).

Despite the fact that the ILAE does not recognize a syndrome called temporal lobe epilepsy (TLE) and that the classification of epilepsies, based on the anatomical focus of seizure origin, belongs to previous classifications, TLE is addressed as the most common form of focal epilepsy with chronic seizures in the temporal lobe of the brain (Berg et al., 2010; Fisher et al., 2017; Murray et al., 1994). Two subtypes of TLE exist:

mesial temporal lobe epilepsy (mTLE), where the seizure onset occurs in the mesial structures of the temporal lobe, mainly in the hippocampus, and neocortical temporal lobe epilepsy (nTLE) with seizure onset from lateral structures of the temporal lobe (Téllez-Zenteno and Hernández-Ronquillo, 2012). Although mesial temporal lobe seizures are more common than lateral temporal lobe seizures, it is difficult to discriminate between mTLE and nTLE, as many symptoms overlap and reciprocal connections between mesial and lateral structures take place, resulting in a mutual spread of ictal discharge (Williamson et al., 1997; Gloor et al., 1982; Kotagal et al., 1995). Therefore, in this work, TLE will be referred to without differentiating between mTLE and nTLE.

1.2 Temporal Lobe Epilepsy

1.2.1 Neuropathological hallmarks

A clinical problem of TLE is given by the fact that one-third of the patients is refractory to pharmacotherapy and the possibilities to surgically intervene, removing the seizure loci in order to reduce or even eliminate seizure activity, is often very low for these patients (Kwan and Sander, 2004; Wiebe et al., 2001; Clusmann et al., 2004; Engel, 2003).
Observations conducted on surgical biopsy specimens have allowed the identification of two main groups of TLE patients, each of them characterized by their neuropathological hallmarks. It must be kept in mind that, being the epileptic focus removed in advanced phases of the disease, the neuronal features are the result of summative pathological and molecular alterations. Nevertheless, approximately 60 % of the biopsy specimens from pharmacoresistant patients show hippocampal sclerosis (HS), which is accompanied by neuronal loss in the CA1 and CA3/CA4 regions and by a dense fibrillary astrogliosis, resulting in contraction and hardening of the tissue (Majores et al., 2007; Blümcke et al., 1999; Sloviter et al., 2004). Neuronal loss affects also other brain regions as the entorhinal cortex layer III and the lateral nucleus of the amygdala (Du et al., 1993; Miller et al., 1994; Pitkänen et al., 1998). Another hallmark of the HS specimens is aberrant axonal reorganization of the dentate granule cells (Blümcke et al., 1999). Under physiological conditions, the granule cells receive excitatory input from the entorhinal cortex and send excitatory output to the CA3 region of the hippocampus

through the mossy fibers. However, several studies showed that granule cell neurogenesis endures postnatally and is stimulated by seizures (Altman and Bayer, 1990; Kuhn et al., 1996; Parent et al., 1997). During the development of TLE, the newly generated granule cells miss the target structures in the CA3 region due to neuronal loss and create aberrant connections with the remaining neurons (Parent et al., 1997).
The second group of TLE drug-refractory patients is characterized by specimens lacking HS and harboring focal lesions within the temporal lobe (Majores et al., 2007). In this case, the biopsies of the resected epileptic focus do not show neuronal loss but a dense astrogliosis responsible for the generation of low-growing brain tumors, such as the low-grade glial and glioneuronal neoplasms (Kim et al., 1990; Miller et al., 1994; Majores et al., 2007).

1.2.2 Epileptogenesis

TLE has a clear *acquired* "*symptomatic"* etiology as it develops as a consequence of an initial precipitating injury (Shorvon, 2011; Pitkänen and Engel, 2014). These brain insults trigger structural and functional neuronal alterations that initiate immediately after the transient brain insult and persist during the establishment of epilepsy (Pitkänen and Engel, 2014). Epileptogenesis is accompanied by changes in synaptic and intrinsic plasticity. Changes in synaptic plasticity primarily implicate changes in network connectivity, neurotransmitter release and expression of post-synaptic receptors (Becker et al., 2008). In 1928, Ramón y Cajal was the first to identify changes in network connectivity after a brain trauma. He investigated axonal sprouting of injured human neocortical neurons and appointed the phenomenon responsible for the hyperexcitability of cortical circuits (Cajal, 1913). Later on, many researchers confirmed the axonal sprouting theory and the formation of new post-injury synapses in many sites of the central nervous system (CNS) (McNamara, 1999). Particular attention was given to the "Mossy-fiber sprouting" (MFS) phenomenon which takes place during epileptogenesis. This event consists of reorganizing the mossy-fiber axons of dentate granule cells into the inner layer of the dentate gyrus of the hippocampus and of generating numerous excitatory synapses between dentate granule cells with consequent formation of a hyperexcitable hippocampal network (Sutula et al., 1988; Represa et al., 1993; Okazaki et al., 1995; McNamara, 1999). Another process by which the excitation-inhibition

balance is shifted towards excitation in TLE is through alteration of the glutamate and gamma-aminobutyric acid (GABA) signaling during epileptogenesis. $GABA_A$ receptor subunit composition, number and distribution are altered in various animal models of TLE and several studies reported changes in glutamate receptor expression in the hippocampus and other brain regions after seizures (Bouilleret et al., 2000; Brooks-Kayal, 2005; Elliott et al., 2003; Peng et al., 2004; Ransom and Blumenfeld, 2007). For instance, a reduction of neocortical and hippocampal levels of glutamate AMPA receptor subunit 2 (GluR2) was observed already a few days after SE in rats (Pollard et al., 1993; Friedman et al., 1994). While an increase in expression of the metabotropic glutamate receptor 1 (mGluR1) was shown in the dentate gyrus (DG) of an animal model of limbic seizures and also in patients affected by TLE (Blümcke et al., 2000). Epileptogenesis is also characterized by changes in neuronal intrinsic plasticity. This phenomenon is caused by long-term changes in the expression and activity of ion channels (Beck and Yaari, 2008; Graef and Godwin, 2010). Those are pore-forming proteins implicated in ion homeostasis and in the generation and transmission of neuronal action potentials. Therefore, changes in intrinsic plasticity correspond to alterations of neuronal electric properties. Experiments conducted using animal models of epilepsy along with advance genomics techniques have provided a list of genes which contribute to the alteration of intrinsic plasticity and epilepsy pathogenesis (Monaghan et al., 2008; Young et al., 2009; Arnold et al., 2019). Wang and his colleagues (2017) reported around 1000 genes to be associated with the epilepsies; eighty-four were classified as “real” epilepsy genes, 73 were associated with neurodevelopment disorders, 536 were defined as epilepsy-related genes and 284 were considered as putative epilepsy genes. In addition, a numerous amount of those genes were ion-channels genes, including sodium (Na^+), potassium (K^+), chloride (Cl^-) and calcium (Ca^{2+}) channels (Wang et al., 2017). Genes were reported as susceptible based on observed mutation(s) and/or abnormal regulation, resulting in changes at the expression level. In the acquired epilepsies, the molecular mechanisms underlying expressional or functional changes involve transcriptional and post-transcriptional regulation of gene expression and trafficking. On the transcriptional level, miRNAs, epigenetic mechanisms and (in)activation of transcription factors (TFs) can modulate the expression of epilepsy-susceptibility genes (Catalanotto et al., 2016; Sosanya et al., 2013; Gross et al., 2016; Schuster et al., 2019;

Tan et al., 2017; Zhang et al., 2018; Dong et al., 2014; Yao et al., 2016). While on the post-transcriptional level, (de)phosphorylation, ubiquitylation, sumoylation and subunit proteolytic cleavages can enable their availability and functionality (Misonou et al., 2004; Bernard et al., 2004; Martin et al., 2007; Kim et al., 2007).

1.3 Ion Channelopathies

Since one third of the genes correlated with epilepsy encode for ion channels, epilepsy is often addressed as an ion channelopathy disorder (Wallace et al., 1998; Reid et al., 2009). Two types of ion channels exist: ligand-gated ion channels, which require a molecular interaction between a neurotransmitter and an orthosteric site in order to be gated, and voltage-gated ion channels, meaning that they change status in response to changes of transmembrane voltage (Alexander et al., 2011; Sands et al., 2005). Examples of epilepsy-associated ligand-gated channels are the excitatory ionotropic glutamate and nicotinic acetylcholine receptors, and the inhibitory, anion-selective, $GABA_A$ receptors (Lerche et al., 2013; Wei et al., 2017; Wang et al., 2017).

1.3.1 The low-voltage activated Ca_V3 channel family

One group of epilepsy-associated voltage-gated ion channels are the calcium channels. Six different calcium channel types exist, i.e. the L-, N-, P-, Q-, R- and T-type calcium channels (Catterall, 2000). They can be divided in high-voltage (HVA; L, N, P, Q, R.) and low-voltage (LVA; T.) gated channels, depending on the membrane potential range over which the channel is open (Catterall, 2011).

The calcium channel subfamily Ca_V3 mediates the T-type, low-voltage activated Ca^{2+} current (I_{CaT}) which consists of a fast inactivation current (Transient), a small current conductance (Tiny) and a current activation at a potential near to the resting membrane potential (Nilius et al., 1985; Nowycky, et al., 1985). The Ca_V3 family has three family members: $Ca_V3.1$ (*Cacna1g*), $Ca_V3.2$ (*Cacna1h*) and $Ca_V3.3$ (*Cacna1I*) (Perez-Reyes et al., 1998; Cribbs et al., 1998; Lee et al., 1999). Interestingly, all three channels have been reported to be involved in the epilepsies (Kim, 2015; Becker et al., 2008; El Ghaleb et al., 2021).

Different splice variants of the three genes can generate different forms of T-type channels which are expressed in a region-specific manner (Zamponi et al., 2015). In the brain, Ca_v3 channels are mainly expressed in the olfactory bulb, amygdala, cerebral cortex, hippocampus and hypothalamus, with a different distribution within the single structures. Notably, the granule cells layer of the olfactory bulb and the CA1 and CA3 regions of the hippocampus express all three types of Ca_v3 channels (Talley et al., 1999). Besides in the brain, T-type calcium channels are expressed in the spinal cord, peripheral sensory ganglia, heart, smooth muscle cells and endocrine cells (Talley et al., 1999; Yunker et al., 2003; McGivern, 2006).

Under physiological conditions, besides the regulation of neuronal excitability through the low-threshold spike/rebound bursting phenomenon, Ca_v3 channels are responsible for neurotransmitter and hormone release, sensory processes, sleep spindles, feeding behaviors, pacemaker activity in the heart, and control of cell growth and proliferation in smooth muscles (Lory et al., 2020; Cain and Snutch, 2010; Atlas, 2013; Chen et al., 1999; Agoston et al., 2004; Krahe and Gabbiani, 2004; Todorovic et al., 2002; Astori et al., 2011; Uebele et al., 2009; Mangoni et al., 2006).

Their regulation is modulated by several molecules, ions and post-translational modifications, including phosphorylation, glycosylation and ubiquitination (Hu et al., 2009; Chemin et al., 2019; Weiss et al., 2013; García-Caballero et al., 2014). Bioactive lipids such as arachidonic acid, a 20-carbon omega 6 polyunsaturated fatty acid, and anandamide, one of the endogenous cannabinoid 1 receptor agonist, negatively regulate T-type Ca^{2+} currents through a direct interaction in a micromolar physiological range (Schmitt and Meves, 1995; Talavera et al., 2004; Chemin at al., 2014; Chemin et al., 2007; Chemin et al., 2001). Some molecules activate or inhibit T-type channels depending on the tissue and species. In the majority of cases, neurotransmitters and hormones inhibit the LVA calcium currents. For instance, dopamine inactivates the calcium current via the D2 receptor in rat pituitary lactotroph cells or via the D1 receptor in bass retinal horizontal cells, and acetylcholine induces the same effect via direct binding to acetylcholine receptors in human ovarian follicular granulosa cells (Lledo et al., 1990a; Lledo et al., 1990b; Pfeiffer-Linn and Lasater, 1993; Platano et al., 2005). Among hormones, oxytocin, somatostatin and vasopressin provoke a downregulation of the Ca_v3 channels (Liu et al., 2005; Agoston et al., 2004; Grazzini et al., 1996).

Downregulation of Ca_v3 isoforms occurs also in the presence of divalent cations such as nickel (Ni^{2+}), cadmium (Cd^{2+}), zinc (Zn^{2+}), copper (Cu^{2+}) and magnesium (Mg^{2+}) (Lee et al., 1999; Swandulla and Armstrong, 1989; Büsselberg et al., 1992; Jeong et al., 2003; Zamponi et al., 2015). The $Ca_v3.2$ subunit presents the highest affinity to the divalent cations in comparison to the other Ca_v3 isoforms: Ni^{2+} has a IC_{50} of ~10 µM for the $Ca_v3.2$ isoform while it has a IC_{50} of above 100 µM for the $Ca_v3.1$ and $Ca_v3.3$ isoforms (Lee et al., 1999). In addition, Zn^{2+} shows a IC_{50} of ~0,8 µM for $Ca_v3.2$ and a IC_{50} 100- and 200- fold higher for $Ca_v3.3$ and $Ca_v3.1$, respectively (Traboulsie et al., 2007). These cations act as competitive antagonist for the calcium binding site, occluding the pore of the channel and lowering the channel conductance (McGivern, 2006).

As a consequence of their physiological roles, the Ca_v3 channels have been linked to several pathological conditions including loss of motor coordination, epilepsy, neuropathic pain and bradycardia (Chang et al., 2011; Beck et al., 1998; Ernst et al., 2009; Bourinet et al., 2005; Mangoni et al., 2006).

In recent years, knock-out (ko) and transgenic animal models for the T-type calcium channels have been generated to better understand their specific implications in diseases. It has been shown that single nucleotide mutations within the Ca_v3 genes can lead to neurodevelopmental disorders. A point mutation in *CACNA1G* causes adult-onset mild ataxia phenotype, while other gain of function mutations within the same gene are responsible for childhood cerebral atrophy (Coutelier et al, 2015; Chemin et al., 2018). In addition, gene mutations in *CACNA1I* have been identified as a risk factor for neuropsychiatric diseases like schizophrenia (Gulsuner et al., 2013; Schizophrenia Working Group of the Psychiatric Genomics Consortium, 2014). $Ca_v3.2$ ko animals are affected by elevated anxiety and attenuated pain (Chen et al., 2012; Choi et al., 2007). The attenuated pain confirms a key role of $Ca_v3.2$ in nociception.

Both $Ca_v3.1$ and $Ca_v3.2$ isoforms have been extensively studied in different forms of epilepsy. $Ca_v3.1$ ko animal models are less susceptible to develop tonic seizures compared to wild type littermates in an electroshock test, while the $Ca_v3.2$ T-type calcium subunit was reported to be involved in the pathogenesis of TLE (Sakkaki et al., 2016; Becker et al., 2008).

1.3.2 The $Ca_v3.2$ subunit in Temporal Lobe Epilepsy

Sanabria et al. (2001) were the first to observe an increase of intrinsic bursting in CA1 pyramidal neurons within the pilocarpine-induced SE animal model of TLE (an animal model to study epilepsy-pathogenesis; see below) and to identify a subset of pyramidal cells (PCs) which act as pacemakers of interictal-like bursting. This subset of neurons recruits the entire CA1 pyramidal neurons, bursting and not bursting, into a synchronized discharge (Sanabria et al., 2001). Initially, the above-mentioned phenomenon was attributed to a *de-novo* calcium current which in the course of the years has been revealed to be the T-type calcium current (Sanabria et al., 2001). In fact, electro-pharmacological studies suggested that the switch from normal firing to a bursting mode after a single episode of SE was caused by an increase of the Ni^{2+}-sensitive T-type calcium current density (Su et al., 2002). Molecular investigations confirmed that early after SE, the $Ca_v3.2$ subunit is transiently, transcriptionally and functionally upregulated leading to an enhancement of T-type calcium current and intrinsic firing in the hippocampal CA1 pyramidal neurons (Becker et al., 2008). Congruently, $Ca_v3.2$ ko mice resulted to be less affected by the SE-induced augmentation of the I_{CaT} and did not show any neuropathological hallmarks, such as neuronal loss, typical for the development of TLE (Becker et al., 2008). All these findings pointed towards a key role of $Ca_v3.2$ in the process of epileptogenesis and in converting a normal neuronal network hyperexcitable.

1.3.3 $Ca_v3.2$ transcriptional regulation

One of the mechanisms responsible for an altered expression, distribution and activity of ion channels during the process of epileptogenesis includes the differential expression of transcriptional activators or repressors. Interestingly, the *Cacna1h* promoter presents binding sites for several transcription factors which can regulate *Cacna1h* gene expression. The Early Growth Response 1 transcription factor (Erg1/Zif268/Krox-24), which is known to be involved in neuronal activity and in the regulation of synaptic plasticity, is one of them (Duclot and Kabbaj, 2017). Erg1 binds the $Ca_v3.2$ promoter via three Cysteine2Histidine2 (C_2H_2)-type Zn^{2+} finger DNA-binding domains, inducing a transcriptional upregulation of the channel and increasing I_{CaT}. The Erg1-induced activation of the *Cacna1h* promoter can be antagonized by the repressor element 1-

silencing transcription factor (REST1), also known as Neuron-Restrictive Silencer Factor (NRSF) which is a repressor of neuronal gene expression and which is highly expressed after extended periods of neuronal hyperactivity, typically occurring during seizures (van Loo et al., 2012). Another transcription factor capable of binding the $Ca_V3.2$ promoter and of regulating the $Ca_V3.2$ expression is metal-response element binding transcription factor-1, also termed metal-regulatory transcription factor 1 or metal-responsive transcription factor 1 and shortened as Mtf1(van Loo et al., 2015).

1.4 Structure and role of Mtf1

Mtf1 is evolutionarily a well conserved protein, from insects to mammals (Günther et al., 2012). The primary structure of the protein consists of six C2H2 type Zn^{2+} finger domains, three transcriptional activation domains - rich in acidic residues, prolines and serines/threonines, a nuclear localization signal (NLS) motif, a nuclear export signal (NES) motif and a homodimerization sequence (Radtke et al., 1993; Seipel et al., 1992; Radtke et al., 1995; Saydam et al., 2001; Lindert et al., 2009). The amino acids (a.a.) length of human MTF1 is slightly longer at the C-terminus but nevertheless quite similar to the mouse Mtf1 protein (753 *vs* 675 a.a.) (Brugnera et al., 1994) (**Fig. 1**).

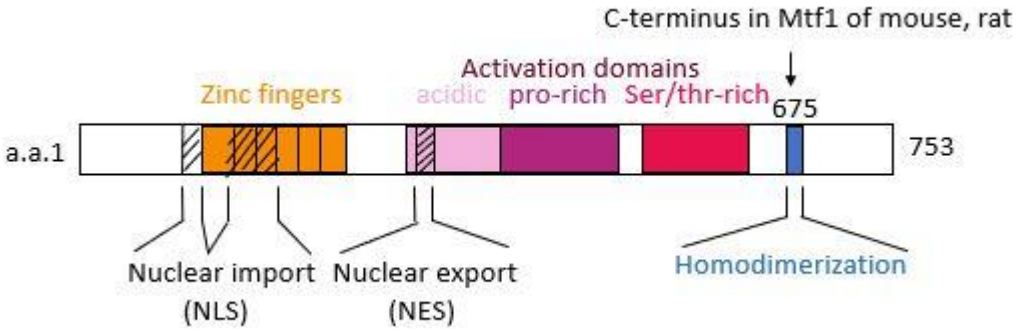

Fig. 1: Representation of the domain structure of mammalian Mtf1. The six Zn^{2+} fingers, the nuclear import and nuclear export motif, the three activation domains and the homodimerization motif. The different arrows show the Mtf1 C-terminus of different mammals. Modified from Günther et al., 2012.

Under physiological conditions, Mtf1 localizes within the nucleus and the cytoplasm, and can be shuttled out of the nucleus by a protein called Chromosomal Maintenance 1

(Crm1) (Lindert et al., 2009; Nguyen et al., 2012). Once Mtf1 is activated in response to heavy metal exposure, such as Zn^{2+} and Cd^{2+}, or forms of stress like hypoxia or oxidative stress, it accumulates in the nucleus (Saydam et al., 2001). Here, it binds via its six Zn^{2+} finger domains to Metal Responsive Elements (MREs) sequences generally located within target gene promoters (Stuart et al., 1984; 1985). Nevertheless, MREs can also be located downstream of the transcriptional start site (TSS) (Günther et al., 2012; Lichten et al., 2011). MREs are DNA-binding consensus 5'-TGCRCNC-3' sequences (with R = A or G and N = any nucleotide) (Wang et al., 2004a). In order to drive expression of target genes, Mtf1 interacts with other transcription factors and coactivators, including Sp1 and p300 (Li et al., 2008; Okumura et al., 2011) (**Fig. 2**). The activity of Mtf1 can be regulated at the post-translational level, for instance by phosphorylation or homodimerization, which is fundamental for the recruitment of other proteins involved in the transcriptional machinery, or can be regulated at the nucleus-cytoplasmic shuttling level (Günther et al., 2012).

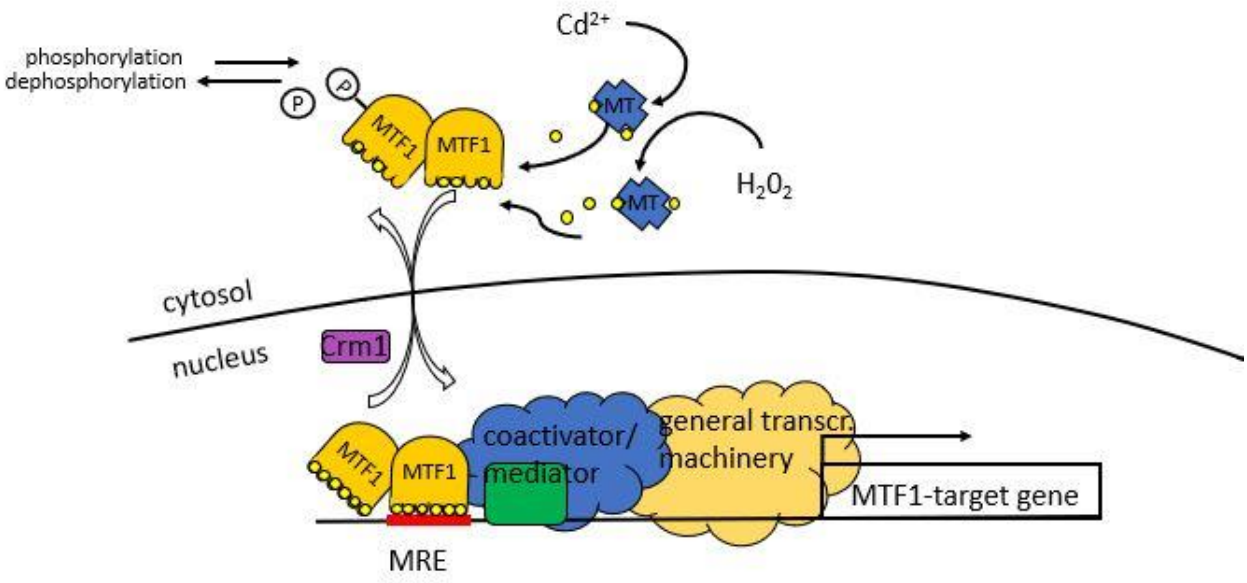

Fig. 2: Schematic overview of mammalian Mtf1 regulation. Under normal conditions, Mtf1 shuttles between the cytosol and nucleus and is carried out of the nucleus via Crm1 interaction. After direct or indirect Zn^{2+} activation, Mtf1 internalizes in the nucleus, binds to MREs within the promoter region of target genes, recruits other transcription factors and activators and regulates target gene expression. Modified form Günther at al., 2012.

Mtf1 plays a central role in heavy metal homeostasis and detoxification by controlling expression of genes that directly influence intracellular heavy metal levels or their availability, with particular regard to Zn^{2+} (Guo et al., 2010; Langmade et al., 2000; Wimmer et al., 2005; Bellingham et al., 2009; Grzywacz et al., 2015). Zn^{2+} is the second most abundant transition metal ion and it is needed by all organisms for cell metabolism and for providing a structural scaffold to many proteins (Choi and Bird, 2014; Vallee and Auld, 1990; Laity et al., 2001). However, a shortage or excess of the ion causes diseases like immune dysfunction, growth retardation or sensory and motor neuropathies (Black, 1998; Andrews, 1992; Afrin, 2010; Hedera et al., 2009). In mammals, Mtf1 has a relevant role in liver development, as shown by Mtf1 ko mice which die at embryonic day 14 due to liver degeneration (Günes et al., 1998; Wang et al., 2004b). The best characterized genes regulated by Mtf1 are the ones encoding for the metallothioneins-I (MT-I) and II (MT-II) which are small cysteine-rich proteins able to bind Zn^{2+}, Cd^{2+} or hydrogen peroxide (H_2O_2) produced in oxidative stress conditions (Radtke et al., 1993; Kagi and Valee, 1960; Andrews, 1992). When intracellular levels of Zn^{2+} are too high, Mtf1 augments expression of MT genes which then chelate the Zn^{2+} in excess with consequent protection of the cell from the ions toxicity and inactivation of Mtf1 (Heuchel et al., 1994). Other well-known mammalian genes that are activated by Mtf1 are *Scl30a1* and *Scl30a2*, encoding for the Zn^{2+} exporter ZnT-I and ZnT-II, *Slc39a10* which encodes for the Zn^{2+} importer Zip10, and the ɣ-glutamate-cysteine-ligase (*Gcl)* which encodes for the subunit of glutamate-cysteine ligase, an enzyme that catalysis the glutathione biosynthesis (Palmiter and Findley, 1995; Guo et al., 2010; Lichten et al., 2011; Kaler and Prasad, 2007; Günes et al., 1998).

1.5 The Zn^{2+}-Mtf1-$Ca_V3.2$ cascade of epileptogenesis

As mentioned above, Mtf1 also regulates the transcription of *Cacna1h*, encoding for the Cav3.2 channel subunit. Indeed, bioinformatic analyses of the $Ca_V3.2$ promoter revealed MREs located upstream of the *Cacna1h* TSS. This discovery explained the Zn^{2+}-induced upregulation of I_{CaT} observed in an animal model of TLE and sees Mtf1 as a mediator of a new mechanism of neuronal plasticity (Suh et al., 2001).

On one side, it was already known that Zn^{2+} is released from glutamatergic terminals during a strong neuronal activity such as SE (Suh et al., 2001) and that it accumulates in

the somata of CA1 neurons already one day after SE where it remains for one week (van Loo et al., 2015). In addition, it was demonstrated that Zn^{2+}, although it acutely and reversibly inhibits Ni^{2+}-sensitive calcium currents, causes a long-term upregulation of I_{CaT} in hippocampal PCs of intracranially Zn^{2+}-injected mice (Traboulsie et al., 2007; van Loo et al., 2015). On the other side, Becker et al. (2008) observed that after a single episode of SE, $Ca_v3.2$ expression is augmented in CA1 neurons, with a transient transcriptional and protein peak respectively 3 and 5 days after SE-induction, and that $Ca_v3.2$ ko animals are less prone to develop seizures after the chemical convulsant pilocarpine administration. Further experiments pointed out how Mtf1 overexpression *in vitro* as well as *in vivo* provokes an increase of $Ca_v3.2$ expression and $I_{CaT,}$ similar to the one induced by Zn^{2+}. In addition, overexpression of a dominant-negative form of Mtf1 (dnMtf1, Mtf1ΔC) which acts as a competitive antagonist for the MREs, reduces the Zn^{2+}-induced $Ca_v3.2$ activation and seizure progression (van Loo et al., 2015). These results indicate a role for Mtf1 in mediating the stimulatory effects of Zn^{2+} on the $Ca_v3.2$ promoter. Altogether, these findings allowed the identification of a new mechanism of neuronal plasticity to which we refer to as the "*Zn^{2+}-Mtf1-$Ca_v3.2$ cascade of epileptogenesis*". Here, the intracellular rise of Zn^{2+} activates Mtf1 which then binds to the MREs present within the *Cacna1h* promoter, resulting in a transcriptional and functional upregulation of the $Ca_v3.2$ channel. The enhancement of $Ca_v3.2$ channel expression results in an enlargement of I_{CaT} and in the conversion of regular firing CA1 neurons to intrinsic burst firing cells, strengthening the excitability of the hippocampal network (van Loo et al., 2015) (**Fig. 3**).

The positive correlation between high levels of MTF1 and Cav3.2 mRNA also in pharmacoresistant patients affected by TLE with HS would indicate that interfering with this intracellular cascade could pave the way to halt the development of TLE or attenuate the progress of the disease (van Loo et al., 2015).

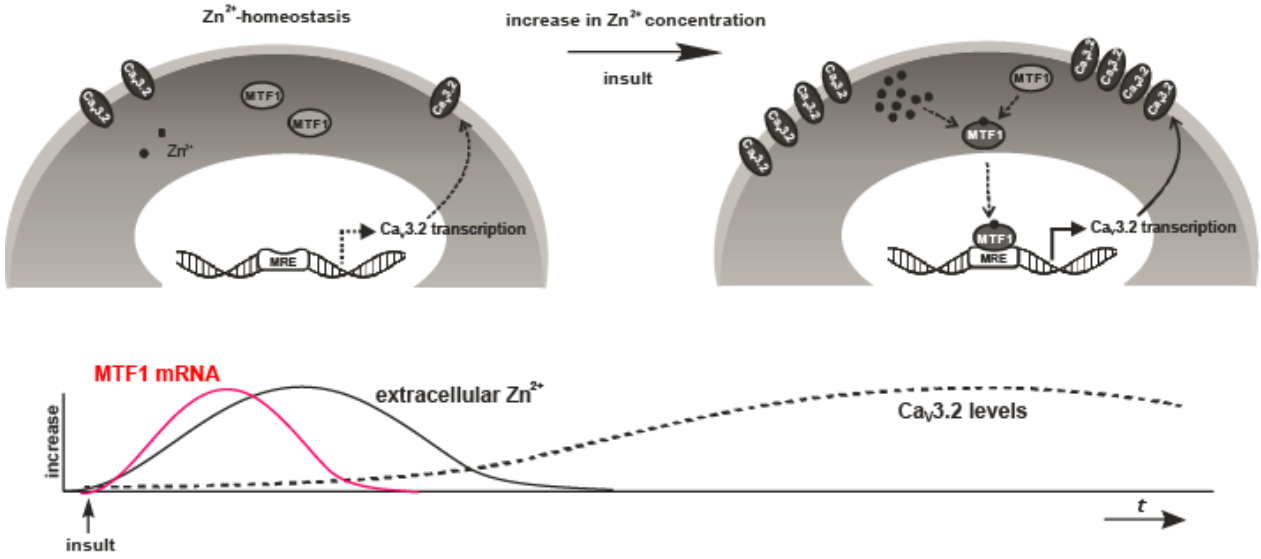

Fig. 3: Timeline of the Zn^{2+}-Mtf1-$Ca_V3.2$ cascade of epileptogenesis. Zn^{2+} released from glutamatergic neurons during neuronal activity underlying SE is internalized postsynaptically and accumulates in pyramidal neurons within 1 day, with a peak at 2-4 days after SE. Zn^{2+} activates Mtf1, and consequently increases $Ca_V3.2$ transcription and channel expression, leading to a robust increase of I_{CaT} and hippocampal hyperexcitability. Image courtesy of Dr. van Loo.

1.6 Animal models of epilepsy

In the last decades, different approaches have been adopted to investigate the process of epileptogenesis. For example, genetic screenings and transcriptomic approaches, specifically at the single-cell level, allow us to couple individual-specific expression differences with genetic variations. As for obvious moral reasons, it is not possible to obtain brain tissue from epilepsy patients during the earlier phases of epileptogenesis. To study the early phases of epileptogenesis, and to have a better insight into the chronic stages, animal models may be useful. For example, the kindling model in rodents is a well-established method where the animal receives daily electrical or chemical stimuli in cortical or limbic structures, most commonly in the amygdala, with gradual development of seizures which increase in severity and duration with ongoing stimulation. With this animal model is possible to mimate some hallmarks of epilepsy such as chronic seizures, neuronal damage and cognitive deficits (Löscher, 2017). The pentylenetetrazol (PTZ) animal model is a chemical kindling model of epilepsy which reassembles the features of absence seizures or “petite mal” seizures (Dhir, 2012). It is

the preferred animal model to test antiepileptic medicines by using repeated administration of the non-competitive antagonist of $GABA_A$ receptor PTZ (De Deyn et al., 1992). Interestingly, although this is a widely used animal model of epilepsy, the mechanism by which PTZ is capable to trigger seizures is not well understood, as some anticonvulsant drugs, known to bind to allosteric sites of the $GABA_A$ receptor, show divergent results both in the PTZ-acute and kindled model (Hansen et al., 2004).

Two other animal models in epilepsy research are the systemic application of the convulsant drugs kainic acid- and pilocarpine to induce the disease. Kainic acid is a cyclic analog of L-glutamate and an agonist of the kainite sensitive glutamate receptor while pilocarpine is a natural heterocyclic compound imidazole-derivate, which acts as an agonist of the muscarinic receptor M3. The approach consists in the induction of an initial brain injury, namely SE, which is defined as a period of seizure activity persisting for at least 30 min without full consciousness recovery, followed by a latent phase of 3-4 weeks before the manifestation of spontaneous seizures (Lowenstein et al., 1999; Scott, 2014; Sloviter et al., 2004; Lévesque et al., 2016).

1.6.1 The Pilocarpine-induced SE animal model of Temporal Lobe Epilepsy

The pilocarpine-induced SE model of TLE is a well-established and clinically translatable model which has allowed to uncover most of the knowledge acquired about TLE pathogenesis. The model was first described in 1983 by Turski et al., who documented how intraperitoneally administration of the drug was followed by limbic seizures culminating with SE. In detail, animals face four different stages before entering SE. Briefly, in the first stage, animals assume a rigid posture; in the second stage, they experience repetitive movements like head bobbing; in the third stage, animals develop severe seizures with rearing without falling, followed by a fourth stage where they have severe seizures with rearing and falling (Pitsch et al., 2007).

The pilocarpine model has been optimized during the years in order to reduce the high mortality and low induction rate (Ahmed Juvale and Che Has, 2020). In order to reduce peripheral muscarinic effects, 20 min before pilocarpine administration, animals receive a first injection of N-methyl scopolamine, an antagonist of the muscarinic acetylcholine receptor not able to cross the blood brain barrier. Usually animals recover from SE within 5-6 hours (h), however, in order to reduce its mortality rate, 40 minutes (min) after

SE onset, mice receive a subcutaneous administration of the anticonvulsant diazepam, agonist of the $GABA_A$ receptor. The pilocarpine-model induces neuronal loss, particularly in the dentate gyrus and CA1/CA3 region of the hippocampus, and mossy fiber sprouting, highly resembling the neuropathological hallmarks found in the surgically resected hippocampi of pharmacoresistant patients with TLE (Fritsch et al., 2010; Sharma et al., 2007; Blümcke et al., 1999).

1.7 Aims of the study

Changes in synaptic and intrinsic plasticity are responsible for the process of epileptogenesis in TLE. Recently, a new mechanism of aberrant intrinsic plasticity has been discovered, in which Mtf1 plays a key role. This transcription factor, upon Zn^{2+} activation, is able to convert CA1 hippocampal neurons from regular firing into a mode with intrinsically increased propensity for burst discharges by specifically inducing the transcriptional and functional levels of the T-type pore-forming calcium subunit $Ca_V3.2$. Interfering with this cascade by $Ca_V3.2$ deletion or by virus-mediated expression of a dominant-negative form of Mtf1 attenuates the emergence of spontaneous seizures in the chronic phase of the pilocarpine-induced SE mouse model. The findings obtained until now suggest this cascade as a putative new target for pharmacological treatment aimed to delay the development of the disease.

However, the pathophysiological context of Mtf1 in insult-induced conversion of a neuronal network from normal function to hyperexcitability goes beyond the '$Ca_V3.2$'-cascade but remains largely unknown.

Therefore, the overall goal of this study is to gain new insights in the role of Mtf1 in the process of epileptogenesis.

The first aim was to identify Mtf1-expressing neurons in mouse brain tissue by developing a minimal promoter to genetically label Zn^{2+}/Mtf1-positive cells.

The second aim was to determine the involvement of the Zn^{2+}/Mtf1 pathway in TLE pathogenesis by monitoring Mtf1 activation at different stages of epileptogenesis.

The third aim was to examine to what extent the Zn^{2+}/Mtf1-positive cells overlap with and contribute to the $Ca_V3.2$-expressing cells in the process of epileptogenesis

The fourth aim was to identify comprehensively downstream targets of the Zn^{2+}/Mtf1-cascade involved in the process of epileptogenesis.

2. Material and methods

2.1 Oligonucleotides

Oligonucleotides were synthesized by Invitrogen (Karlsruhe, Germany). Lyophilized oligonucleotides were dissolved in Ampuwa water (Fresenius Kabi, Germany) to a final concentration of 100 µM.

2.1.1 Cloning primers

Tab. 1: Cloning primers

PCR fragment	Direction	Primer sequence (5' to 3)	Enzyme	Plasmid
Luciferase	Fw	cagcttacaaccatgatggaagatgccaa aaacattaagaagg	NcoI	pAAV-MREs-Luciferase
Luciferase	Rv	atctcttacttgtacttacacggcgatcttgccgc	BsrGI	pAAV-MREs-Luciferase
LacZ	Fw	Cagcttacaaccatgatgaccatgattacgg attcactgg	NcoI	pAAV-MTI-*LacZ*
LacZ	Rv	atctcttacttgtacttatttttgacaccagaccaactggt	BsrGI	pAAV-MTI-*LacZ*
$Cav_{3.2}$-1020	Fw	gcgacgcgtcagtgaagggaaggggcggcgc	BamHI	pAAV-Cav3.2-*LacZ*
$Cav_{3.2}$-1020	Rv	gcggtcgacgtggcggagggcagcac	SalI	pAAV-Cav3.2-*LacZ*

Mtf1	Fw	ccggggatcctctagaatgggggaacacagtccagac	XbaI	pAAV-hSyn-Mtf1
Mtf1	Rv	tgtttcagggtggcagctgcagg		pAAV-hSyn-Mtf1
2A-SBFP2	Fw	gccacccgtgaaacagactttgaattttgaccttctcaag		pAAV-hSyn-2A-SBFP2
2A-SBFP2	Rv	tgctcgaggcaagctttcacttgtacagctcgtccatgc	HindIII	pAAV-hSyn-2A-SBFP2
MRE-MTI	Fw	ctgcggccgcacgcgggtacctgagctcgctagcctcg	MluI	pAAV-MTI-iRFP^{713}
MRE-MTI	Rv	ccatggtggctctagggtggctttaccaacagtaccg	XbaI	pAAV-MTI-iRFP^{713}
mRuby3	Fw	cagcttacaaccatggtgtctaagggcga	NcoI	pAAV-MTI-mRuby3
mRuby3	Rv	atctcttacttgtacttacttgtacagctcgtccatgcc	BsrGI	pAAV-MTI-mRuby3

2.1.2 Sequencing primers

Tab. 2: Sequencing primers

Template	Direction	Sequence (5’ to 3’)
Poly-A	Rv	ttgccccttgctccatac
hSyn	Fw	acgcgaggcgcgagatag
Mtf1	Rv	ggagggagcaggtggaggag
2a-sbfp2	Fw	aagcatcgaaagtggaggag

2.1.3 Quantitative real time RT-PCR primers

Tab. 3: RT-PCR primers

Gene	Fw primer (5’ to 3’)	Rv primer (5’ to 3’)
Cacna1b	cgcctttggggtattgaact	agaggcgaaggaagcttagg
Creb1	gcccctggagttgttatggc	tcttgctgcctccctgttctt
Cplx2	actctgcttggtgtctgactct	tttgggaaatgagcccacctgt
Gabra4	ggacccctgatactttcttcagg	cgcacttatggtgagtctcattg
Gabrb3	tgaaaaaccgcatgatccgc	gctgtcgtagtgatcctgagc
Gabrd	attttatacagcatccgcatcacc	catccagtgggtacttggcg
Git1	acagatggctgacagcttgg	atggcaagttcctcaaaaagcc
Gria1	tgatggaatccgcaagattggtt	cgaggatagtcgtgacgatgtag
Grin2b	aacggtcagaggtggttgac	cgtcagcactgaatggctctaa
Kalrn	acacatacctccaccggaga	ctccttcgtttgcttggcag
Kcnh1	caacctgaggaagaggattgtgt	tttctgctggcggaaccttt

Kctd13	cactatgcctcatccccaca	agttgtcatctgaagtgctggt
Lrrtm2	agttgtcatctgaagtgctggt	gcttctcacagcggcatttag
Nrxn3	tggcaaataccacgttgtgc	cgttcattatcagtgttgcctgta
Ntrk2	acctcactgtgcattttgcg	tagaaccactgaagcgcagg
Ptprs	acccacaccctacaagattcag	aaggtgtgtggcttgaggtg
Rims3	aatccctcccagccacctat	gcttgctggtacaagggatca
Syn	ttcaggactcaacacctcggt	cacgaaccataggttgccaac
Unc13a	atggttcaaaggcggtcctg	ccttccgagactgcaccaat

2.2 Plasmids

2.2.1 Generated plasmids

Tab. 4: Generated plasmids

Name	Insert	Plasmid
pAAV-pGl4.23-Luciferase	Luciferase (Firefly)	pAAV-pGl4.23-Venus
pAAV-MREd/c-Luciferase	Luciferase (Firefly)	pAAV-MREd/c-Venus
pAAV-MRE3/4-Luciferase	Luciferase (Firefly)	pAAV-MRE3/4-Venus
pAAV-MTI-Luciferase	Luciferase (Firefly)	pAAV-MTI-Venus
pAAV-hSyn-Mtf1-2A-SBFP2	Mtf1-2A-SBFP2	pAAV-hSyn-MCS
pAAV-MTI-*LacZ*	*LacZ*	pAAV-MTI-Venus
pAAV-Ca_v3.2-*LacZ*	Ca_v3.2-1020	pAAV-MCS-*LacZ*
pAAV-MTI-mRuby3	mRuby3	pAAV-MTI-Venus

pAAV-MTI-iRFP^{713}	MRE-MTI	pAAV-hSyn-iRFP^{713}

2.2.2 Plasmids generated prior this study

pAAV-pGl4.23-Venus, pAAV-MREd/c-Venus, pAAV-MRE3/4-Venus, pAAV-MRE-MTI-Venus, pAAV-Ca_V3.2-Venus, pAAV-hSyn-GFP, pAAV-hSyn-Mtf1-IRES-Venus, pAAV-hSyn-dnMtf1-IRES-Venus, pAAV-hSyn-RL-TK.

2.3 Molecular Biology Methods

2.3.1 Polymerase chain reaction

DNA fragments were amplified by polymerase chain reaction (PCR) (**Tab. 5**). The PCR reaction mix contained double stranded DNA of the sequence of interest, single stranded primers, deoxyribonucleotides (dNTP) (Life Technologies) and the required amount of buffer and water. The Phusion High-Fidelity DNA Polymerase (Thermo Fisher Scientific) was used to amplify the DNA.

Tab. 5: PCR protocol

PCR reaction mix	50 µl reaction
5X HF buffer	10 µl
Fw primer (10 pmol/µl)	2,5 µl
Rv primer (10 pmol/ µl)	2,5 µl
Template DNA	100 ng
dNTP-Mix (25 mM)	1 µl
Nuclease-free Water	to 50 µl

The reaction was performed in a Thermal Cycler T100 (Bio-Rad). Different temperature steps were used to amplify the DNA fragment with 36 cycles of steps 2-4 (**Tab. 6**)

Tab. 6: PCR program

Step	Temperature	Time
1. Initial Denaturation	94 °C	1 min
2. Denaturation	94 °C	10 sec
3. Annealing	55-60 °C	30 sec
4. Extension	72 °C	15-30 sec/kb
5. Final extension	72 °C	10 min

2.3.2 Cloning

For the generation of new plasmids, template DNAs were amplified via PCR with appropriate primers (all primers including restriction sites recognition sequences are listed in **Tab. 1**). Primers were designed using SnapGene and synthesized by Invitrogen Life Technology. Final vectors and purified PCR amplicons were digested with the appropriate enzymes for 2 h at 37 °C. Following restriction, vector and amplified DNA fragments were complemented with 6x loading dye (Life Technologies) and separated on 1 % agarose (Sigma Aldrich) gels containing 4 % peqGreen RNA/DNA dye (PeqLab) for 30-60 min at 80-150 V. For an estimation of band sizes, GeneRuler 1kB DNA (Thermo Fisher Scientific) was also loaded on the agarose gels. DNA bands were visualized by UV-light via Chemidoc (Bio-Rad), cut out the gel for further vector generation and purified with the NucleoSpin® Gel and PCR Clean-Up kit (Macherey Nagel). Vectors and PCR fragments were ligated following the manufacturer's instructions of the In-Fusion® HD Cloning Kit (Takara Clontech). After ligation, 5 µl of product were used for chemical transformation of bacteria as described in section 2.3.3.

2.3.3 Chemical transformation of bacteria with plasmid DNA

To transform or re-transform the plasmid of interest, 50 µl of Stellar competent cells (Takara Bio) or 5-α *E. coli* recombinant cells (RC) (New England Bio Labs) were thawed on ice. For a transformation 5 µl of ligation product, and for a re-transformation 1 µg DNA were added to the bacteria and incubated for 20 min on ice. A heat shock followed at a temperature of 42 °C for 45 sec. The bacteria were placed on ice for 2 min before the addition of 150 µl of LB medium (Carl Roth) for RC cells or SOC medium (Takara Bio) for Stellar cells. Bacteria were incubated for 1 h at 37 °C in a thermo shaker. Afterwards, bacteria were plated on an agar-plate with ampicillin (Carl Roth) antibiotic as selection marker (100 µg/ml) and incubated overnight at 37 °C.

2.4 Bacteria Culture

To cultivate bacteria expressing the plasmid of interest, a single colony grown on an ampicillin agar-plate was incubated in 5 ml of LB medium and 0,1 % of ampicillin overnight at 37 °C at 180 rpm.

2.5 DNA plasmid purification

Purification of DNA plasmids was done using commercial kits (“mini”, “midi” and “maxi” purification kits (Qiagen, Germany)), following the manufacturer’s instructions. DNA concentrations were determined by spectrophotometric analysis. The plasmids obtained with the mini kit were used for restriction analysis and sequencing of the ligation product. The plasmids obtained with the midi kit were utilized for digestion, cloning and cell transfection. Plasmids used for purified virus production and neuron transfection were obtained with the endotoxin-free maxi kit in order to obtain high quality of DNA.

2.6 Sequencing

The correctness of the plasmid was confirmed by sequencing analyses, 15 µl of plasmid (~100 ng/µl) with 2 µl of sequencing primer were sent to Eurofins Genomics service (Germany).

2.7 Total RNA, messenger RNA (mRNA) isolation and cDNA synthesis

Total RNA was obtained from mouse micro-dissected CA1 hippocampal regions using the RNeasy Plus Micro Kit (Qiagen). mRNA was obtained from neuronal cultures in 24 wells-plate (70,000neurons/well) using the Dynabeads® mRNA DIRECT™ Micro Purification Kit (Life Technologies). First, neurons were washed with phosphate-buffered saline (PBS) and 50 µl of lysis buffer from the kit was added to the wells. Then, cells were stored at -80 °C for 10 minutes in order to promote the detachment of neurons from the bottom of the plate and the disruption of the neuronal membrane. The mRNA was isolated following the manufacturer's instructions. cDNA was synthesized from the purified mRNA by reverse transcription using the RevertAid H Minus First Strand cDNA Synthesis kit (Thermo Fisher Scientific), following the manufacture's protocol and in a T3 Thermo Cycler (Biometron). cDNA samples were stored for subsequent analysis at -20 °C.

2.8 Real time PCR

For quantitative real time PCR (RT-PCR), the Maxima SYBR Green/ROX qPCR Master Mix (ThermoFisher Scientific) was mixed with other components as listed in **Tab. 7.**

Tab. 7: RT-PCR reaction mix for one replicate

Components	Volume
DEPC H_2O	1,5 µl
Master Mix	3,125 µl
Fw primer (10pmol/µl)	0,1875 µl
Rv primer (10pmol/µl)	0,1875 µl
cDNA	1,25 µl
Σ	6,25 µl

The Taqman gene expression assay was performed in a C100 Touch Thermal Cycler CFX84^{TM} Real-Time system (Bio Rad Laboratories) following the protocol showed in **Tab. 8**. Steps 3-5 were repeated for 40 cycles and step 7 was added to the normal protocol in order to obtain a melting curve and consequent product size specificity.

Tab. 8: RT-PCR protocol

Step	Temperature	Time
1	50 °C	2 min
2	95 °C	10 min
3	95 °C	20 sec
4	60 °C	30 sec
5	72 °C	40 sec
6	95 °C	15 sec
7	60 °C	15 sec
	0.5 °C increment	15 sec/temperature
	95 °C	15 sec

Samples were pipetted in triplicate; one replicate was obtained by pooling together 2 wells of 24 well-plates with 70,000/well neurons. Gene expression measurements were done on an Abi Prism 7900HT system (PE Applied Biosystem). To analyse the expression of the gene of interest, synaptophysin was used as reference gene. Quantification was performed according to the $2^{-\Delta\Delta Ct}$ method. ΔCt (Cycle threshold value) = Ct of gene of interest – Ct of synaptophysin. ΔΔCt = ΔCt (treated samples) – ΔCt (untreated samples). Results are expressed as relative mRNA expression.

2.9 RNA sequencing

mRNA sequencing of resected CA1 hippocampal regions was performed in collaboration with the Cologne Center for Genomics (CCG), university of Cologne. RNA library preparation was obtained with the NEBNext® Ultra™ Directional RNA Library Prep Kit for Illumina® (New England BioLabs) (mRNA input:16 ng) and an RNA sequencing library was generated from 25 million reads of 100 bp paired ends.

2.10 Bioinformatic analyses

A list of genes involved in the synaptic transmission was obtained from the Synapse GO annotation database (http://www.informatics.jax.org/vocab/gene_ontology/GO:0007268). Putative MREs at the promoter region of the synaptic-related genes were detected using the Jaspar database in the Signal Search Analysis Server (SSA- https://ccg.epfl.ch/cgi-bin/ssa/findm_form_parser.cgi) and the tool finding motif around functional site (FindM). As input parameters for the promoter region, we used 1100 bp upstream and 100 bp downstream from the TSS. As cut-off value we selected genes with a binding sequence affinity > 98 %.
Bioinformatic analyses for the RNAseq experiment were conducted by our collaborator Dr. Ashley van Waanderberg, i-Synapse, Queensland, Australia. The following Bioconductor packages were used to analyze gene expression data: EdgeR, DESeq2 and voom/lomma (Robinson et al., 2010; Ritchie et al., 2015; Love et al., 2014; Law et al., 2014).

2.11 Cell culture

2.11.1 Human Embryonic Kidney 293 cells

Human Embryonic Kidney 293 (HEK293) cells (Stratagene) were kept in high glucose Dulbecco's Modified Eagle Medium (DMEM) (Life Technologies) supplemented with 10 % fetal calf serum (FCS) (Gibco®), 100 units per ml penicillin/streptomycin (Thermo Fischer Scientific) and 2 mM glutamine (Thermo Fisher Scientific), and incubated at 37 °C and 5 % CO_2. Cells were passaged every 2-3 days at a confluence of 60-80 % and plated in a dilution 1:10.

2.11.2 Transfection of HEK293 cells for Adeno-Associated Virus $_{1/2}$ (rAAV$_{1/2}$) production

To produce crude AAV$_{1/2}$ particles, HEK293 cells were seeded with a density of 1.5 x 10^6 cells/10 cm dish in DMEM medium. The next day, 4 h prior transfection, normal medium was removed and cells were incubated with Iscove's Modified Dulbecco's Medium (IMDM) (Thermo Fischer Scientific), supplemented with 5 % FCS. The transfection mixture per 10 cm dish is listed in **Tab. 9**

Tab. 9: HEK293 transfection mixture for AAV$_{1/2}$ virus production

Components	Amount
H_2O	1 ml
$CaCl_2$	145 µl; 2.5 M
pFdelta6 – adenoviral helper virus	11 µg
pH21 – serotype 2	2.64 µg
pNLrep /pRV1 – serotype 1	2.64 µg
AAV plasmid	5.5 µg
2x HeBS	1.2 ml

The helper plasmid pNLrep/pRV1 encodes for the rep gene while the helper plasmid pH21 encodes the cap gene. The 2X HEBS is composed by 50 mM HEPES (Carl Roth) with a pH=7.05, 280 mM NaCl (Sigma-Aldrich) and 1.5 mM Na_2HPO_4 (Sigma-Aldrich) and was added in a drop-wise manner while vortexing. The transfection mixture was incubated at room temperature (RT) for 2 min to allow complex formation before addition to the HEK293 cells. The IMDM medium was removed 24 h after the transfection and replaced with DMEM medium. To harvest the virus, the DMEM medium was collected 48 h after transfection in a falcon together with 1 ml of PBS which was added to the 10 cm dish in order to scrap the cells off. To disrupt the cells membrane, the suspension was

frozen at -80 °C and thawed at 37 °C for three times. After that, suspension was centrifuged for 3 min at 4500 rpm and virus-containing supernatant was stored at 4 °C. $rAAV_{1/2}$ viral particles were purified from the cell lysate by HiTrap heparin column purification (GE Healthcare), and then concentrated to a final stock volume of 500 ml using Amicon Ultra Centrifugal Filters (Millipore). Purity of the viruses was validated by coomassie blue staining of SDS–polyacrylamide gels. Functional titers (transducing units) of the fluorescent protein vectors were determined by transduction of cultured primary neurons.

2.11.3 Primary Neurons

Primary hippocampal neurons were prepared from C57Bl/-6N mice. Pregnant mice were sacrificed under deep isoflurane anaesthesia (Piramal Critical Care) and the uterus containing embryos (embryonic days 14-18) was removed. Hippocampi and cortex were isolated from the embryos and tissue was washed 3 times with cold Ca^{2+}/Mg^{2+} free Hanks' Balanced Salt Solution (HBBS) (Gibco®) before being digested with 200 µl 2.5 % trypsin (10X) (Gibco®) for 20 min at 37 °C. After 3 washing steps with HBSS, medium was aspirated and 200 µl 1 mg/ml DNase-I (Roche) together with 800 µl 1X basal medium eagle (BME) (Gibco®) was added. Tissue was mechanically dissociated by trituration using a 1 ml plastic tip. Neurons were counted, seeded in a 24 wells plate coated with Poly-D-Lysine (Sigma) and kept at 37 °C, 5 % CO_2 in BME supplemented with 0.5 % glucose (Sigma-Aldrich), 1 % FCS, 2 % B-27 (Life Technologies) and 0.5 mM L-glutamine (Gibco®).

2.11.4 Transduction of cultured primary neurons and Zn^{2+} loading

Primary neurons were transduced at DIV1-7 depending on the type of experiment with viral particle extracts containing ~10^8 transducing units (rAAV serotype 1/2). On DIV14, neurons were incubated with 1 µM $ZnCl_2$ for 1 h. Control neurons were treated in the same way but incubated with normal medium. Transduced neurons were further cultivated at 37 °C and 5 % CO_2.

2.11.5 Luciferase assay on hippocampal neurons

For Luciferase experiments, hippocampal neurons (24 wells plate, 40,000 neurons/well) were co-transduced on DIV7 with rAAV-MREs-Luciferase, rAAV-TK-Renilla and with rAAV-hSyn-Mtf1-IRES-Venus viral suspension. On DIV14, neurons were incubated with 1 µM $ZnCl_2$ for 1 h. Luciferase activities were determined after 4 h using the Dual Luciferase Report Assay System (Promega). Briefly, cells were washed with PBS and incubated for 15 min with the appropriate amount of Passive Lysis Buffer. After that, 20 µl/well of cell lysate was transferred in a 96 well Lumitrac™ plate (Greiner Bio-one, Germany) and combined with 100 µl Luciferase Assay Reagent II (LAR II) and 100 µl Stop & Go®. *Renilla* and firefly luciferase activity were measured using the Glomax Luminometer (Promega). If not mention elsewhere, results are given as firefly/*Renilla* relative light units.

2.12 Stereotactic $rAAV_{1/2}$ vector injection

Adult male mice (~56 days, > 20 gr) were obtained from Charles River Laboratories (C57Bl/6-N) and housed under a 12 h light/dark cycle, in a temperature (22 ± 2 °C) and humidity (55 ± 10 %) controlled environment and with food and water *ad libitum*. Animals were allowed of 1 week of adaptation to the animal facility before surgery. Mice were anesthetized with 0.05 mg kg^{-1} fentanyl (B. Braun, Germany), 5.0 mg kg^{-1} midazolam (Rotexmedica GmH, Germany) and 0.5 mg kg^{-1} medetomidine (Dorbene, Parsippany, NJ), intraperitoneal (i.p.). Thirty minutes before the anesthesia, mice received a subcutaneous (s.c.) injection of 5 mg kg^{-1} ketoprofen (Rifen, Vetoquinol). Intracerebral AAV injections in the left and right CA1 hippocampal region were performed stereotaxically at the coordinates (in mm) -2 posterior, -1.5/1.5 lateral and 1.5 ventral relative to Bregma. Holes the size of the injection needle were drilled into the skull, and 1 µl of viral suspension was injected through a 10 µl Hamilton syringe at a rate of 200 $nl\,min^{-1}$ using a microprocessor-controlled mini-pump (World Precision Instruments). One µl of viral suspension contained ~10^8 transducing units. After injection, the needle was left for 5 min in place before removal, the incision was closed and mice were allowed to recover on a heating plate. Mice were monitored twice per day and received a s.c. analgesic (Ketoprofen, Rifen, Vetoquinol) injection for 3 days post-operation. All

experiments were performed in accordance with the guidelines of the European Union and the University of Bonn Medical Center Animal Care Committee.

2.13 Pilocarpine-induced SE

To induce SE, adult C57Bl/6-N mice (P~60; >20 g) were injected with a single dose of muscarinic agonist pilocarpine hydrochloride (335 mg kg^{-1}, s.c., Sigma). To avoid peripheral muscarinic effects, scopolamine methyl nitrate (1 mg kg $^{-}$1, s.c., Sigma) was administered 20 min before injection of pilocarpine. Forty min after SE onset, the mice were injected once with diazepam (4 mg kg^{-1}. s.c., Ratiopharm). SE was defined as steady series of generalized tonic-clonic convulsions (stage V of the previously described classification of spontaneous seizures according to (Pitsch et al., 2007). Control mice were given scopolamine methyl nitrate and diazepam, but 0.9 % NaCl (Fresenius) instead of pilocarpine. After SE, all animals were fed with a 5 % glucose solution (Fresenius) and soaked rodent food and checked twice per day.

2.14 Near-infrared *in vivo* imaging

Mice were injected either with rAAV-MTI-iRFP or rAAV-MTI-iRFP combined with rAAV-hSyn-Mtf1-2A-SBFP2 particles (rAAV-Mtf1) or rAAV-MTI-iRFP combined with rAAV-hSyn-GFP (rAAV-GFP). Three weeks after injection, mice were anesthetized and basal iRFP values were measured through the skull. Three days after basal iRFP measurements, mice underwent pilocarpine-induced SE or sham-treatment. iRFP values were again determined 2, 10 and 28 days after pilocarpine-induced SE (time points were selected based on the results described in Kulbida et al. (2015)). The iRFP intensity signal of animals injected with an overexpression of rAAV-GFP and rAAV-Mtf1 was measured 2 weeks after injection.

Near-infrared imaging was performed with a Pearl® Impulse Small Animal Imaging System (Li-COR Biosciences GmbH, Bad Homburg, Germany). The iRFP signal was determined using a highly sensitive charged coupled device (CCD) camera. Excitation and emission wavelengths were fixed at 690 and 710 nm, respectively. Pictures were analyzed using the Pearl® Impulse Image Studio Software v3.1 (Li-COR Biosciences GmbH, Bad Homburg, Germany). Fluorescent signals were normalized to background

levels and quantified by placing two round regions of interest above the hippocampal region. Fluorescent signals are presented as arbitrary units (a.u.).

2.15 β-Galactosidase staining

Adult male C57Bl/6-N mice were injected as described above, either with rAAV-MTI-*Lac*Z or a combination of rAAV-MTI-*Lac*Z and rAAV-hSyn-Mtf1-2A-SBFP2 (rAAV-Mtf1) or a combination of rAAV-MTI-*Lac*Z and rAAV-hSyn-GFP (rAAV-GFP). For the $Ca_V3.2$-*Lac*Z experiments, adult male mice C57Bl/6-N were injected with rAAV-$Ca_V3.2$-*Lac*Z. Two weeks after injection, mice were sham- or pilocarpine-SE treated. Three days after SE, mice were decapitated under deep isoflurane anaesthesia. Brains were rapidly removed, coronal slices (400 µm) were made on a vibratome (Thermo Fisher Scientific) and β-Galactosidase staining was performed according to the manufacturer's protocol (Sigma Aldrich, #GALS_1 kit). Slices were recut in 50 µm, coverslipped in Mowiol mounting medium (Roth, Germany) and acquired using the Zeiss Axion Z1 slide scanner, provided by the Microscope Core Facility of the University of Bonn. Mice injected with an overexpression of rAAV-GFP and rAAV-Mtf1 were sacrificed 2 weeks after injection and *Lac*Z staining was performed as described above.

2.16 Immunofluorescence on paraffine imbedded sections

Adult male C57Bl/6-N mice were injected with rAAV-MTI-Venus. Two weeks after injection, animals experienced sham or pilocarpine-SE treatment. Mice were perfused 1 day after SE with 4 % PFA. This timepoint was selected as Mtf1 and Creb1 showed significant increased transcript levels already 12 h after SE, therefore we assumed that 1 day after SE the proteins would be expressed. Brains were removed, left overnight in 4 % paraformaldehyde (PFA) and subsequently embedded in paraffin. Immunofluorescence was conducted on coronal slices (4 µm) made using a microtome (Thermo Fisher Scientific). Standard staining protocols were used for immunofluorescent stainings against Venus (indicator for Mtf1-positive neurons) and Creb1. Paraffin sections were de-paraffinized in xylene (PanReac AppliChem) for 10 min, followed by incubation in a decreasing EtOH series (100 %, 95 %, 75 %, 50 %) for 1 min at each concentration. Slices were then rinsed in ddH_2O for 2 min. After washing, slices were

subjected to a citric acid (10 mM, pH=6) antigen retrieval treatment, followed by 5 min washing step in PBS. Slices were permeabilized with 0.5 % Triton™ X-100 (Merck) in PBS solution for 30 min at RT, prior being incubated for 2 h at 37 °C in blocking buffer (10 % normal goat serum (NGS), 1 % bovine serum albumin (BSA), 0.3 % Triton™ X-100 in PBS) in order to avoid non-specific antibody binding. After blocking slices were incubated with primary antibody overnight at 4 °C; Venus (Abcam, ab290, 1:1000) and Creb1 (Invitrogen, MA1083, 1:200) The next day, slices were washed three times for 5 min in PBS and incubated with the respective secondary antibodies (goat anti-rabbit Alexa Fluor 488 against Venus and goat anti-mouse Alexa Fluor 568 against Creb1) for 2 h at RT. After 3 washing steps for 5 min in PBS, slices were incubated in DAPI counterstaining 1:100 (Life Technologies). Images (40X) were taken with a Nikon Eclipse Ti microscope.

2.17 Tissue dissociation and FACS sorting

Two weeks after rAAV-hSyn-tdTomato and rAAV-MTI-Venus injection, C57Bl/6-N adult mice experienced sham- or pilocarpine-induced SE treatment. Three days later, mice were deeply anesthetized with isoflurane (Piramal Critical Care) and decapitated. The brain was extracted and the hippocampus isolated on ice and washed with cold PBS. Cell suspension isolation and debris and red blood cell removal occurred using the Adult Brain Dissociation Kit (MACS Miltenyl Biotec, Germany) following the manufacturer's protocol. The samples were sorted on a BD FACS Aria III, provided by the Flow Cytometry Core Facility of the University of Bonn. For the detection of the tdTomato signal, neurons were excited under a 561 nm laser and detected by a 582/15 filter. For the detection of the Venus signal, neurons were excited under a 488 nm laser and detected by a 530/30 filter. DAPI staining was used as a marker for dead cells and detected by a 450/50 filter. After sorting, cells were spun down at 4 °C for 2 min. The collection medium (PBS with 1 % heated inactivated and filtered FCS) was aspirated and tubes were immediately frozen in liquid nitrogen and stored at -80 °C until RNA extraction.

2.18 Hippocampal CA1 isolation

For the RNA-seq experiments, animals were divided in five experimental groups: 1) hSyn-GFP-injected (sham-treated), 2) hSyn-Mtf1-IRES-Venus-injected (sham-treated), 3) hSyn-dnMtf1-IRES-Venus-injected (sham-treated), 4) hSyn-GFP-injected (pilocarpine-SE), 5) hSyn-dnMtf1-IRES-Venus-injected (pilocarpine-SE). Animals were injected with the corresponding rAAVs two weeks before sham/pilocarpine treatment. Three days after sham/SE induction, animals were deeply anesthetized with isoflurane (Piramal Critical Care) before decapitation. Brains were extracted and coronal slices (300 µm) were made on a vibratome (Leica). The CA1 hippocampal region was microdissected under a fluorescent light microscope (Nikon) and samples were immediately frozen in liquid nitrogen.

2.19 Microscopy

2.19.1 Time Lapse Imaging

Hippocampal neurons (24 well plates, 40,000 neurons/well) were transduced on DIV1 with 5 µl rAAV-MTI-Venus viral suspension. Experimental wells were transduced with 5 µl rAAV-Mtf1-2A-SBFP2 viral suspension on DIV7 and treated for 1 h with 1 µM $ZnCl_2$ on DIV 14. Control wells were treated in the same way without $ZnCl_2$ but incubated with normal medium. Neurons were monitored and photographed under a fluorescence microscope (Axio Observer, A.1, Zeiss) in order to observe changes in fluorescence intensity before Zn^{2+} stimulation. Pictures (20X) were taken under the same conditions using a Jenoptik ProgRes MF Cool camera. Two hours after Zn^{2+} stimulation, changes in fluorescence intensity were examined using time-lapse imaging (Nikon Eclipse Ti microscope) for 15 h. Photographs (40X) were taken using a DS-Qi2 camera (Nikon).

2.19.2 Brain slices images

Adult male C57Bl/6-N mice were injected either with a combination of rAAV-MTI-mRuby3 and rAAV-Ca_V3.2-Venus, with and without rAAV-hSyn-Mtf1-2A-SBFP2. Three weeks after injection, animals experienced sham or SE-pilocarpine treatment. Mice were perfused at 1 and 3 days after SE with 4 % PFA. Brains were removed and left overnight

in 4 % PFA. Coronal slices (25-50 μm) were made using a vibratome (Thermo Fisher Scientific) and mounted with Mowiol. Images were made with the objective PlanApochromat 20X using a laser-scanning Visitrone Visiscope confocal provided of two pco.edge sCMOS cameras, offered by the Microscopy core facility of the University clinic of Bonn and the VisiView Software.

2.20 Creb1 fluorescence intensity analysis

Immunofluorescence stainings of Venus and Creb1 from mice hippocampi were acquired using a laser-scanning Nikon A1/Ti confocal microscope with a Plan APO IR 40x WI objective and the Nikon NIS Elements 4.0 acquisition software. The analysis was performed in ImageJ (Schindelin et al., 2012). Venus-expressing neurons were identified by subtracting a background and then by defining an intensity image threshold equal to the 10 % of the max intensity image after background subtraction. Regions of interest (ROIs) were manually detected and overlapped to the Creb1-expressing neurons. The mean grey value was used as parameter to measure the Creb1 fluorescence intensity in Mtf1-positive (Mtf1+) and Mtf1-negative (Mtf1-) neurons.

2.21 Human TLE patients and mRNA expression analyses

For the MTF1-target gene and MTF1 mRNA correlation, 2 different cohorts were analysed. The first cohort is composed by hippocampal biopsy tissue from patients with HS (*N*=79) versus patients with lesion-associated (low-grade neoplasms or dysplasia; *N*=35) chronic TLE, who underwent surgical treatment in the Epilepsy Surgery Program at the University of Bonn Medical Center due to pharmacoresistance. In all patients, presurgical evaluation using a combination of non-invasive and invasive procedures revealed that seizures originated in the mesial temporal lobe (Kral et al., 2002). Clinical characteristics per subgroup are described in **Tab. 10.** In the HS patient group, no individual was suffering from recurrent seizures at the time of birth but developed chronic recurrent seizures and HS later in life and many patients in the HS cohort could recall transient insults during childhood. In contrast, in the lesion-associated group, TLE is provoked by tumor or malformation in the proximity of the hippocampal formation. Furthermore, lesion-associated patients do not have clinical histories of initial

precipitating events/epileptogenesis and the hippocampal formation does not show HS. Taking into consideration the definition of TLE as an acquired form of epilepsy, Lesion-associated TLE hippocampi can be assessed as a control group for epileptogenic HS hippocampi. All procedures were conducted in accordance with the Declaration of Helsinki and approved by the Ethics Committee of the University of Bonn Medical Center. Informed written consent was obtained from all patients. mRNA analyses for MTF1-target genes and MTF1 were carried out as described in Pernhorst et al. (2013). RNA from biopsies representing all hippocampal subfields served to generate 750 ng cRNA used for hybridization on Human HT-12 v3 Expression BeadChips with Illumina Direct Hybridization Assay Kit (Illumina, San Diego, CA) according to standard procedures. Data for MTF1-target genes and MTF1 analysed by Illumina's GenomeStudio Gene Expression Module and normalized using Illumina BeadStudio software suite by quantile normalization with background subtraction. The second cohort consisted of 55 biopsy specimen of HS patients. Patients underwent surgical treatment in the Epilepsy Surgery Program at the University of Bonn Medical Center due to pharmacoresistance. Clinical parameters considered were number of seizures before surgery, age at the surgery, cell loss count in CA1, CA2, CA3 and DG and the drug therapy followed (LEV-combination, non LEV-combination and monotherapy) (**Tab. 11**). Samples' RNA isolation, cDNA synthesis and RNA-seq were performed in the lab of Dr. Per Hoffman (Life and Brain, Bonn, Germany).

Tab. 10: Clinical parameters distribution of 114 TLE-affected patients. Parameters as gender, post-operative outcome and drug therapy are presented in percentuage values. Age at seizure onset in years, age at epilepsy surgery in years, seizure frequency per month are presented in mean ± SEM values. The post-operative outcome is classified according Engel classification (class I A: completely seizure free; class IV B. no seizure reduction) (Engel J., 1993).

Parameters	Lesion-associated	n	HS	n
Number of patients	35		79	
Gender (male vs. female)	62.9 % vs. 37.1 %	35	48.1 % vs. 51.9 %	79

Age of seizure onset (years)	12.5 ± 1.6	29	12.7 ± 1.6	70
Seizure Frequency per month	27.8 ± 8.1	34	8.1 ± 1.0	79
Drug therapy (sodium-channel blocker monotherapy vs. LEV combinations vs. non LEV-combinations	17.1 % vs. 34.3 % vs. 48.6 %	35	20.3 % vs. 36.7 % vs. 43.0 %	79
Age at epilepsy surgery (years)	22.8 ± 2.7	35	35.0 ± 1.7	79
Post-operative outcome (Engel I A vs. Engel IV B)	55.9 % vs. 44.1 %	34	61.8 % vs. 38.2 %	76

Tab. 11: Clinical parameters distribution of 55 HS-associated TLE-affected patients. Parameters as gender, age duration of epilepsy until surgery, seizures per month, drug therapy, cell loss in CA1,CA2,CA3 and DG are presented in percentuage values. Age at epilepsy surgery in years.

Parameters	Values
Number of patients	55
Gender (male vs female)	58 % vs 42 %
Age duration of epilepsy until surgery (≤ 10 vs. 11-20 vs. > 20 years)	43 % vs. 30 % vs. 27 %
Age at epilepsy surgery (years)	36.96
Seizures per month (≤ 5 vs.6-15 vs. >15)	47 % vs.33 % vs.20 %
Drug therapy (sodium-channel blocker monotherapy vs. LEV combinations vs. non LEV-combinations)	14.54 % vs. 30.90 % vs.54.56 %
Cell loss CA1 (≤ 50 % vs. > 50 %)	15 % vs. 85 %
Cell loss CA2 (≤ 50 % vs. > 50 %)	63 % vs. 37 %
Cell loss CA3 (≤ 50% vs. > 50 %)	32.72 % vs.67.28 %
Cell loss CA4 (≤ 50 % vs. > 50 %)	18.18 % vs. 81.82 %
Cell loss DG (≤ 50 % vs. > 50 %)	80 % vs. 20 %

2.22 Statistical analyses

Statistical analyses were performed using GraphPad Prism 6.05 software. Tests used to calculate the statistical significance are mentioned in the corresponding figures. Average values in figures and tables are expressed as mean ± standard error of the mean (SEM).

3. Results

3.1. Identification of Zn^{2+}-sensitive Mtf1 transcriptional unit *in vitro*

To characterize Zn^{2+}-inducible Mtf1-positive cells, we first developed a transcriptional reporter unit that can label cells sensitive for Mtf1 in a Zn^{2+}-dependent manner. The project was already initiated, prior to my contribution to the project, by the identification of five different transcriptional units consisting of a minimal promoter, a TATA box and several potential binding sites for Mtf1 (metal-responsive elements; MREs). The potential binding sites were selected based on putative Mtf1 binding and named MRE-d/c, MRE-3/4, MRE-S*4, MRE-Cav and MRE-MTI. MRE-d/c, MR-3/4 and MRE-S*4 were selected based on proven Mtf1 binding *in vitro* (Remondelli et al., 1997; LaRochelle et al., 2008; Stuart et al., 1985). MRE-d/c corresponds to the mouse MTI promoter sequence spanning from nucleotides -150 to -123 and harbors two copies of MREs, respectively MREd and MREc (Durnam and Palmiter, 1981). MRE-3/4 corresponds to the human MTII promoter sequence spanning from nucleotide -149 to -112 and contains two copies of MREs, MRE3 and MRE4 (Karin et al., 1987). MRE*S 4 consists in 4 identical copies of high affinity MRE sequence of the mouse Mtf1 (Remondelli et al., 1997). MRE-Cav was selected for its proven Zn^{2+}-induced Mtf1 binding to the *Cacna1h* promoter (encoding the $Ca_V3.2$ protein) in an animal model for TLE and contains 4 copies of the identified MRE (van Loo et al., 2015). MRE-MTI was based on the endogenous MTI mouse promoter region, harboring five binding sites for Mtf1 (Radtke et al., 1993).

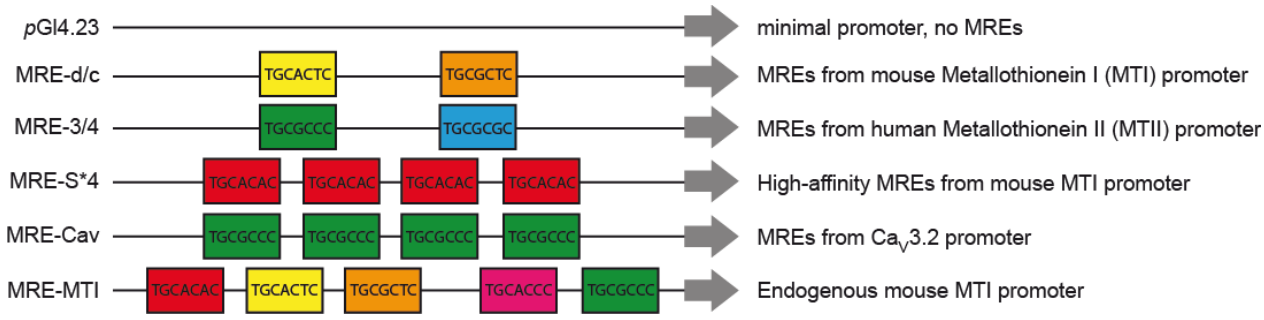

Fig. 4: Schematic overview of the transcriptional units. Five potential MREs are indicated by colored boxes, with each color representing a different MRE consensus sequence. The *p*Gl4.23 transcriptional unit only harbors a minimal promoter without any MREs

The five transcriptional units were tested for their Zn^{2+}-inducible transcriptional activity by performing luciferase assay in neuronal NG108-15 cells. Under basal conditions, a strong luciferase activity was observed for MRE-S*4 and to a lesser degree for MRE-MTI. Almost no activity was observed for the MRE-d/c, MRE-3/4 and MRE-Cav transcriptional units (**Fig 5**, left panel). Subsequent overexpression of the cells with Mtf1, combined with an incubation of the cells in Zn^{2+} solution (200 µM for 4 h; van Loo et al., 2015), resulted in a significant increase in activity for MRE-d/c, MRE-3/4, MRE-Cav and MRE-MTI, whereas MRE-S*4 did not show a further increase in transcriptional activity when compared to basal conditions. No increase in transcriptional activity was obtained when the cells were only incubated in Zn^{2+} solution (**Fig 5**, right panel). This initial experiment narrowed the choice for the best transcriptional reporter unit to MRE-d/c, MRE-3/4, MRE-Cav and MRE-MTI.

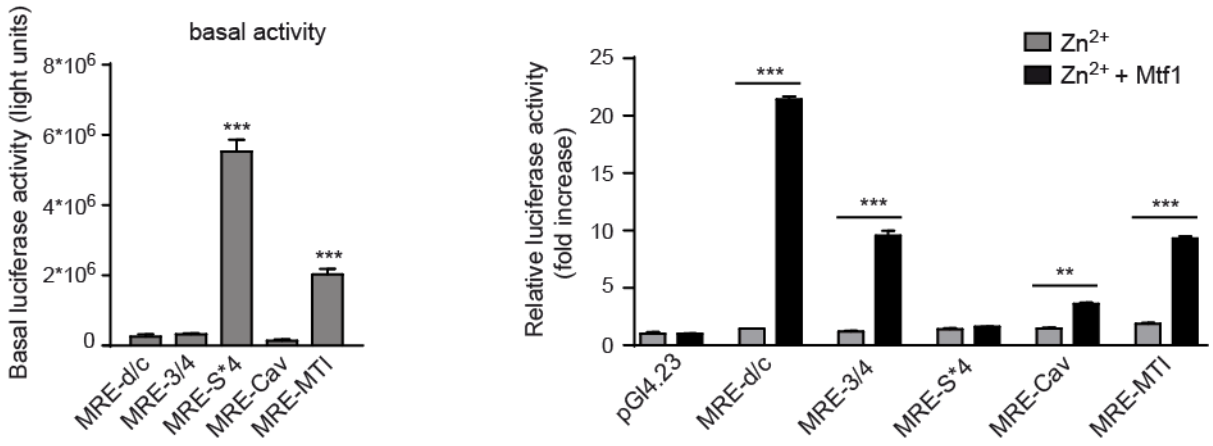

Fig. 5: Increases in Zn^{2+}/Mtf1 activates several MRE-containing transcriptional units in NG108-15 cells. Under normal conditions, a strong basal luciferase activity is observed for MRE-S*4 and MRE-MTI transcriptional units. After Zn^{2+}/Mtf1 treatment, a significant increase in luciferase activity was observed for MRE-d/c, MRE-3/4, MRE-Cav and MRE-MTI transcriptional units (*t-test:* ** $P \leq 0.01$, *** $P \leq 0.001$; N = 3*)*.

3.1.1 MRE-d/c and MRE-MTI transcriptional units respond to Zn^{2+}/Mtf1 challenge in hippocampal neurons

To identify the best Zn^{2+}/Mtf1-responsive transcriptional unit, the four potentially Zn^{2+}/Mtf1-sensitive transcriptional units (MRE-d/c, MRE-3/4, MRE-Cav and MRE-MTI) were tested in primary hippocampal neurons. To that end, primary hippocampal neurons were transduced at days *in vitro* (DIV) 7 with AAVs harboring luciferase under control of the transcriptional units. Application of Zn^{2+}/Mtf1 resulted in a significant increase in luciferase activity only for the MRE-d/c and MRE-MTI transcriptional units (**Fig. 6 A,D**). Since the MRE-MTI transcriptional unit had a 10-fold stronger activation upon Zn^{2+}/Mtf1-stimulation (MRE-MTI: 23.4-fold; $p < 0.0001$) compared to the activation observed for MRE-d/c (2.5-fold; $p = 0.0441$), we decided to focus on the MRE-MTI transcriptional unit in our subsequent experiments.

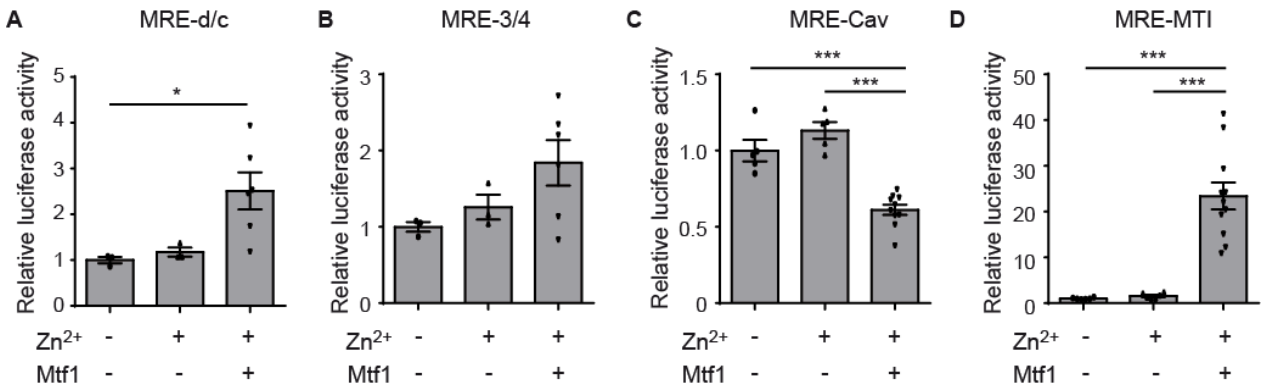

Fig. 6: MRE-d/c and MRE-MTI transcriptional units respond to Zn^{2+}/Mtf1 challenge in hippocampal neurons**.** Luciferase activity of the MRE-d/c (**A**), MRE-3/4 (**B**), MRE-Cav (**C**) and MRE-MTI (**D**) transcriptional units, normalized against the luciferase activity of the *p*Gl4.23 transcriptional unit. Mouse hippocampal neurons were transduced at DIV7 with the transcriptional units, with and without Mtf1. At DIV14, cells were Zn^{2+}-challenged (1 µM, 1 h) and luciferase activity was measured 4 h after Zn^{2+}-challenge. A significant increase after Zn^{2+}/Mtf1-challenge was observed for MRE-d/c (One-way ANOVA, Tukey's multiple comparisons test, * $P \leq 0.05$, $N = 3$, $n \geq 3$) and MRE-MTI (One-way ANOVA, Tukey's multiple comparisons test, *** $P \leq 0.001$; $N = 3$, $n \geq 3$).

3.1.2 The mouse metallothionein I promoter functions as a Zn^{2+}-sensitive Mtf1 reporter unit in hippocampal neurons

To prove unequivocally that the MTI transcriptional unit can be activated by Mtf1 in a Zn^{2+}-sensitive manner, primary hippocampal neurons were transduced (DIV 1) with rAAVs harboring the Venus protein under control of the MRE-MTI transcriptional unit, followed by transduction (DIV 7) with rAAVs harboring an overexpression construct for Mtf1 (rAAV-hSyn-Mtf1-2A-SBFP2). As expected based on the presence of physiological Zn^{2+} within the neurons, one day before Zn^{2+} application (DIV 13), a slight increase in fluorescence intensity was observed for the neurons incubated with Mtf1 (**Fig. 7A**, middle and lower panels). Subsequent incubation of the cells in Zn^{2+} solution (DIV 14; 1 µM Zn^{2+}, 1 h) resulted in a robust increase in fluorescence intensity measured at 2 and 7.5 h after Zn^{2+} application, which returned back to starting levels at 15 h after Zn^{2+} application (**Fig. 7A,B**). Altogether, these findings thus confirm that MRE-MTI represents a transcriptional unit usable for labeling Zn^{2+}/Mtf1-activated cells *in vitro*.

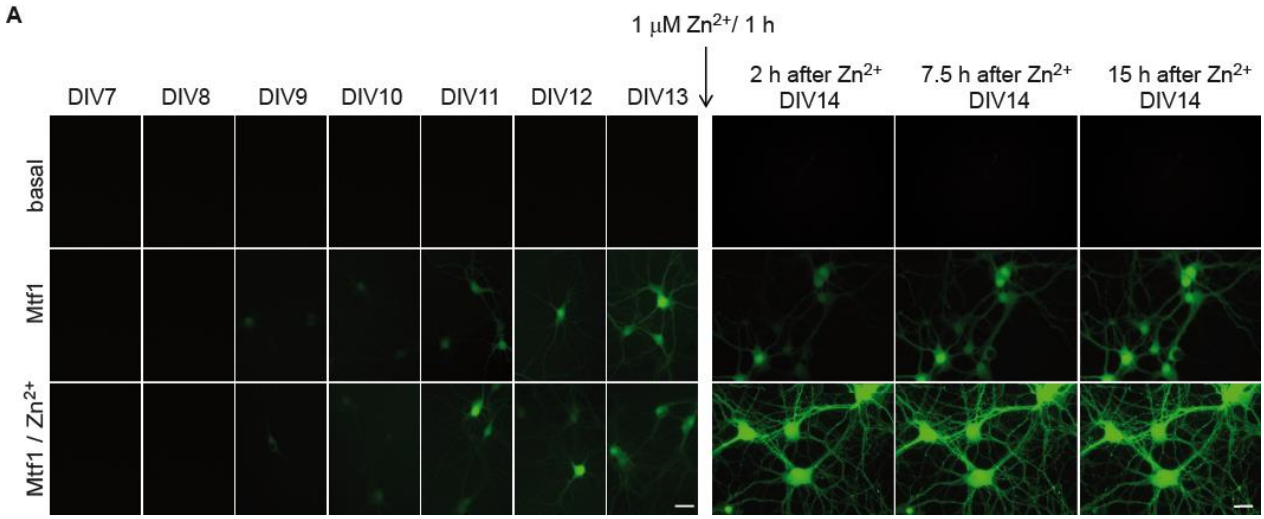

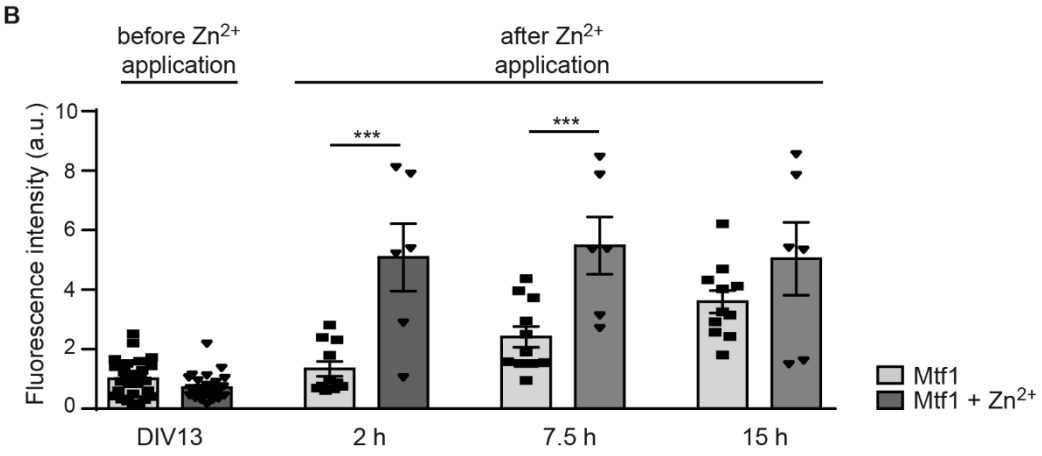

Fig. 7: The mouse metallothionein I promoter functions as a Zn^{2+}-sensitive Mtf1 reporter unit in hippocampal neurons. (**A**) Fluorescence intensity of mouse primary hippocampal neurons transduced with rAAV-MTI-Venus (DIV 1), rAAV-hSyn-Mtf1-2A-SBFP2 (DIV 7) and stimulated with Zn^{2+} solution (DIV 14; 1 µM Zn^{2+} for 1 h). Fluorescence intensity was measured daily from DIV 7 until DIV 13. After Zn^{2+} incubation, fluorescence intensity was measured 2, 7.5 and 15 h after washing out the Zn^{2+} solution. Under basal conditions (rAAV-MTI-Venus), no fluorescence signal was detected longitudinally. After co-transduction with rAAV-hSyn-Mtf1-2A-SBFP2 (Mtf1 panel), fluorescence starts around DIV 9. Subsequent Zn^{2+} incubation (Mtf1/Zn^{2+} panel) results in a strong fluorescence intensity already 2 h after incubation. Scale bars, 25 µm. (**B**) Quantification of the fluorescence intensity shown in A. Data were normalized against the fluorescence intensity before Zn^{2+}-application (DIV 13). (One-way ANOVA, *Tukey's multiple comparisons test*, *** $P \leq 0.001$; N = 3, n ≥ 3).

3.2 Characterization of the MTI-transcriptional unit in the pilocarpine-induced-SE animal model of TLE

3.2.1 The MTI-transcriptional unit as a tool to genetically label Mtf1 expressing neurons in the pilocarpine-SE animal model of TLE

To probe whether the MTI transcriptional unit also reflects the Zn^{2+}/Mtf1-activity *in vivo*, rAAVs harboring the *Lac*Z reporter gene under control of the MTI transcriptional unit (rAAV-MTI-*Lac*Z) were injected into CA1 PCs of adult mice. A strong increase in *Lac*Z staining was observed after co-transduction with Mtf1 viral particles (**Fig. 8 A,C**). In addition, a strong *Lac*Z accumulation was observed three days after pilocarpine-induced SE for the MTI transcriptional unit (**Fig. 8B**; upper panel, **Fig. 8C**), as well as for the Cav3.2 core promoter (**Fig. 8B**; lower panel, **Fig. 8D**), paralleling the "Zn^{2+}-Mtf1-Cav3.2"

cascade of epileptogenesis (van Loo et al., 2015). These findings indicate that the MTI-transcriptional unit works also *in vivo*, in a Zn^{2+}/Mtf1-dependent manner and that it can be used to characterize the Zn^{2+}/Mtf1 pathway in the process of epileptogenesis *in vivo*.

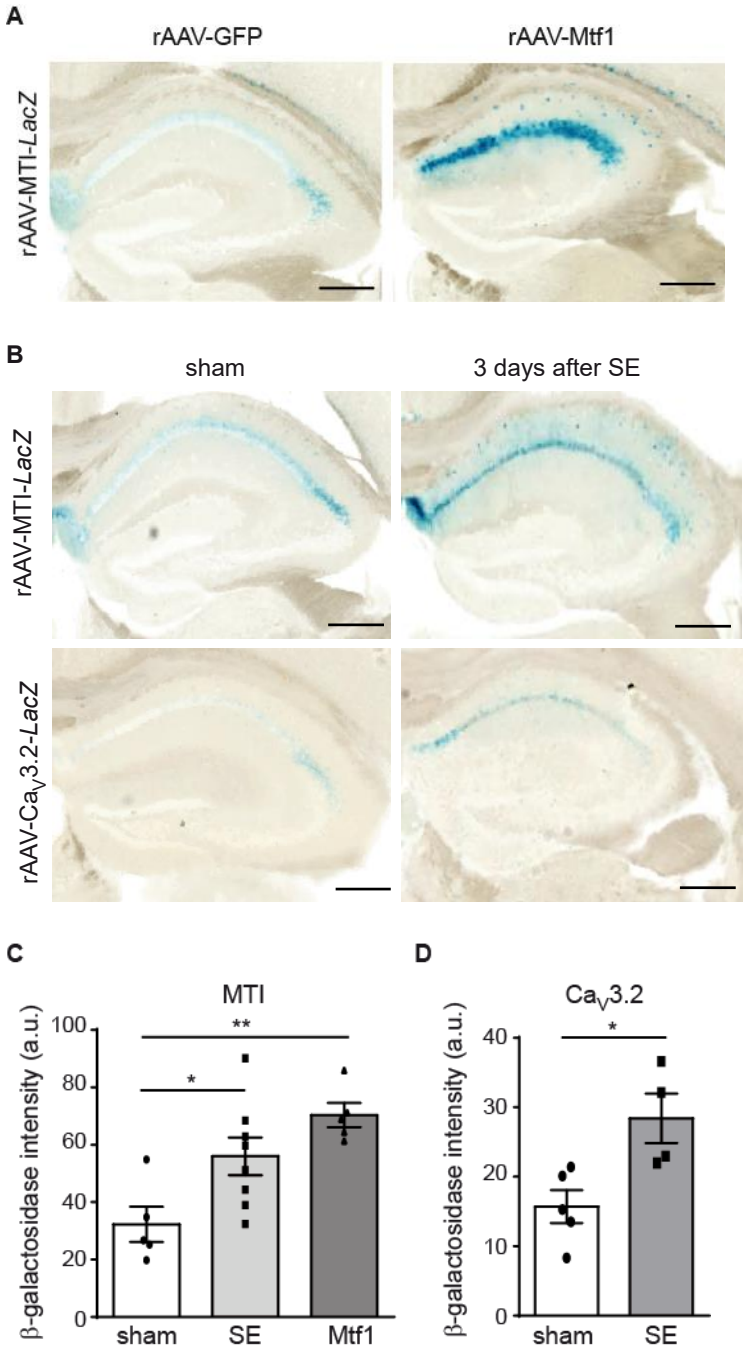

Fig. 8: The MTI-transcriptional unit as a tool to genetically label Mtf1-expressing neurons in an animal model for TLE. (**A**) *Lac*Z staining of the MTI transcriptional unit in the hippocampal region under basal conditions (rAAV-GFP) and two weeks after rAAV-hSyn-Mtf1-2A-SBFP2 (rAAV-Mtf1) transduction. A strong accumulation of *Lac*Z staining was observed in hippocampal CA1 after rAAV-Mtf1 transduction, indicating that the MTI

transcriptional unit is sensitive for Mtf1 *in vivo.* Scale bars, 200 µm. (**B**) *LacZ* staining of the MTI transcriptional unit (upper panels) and *Ca_V3.2* core promoter (lower panels) in sham and pilocarpine-SE mice, three days after pilocarpine-induced SE. Scale bars, 200 µm. (**C**) Quantification of rAAV-MTI-*LacZ* expression of sham-, pilocarpine-induced SE- and Mtf1 treated mice. (One-way ANOVA*, Tukey's multiple comparisons test, *P ≤ 0.05, **P ≤ 0.01,* N = *5 sham, 8 SE, 5 Mtf1). (***D***)* Quantification of *LacZ* expression under the Ca_V3.2 core promoter of sham- and pilocarpine-induced SE-injected animals (*t-test: *P* ≤ 0.05, N = 5 sham, 4 SE*)*

3.2.2 The MTI transcriptional unit is activated early after pilocarpine-induced SE

To unravel the activation of the MTI transcriptional unit at different time points after pilocarpine-induced SE, we next performed *in vivo* imaging using rAAVs harboring the iRFP under control of the MTI transcriptional unit which were injected in the CA1 hippocampal region of adult mice. Enhancement of MTI transcriptional activity was observed after transduction with Mtf1 (**Fig. 9A,B**) and early after pilocarpine-induced SE. The iRFP signal increased significantly already 2 days after pilocarpine-induced SE (1.7 fold, $P \leq 0.001$), slightly decreased but remained significant after 10 days (1.6 fold, $P \leq 0.05$), and returned back to starting levels 28 days after SE in comparison with the sham littermates (**Fig. 9C,D**). These results were congruent with the monitoring of Ca_V3.2 promoter activity after SE showed by Kulbida et al. (2015) and confirmed the activation of the "Zn^{2+}-Mtf1-Ca_V3.2" cascade during the process of epileptogenesis.

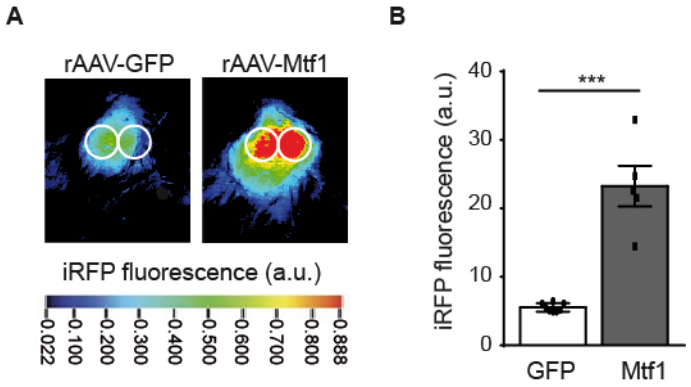

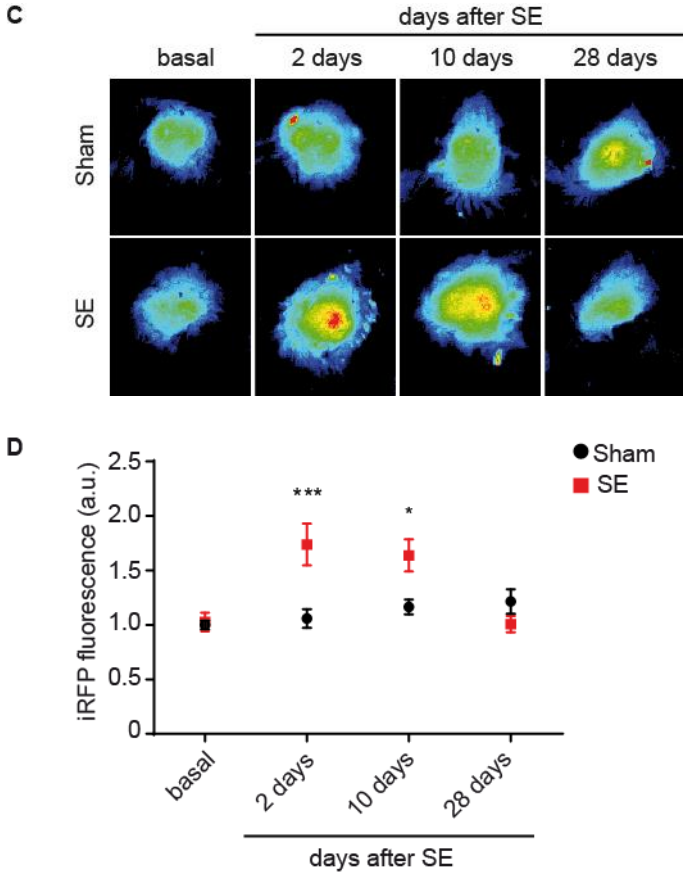

Fig. 9: The MTI transcriptional unit is activated early after pilocarpine-induced SE**.** (**A**) Near-infrared *in vivo* imaging. Representative pseudo color visualization of *in vivo* iRFP signal of a recorded rAAV-MTI-iRFP mouse with exposed skull under basal conditions (rAAV-GFP; left panel) and 14 days after rAAV-Mtf1-2A-SBFP2 transduction (rAAV-Mtf1; right panel). Regions of interest (ROIs) were defined above the hippocampal region and the surface radiance was defined in arbitrary units (a.u.). The color bar indicates the total fluorescence efficiency. (**B***)* Quantification of A *(t-test: *** P* ≤ 0.001, N = 8 GFP, 5 Mtf1*)* (**C**) Representative examples of a recorded rAAV-MTI-iRFP mouse under basal conditions and after pilocarpine-induced SE longitudinally. (**D**) Quantification of iRFP signals of sham- and pilocarpine-induced SE-injected animals (Two-way ANOVA, *Sidak´s multiple comparisons test*, ** P* ≤ 0.05*, *** P* ≤ 0.001, N = 8 sham, 6 SE).

3.2.3 The MTI transcriptional unit co-localizes with $Ca_v3.2$ expression

We then investigated whether Mtf1 and $Ca_v3.2$ are expressed within the same neuronal populations. To this end, we injected a combination of rAAV-$Ca_v3.2$-Venus and rAAV-MTI-mRuby3 particles into the hippocampal CA1 region of mice. After overexpressing Mtf1 viral particles, an increase of Venus and mRuby3 fluorescence intensity as well as a strong overlap of the Venus- and mRuby3 positive cells was observed (**Fig. 10A**). To

analyse whether the obtained results could be reproduced during early epileptogenesis, two weeks after rAAV injections, animals were either subjected to pilocarpine-SE or sham-treatment and sacrificed 3 days thereafter, which is the time point of highest $Ca_V3.2$ mRNA level after SE (Becker et al., 2008). Interestingly, 3 days after SE, an increase of rAAV-$Ca_V3.2$-Venus and rAAV-MTI-mRuby intensity and of overlapping Venus- and mRuby3- positive cells occurred in pilocarpine-SE animals in comparison with their sham-treated littermates (**Fig. 10B**). We next wondered whether the MTI transcriptional unit and the $Ca_V3.2$ promoter would be activated already 1 day after SE, leading to a rise in Venus and mRuby3 fluorescence intensity and indicating that the "Zn^{2+}-Mtf1-$Ca_V3.2$" cascade of epileptogenesis is activated directly after a single episode of SE or brain trauma. To this end, injected animals were sacrificed 1 day after pilocarpine-induced SE or sham-treatment. Interestingly, already 1 day after SE, a rise in mRuby3 and Venus signal and overlapping of double positive cells in pilocarpine-SE-treated animals compared to sham-treated mice was observed (**Fig. 10C**). These results indicate that already one day after pilocarpine-induced SE the rise in [Zn^{2+}] is able to activate Mtf1, which then binds to both the MTI transcriptional unit and the Cav3.2 core promoter (van Loo et al., 2015).

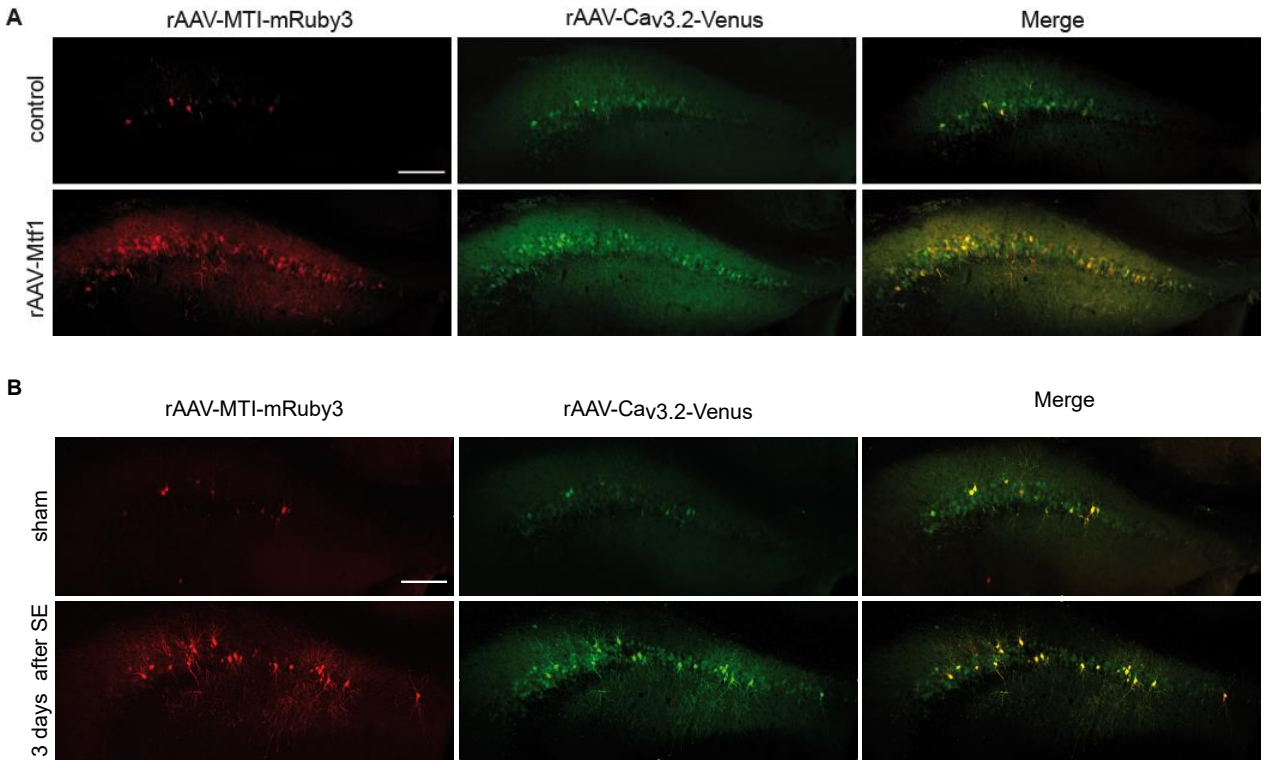

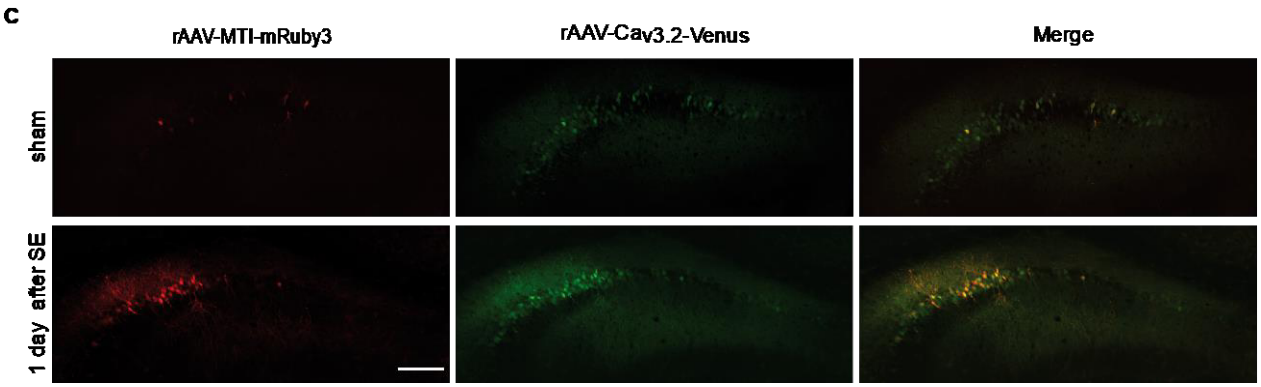

Fig. 10: The MTI-transcriptional unit co-localizes with $Ca_V3.2$ expression. (**A**) Representative image of rAAV-MTI-mRuby3 and rAAV-$Ca_V3.2$-Venus injected animals under basal conditions (control; upper panel) and 14 days after rAAV-Mtf1-2A-SBFP2 transduction (rAAV-Mtf1; lower panel). Scale bar, 200 µm. (**B**) and (**C**) Representative images of rAAV-MTI-mRuby3 and rAAV-$Ca_V3.2$-Venus injected animals 3 days (**B**) and 1 day (**C**) after induced-SE. Scale bars, 200 µm.

3.3 FACS analysis confirms increased Mtf1-expression in a subpopulation of hippocampal neurons after Pilocarpine-induced SE

Whole genome next-generation RNA-seq of CA1 PCs pronounced transcriptional heterogeneity between single CA1 PCs, indicating the existence of defined neuronal populations and shedding a light on the existence of specific neuronal networks (Cembrowski et al., 2016; Földy et al., 2016). In order to determine the transcriptome of Zn^{2+}/Mtf1-positive neurons, we aimed to perform RNA-seq of Mtf1-positive and Mtf1-negative neuronal populations isolated by FACS. For this, hippocampal CA1 regions of adult mice were virally transduced with rAAV-MTI-Venus and rAAV-hSyn-tdTomato and sham-or pilocarpine-SE treated two weeks after injection. Cells activated by the Zn^{2+}/Mtf1-cascade were then labelled in yellow, whereas cells that were negative for the Zn^{2+}/Mtf1-cascade were labelled in red. Animals were sacrificed 3 days after SE, when Zn^{2+} levels were strongly increased in hippocampal CA1 and with a prior accumulation of Mtf1 mRNA levels. Mtf1-positive and Mtf1-negative neuronal populations were separated by FACS (**Fig. 11A**) and more Mtf1-positive cells were observed after pilocarpine-SE treatment (t-test, $^{**}P \leq 0.01$) (**Fig. 11B**). However, the RNA obtained from the different cell populations, especially from the pilocarpine-treated groups, did not satisfy the quality control requirement of a RIN^e value > 7 indicating that the RNA

integrity needed for successful sequencing was not reached. Although different strategies were tried, we unfortunately did not succeed with this experiment and we decided to adopt another approach in order to identify of the molecular profiles of Mtf1-expressing cells (see paragraph 3.4).

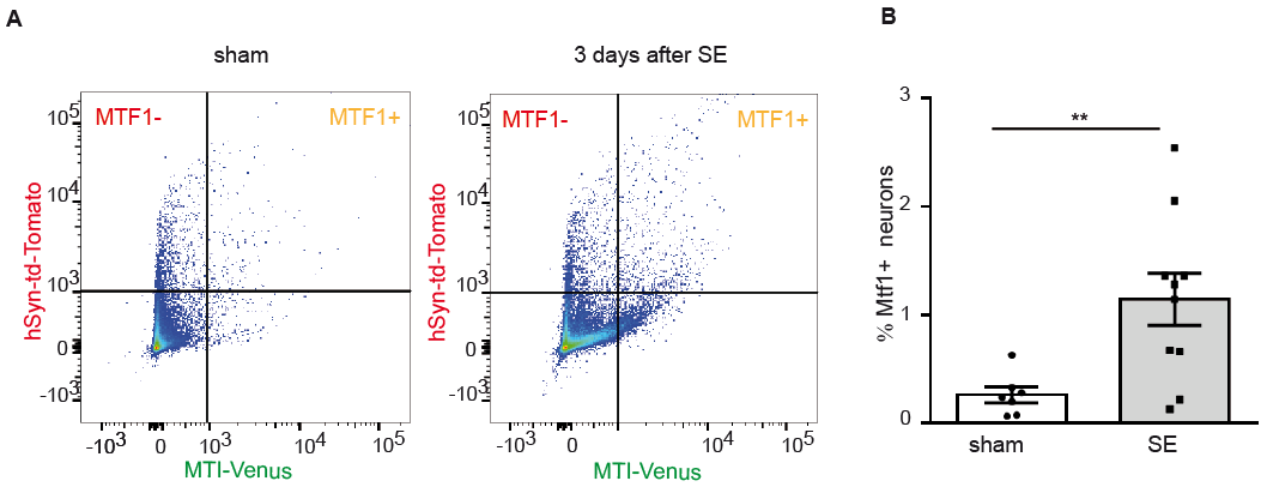

Fig. 11: FACS-sorted Mtf1-positive and Mtf1-negative hippocampal neurons. (**A**) FACS-sorted Mtf1-positive (rAAV-MTI-Venus and rAAV-hSyn-tdTOMATO fluorescence) and Mtf1-negative (only rAAV-hSyn-tdTOMATO fluorescence) neuronal populations of control (left panel) and three days after pilocarpine-induced SE (right panel) mouse hippocampi. (**B**) Quantification of Mtf1-positive neuronal populations in control and three days after SE (t-test, ** $P \leq 0.01$, N = 7 sham, 10 SE).

3.4 Mtf1 regulates the transcription of a broader set of plasticity-related genes

3.4.1 Identification of plasticity-related genes transcriptionally regulated by Mtf1 *in vitro*

Given the lack of success with the FACS sorting experiment to identify the molecular behaviour of Mtf1-positive cells, and the still open question to better understand the role of Mtf1 in converting regular neurons in intrinsic firing bursters, we next pursued a bioinformatics approach in order to identify additional genes whose transcriptional expression is regulated by Mtf1 in a Zn^{2+}-dependent manner.

For this, genes with Mtf1 binding sequences within their promoter region were selected and their transcription levels after Zn^{2+}/Mtf1-challenge were measured by performing Taqman assays in primary hippocampal neurons. First, we bioinformatically identified genes with an Mtf1 binding site located within their promoter region (**Fig. 12A**) using the single search Analysis server (https://ccg.epfl.ch/cgi-bin/ssa/findm_form_parser.cgi) and the Jaspar database (Sandelin et al., 2004). Genes within the range of a binding affinity between 98.0 % and 99.5 % were selected, and resulted in 2208 genes with potential Mtf1 binding sites (**Fig. 12A, B**). Next, we checked whether those genes were associated with the GO term Synapse using the Synapse GO annotation website (http://www.informatics.jax.org/vocab/gene_ontology/GO:0007268). Of the 2208 genes, 100 were annotated within the Synapse GO database, and from these, 18 genes were selected for subsequent *in-vitro* experiments according to their known relevance in synaptic plasticity. (**Fig. 12C**).

To test whether the selected genes were regulated in a Zn^{2+}/Mtf1-manner, primary hippocampal neurons were transduced (DIV 7) with a control rAAV (rAAV-hSyn-GFP) or an overexpression construct for Mtf1 (rAAV-hSyn-Mtf1-IRES-Venus). Subsequent incubation of neurons in Zn^{2+} solution (DIV 14, 1 μM, 1 h) led to an increased gene expression for *Kalrn, Cplx2, Creb1, Rims3, Gria1, Gabra4, Kcnh1 and Unc13a* in the Zn^{2+}/Mtf1-challenged samples compared to transduction with control rAAVs (**Fig. 12D**; left panel, genes with higher binding affinity; right panel, genes with lower binding affinity). To prove unequivocally that the transcriptional expression of the above identified genes is Mtf1-dependent, primary hippocampal neurons were transduced (DIV 7) with GFP (rAAV-hSyn-GFP), Mtf1 (rAAV-hSyn-Mtf1-IRES-Venus) and dnMtf1 (rAAV-hSyn-dnMtf1-IRES-Venus). Incubation of neurons in Zn^{2+} solution (DIV 14, 1 μM, 1 h) resulted in a Mtf1-dependent enhanced gene expression for *Creb1*, *Rims3*, *Gabra4*, *Gabrd* and *Unc13a*, whereas no augmentation for those genes was observed when treating neurons overexpressing the dominant negative variant of Mtf1 with Zn^{2+} solution (**Fig. 12E**).

A

Cut-off	# of genes
99.5	3
99.3	15
99.0	43
98.0	2208

B

C

Candidate gene	Name	MRE consensus sequence
1) Kalrn	Kalirin RhoGEF Kinase	TC**TGCACACG**GCGT / CC**GT****CACACG**ACTG
2) Cplx2	Complexin-2	TG**AGCACACG**GCAC
3) Cacna1b	Calcium voltage-gated channel Subunit α 1 B	TG**TGCTCACG**GTGC
4) Creb1	cAMP responsive element binding protein 1	TG**CGCACTCG**GCAC
5) Git1	GIT ArfGAP 1	GG**TGCACACA**ACAC
6) Ntrk2	Neurotrophic tyrosine kinase receptor, type 2	TG**CGCACTCG**GCAC
7) Rims3	Regulating synaptic membrane exocytosis 3	TT**TGCACCCG**GCGG
8) Gria1	Glutamate ionotropic receptor, AMPA Type Subunit 1	TG**TGCACACA**TCTC
9) Gabra4	GABA A receptor, subunit α 4	TG**TGCGCACG**CCGC / CC**G****GCGCACG**TGTG
10) Gabrb3	GABA A receptor, subunit β 3	TT**TGCAGACA**GTTC
11) Gabrd	GABA A receptor, subunit δ	TT**TGCAGACA**GCAA
12) Grin2b	Glutamate ionotropic receptor, NMDA Type Subunit 2B	GT**TGCACTCT**GCAC
13) Kcnh1	Potassium voltage-gated channel, subfamily H member 1	AC**G****ACAAACG**TCTC
14) Kctd13	Potassium channel tetramerisation domain containing 13	TT**TGCACCCG**CCTT
15) Lrrtm2	Leucine rich repeat transmembrane neuronal 2	C**TA****TCACACG**TTTA
16) Nrxn3	Neurexin III	TT**TGCACACT**TCTT
17) Ptprs	Protein tyrosine phosphatase, receptor type, S	CC**G****GCGCGCG**TGTG
18) Unc13a	Unc-13 homolog A	GC**TGCACCCG**CCGC

D

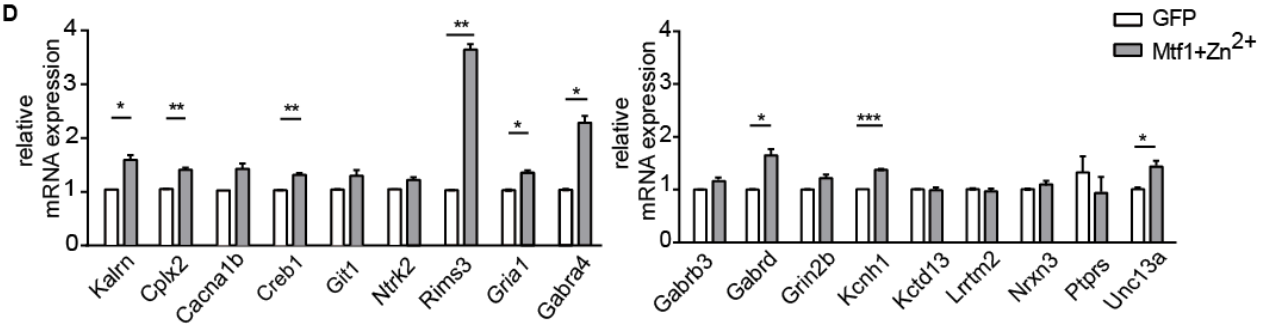

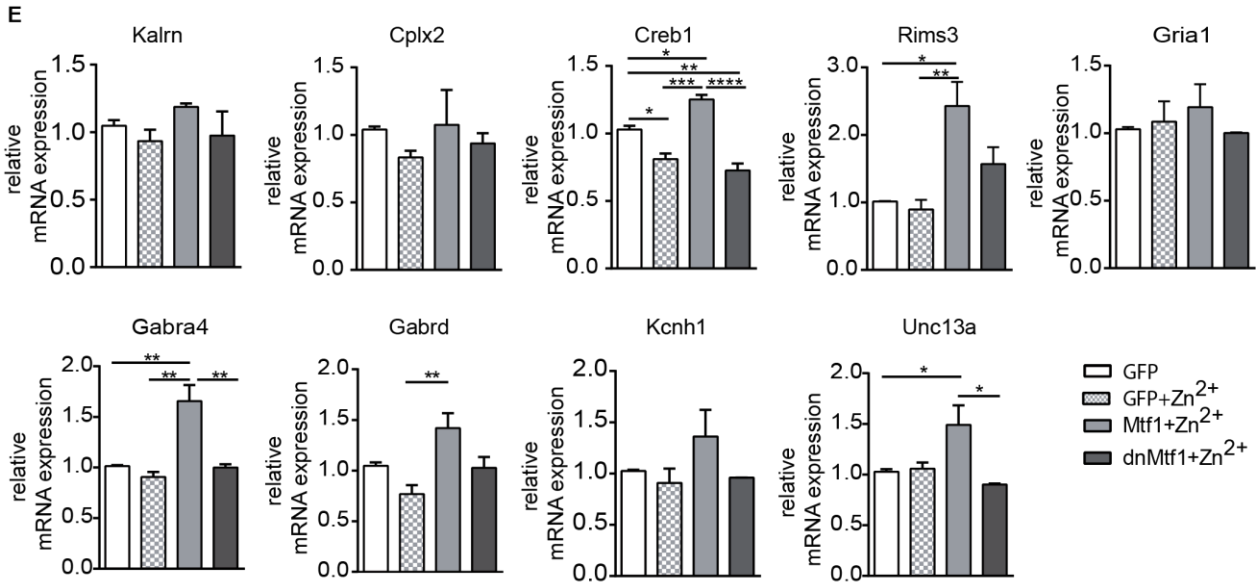

Fig. 12: Identification of plasticity-related genes transcriptionally regulated by Mtf1 *in vitro.* (**A**) Table showing the number of genes with Mtf1 binding sites, separated per different cut-offs, from the highest (cut-off 99.5) to the lowest (cut-off 98.0) binding affinity values. (**B**) Mtf1 consensus binding sequence obtained from Jaspar database. (**C**) List of the selected Mtf1-candidate genes with higher (1-9) and lower (10-18) Mtf1 binding affinities and their respective MREs. Core consensus sequence are given in bold whereas nucleotides that do not match the binding sequence are given in red (**D**) Quantitative RT-PCR for Mtf1 candidate target genes in hippocampal neurons stimulated with Mtf1 and Zn^{2+}. mRNA expression levels were measured 4 h after Zn^{2+} incubation, with synaptophysin as reference gene (t-test, * $P \leq 0.05$, ** $P \leq 0.01$, *** $P \leq 0.001$; N ≥ 3) (**E**) mRNA expression for *Kalrn, Cplx2, Creb1, Rims3, Gria1, Gabra4, Gabrd, Kcnh1* and *Unc13a* in hippocampal neurons stimulated with Mtf1+Zn^{2+} or dnMtf1+Zn^{2+}. mRNA levels were measured 4 h after Zn^{2+} incubation, with synaptophysin as reference gene (One-way ANOVA*, Tukey's multiple comparisons test, * P ≤ 0.05,* ** $P \leq 0.01$, N = 3).

3.4.2 CREB1 and MTF1 expressions positively correlate in 2 human TLE cohorts

To evaluate whether the correlation between Mtf1 and the *in vitro* identified synaptic-related Mtf1-target genes more broadly represents a phenomenon also in human TLE, we next analyzed the hippocampal expression of MTF1 and the *in vitro* identified genes in 2 independent human epilepsy cohorts. In the first cohort, we measured the hippocampal transcript levels of MTF1, KALRN, RIMS3, CREB1, GRIA1, GABRA4 and UNC13A in pharmacoresistant TLE patients with HS versus patients with "lesion-associated" TLE. For some genes (KALRN, CREB1 and UNC13A) different Illumina

probes were analyzed. Interestingly, a strong positive correlation was observed for CREB1 and MTF1, specifically in the HS group, indicating that higher MTF1 levels lead to higher CREB1 expression levels in patients affected by HS (**Fig. 13**). This correlation was also confirmed in a second cohort consisting of 55 pharmacoresistant patients suffering from HS, where transcript levels of MTF1, KALRN, CPLX2 CREB1, GABRD, KCNH1 and UNC13A were measured (**Fig. 14**).

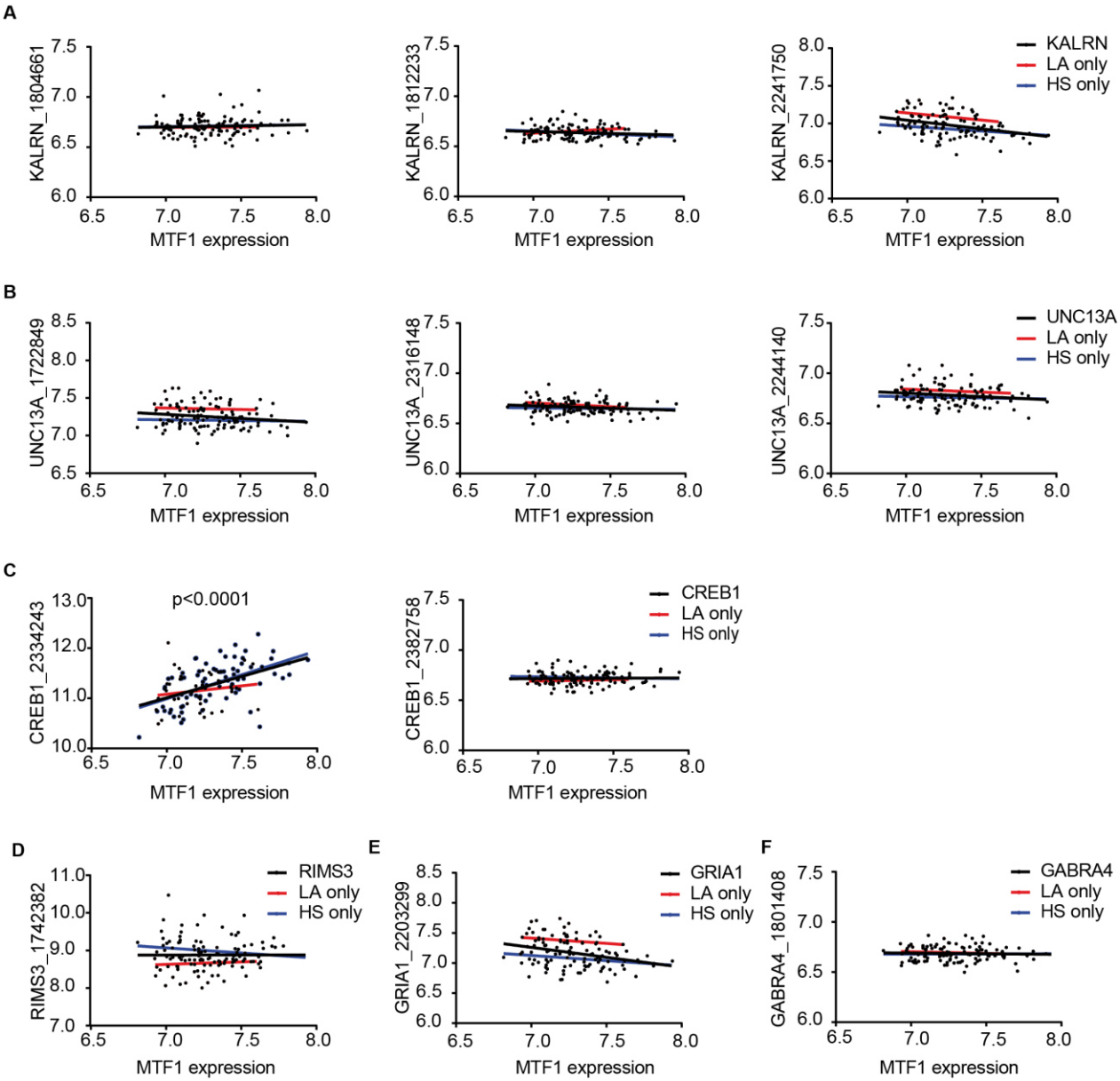

Fig. 13: CREB1 and MTF1 hippocampal expressions correlate in a human cohort of 114 patients affected by TLE. **(A-F)** Regression analyses of MTF1 mRNA versus KALRN mRNA (**A**), UNC13A mRNA (**B**), CREB1 mRNA (**C**), RIMS3 mRNA(**D**), GRIA1 mRNA

(**E**) and GABRA4 mRNA (**F**) in a human cohort composed of 114 patients affected by pharmacoresistant TLE; 79 patients with HS and 35 patients with lesion-associated TLE. Different probes were used for measuring KALRN, UNC13A and CREB1 transcripts. A positive correlation is observed for MTF1 and CREB1 transcript levels in TLE patients affected by HS (Linear regression, **** P ≤ 0.0001, N = 79 HS, 35 lesion-associated TLE).

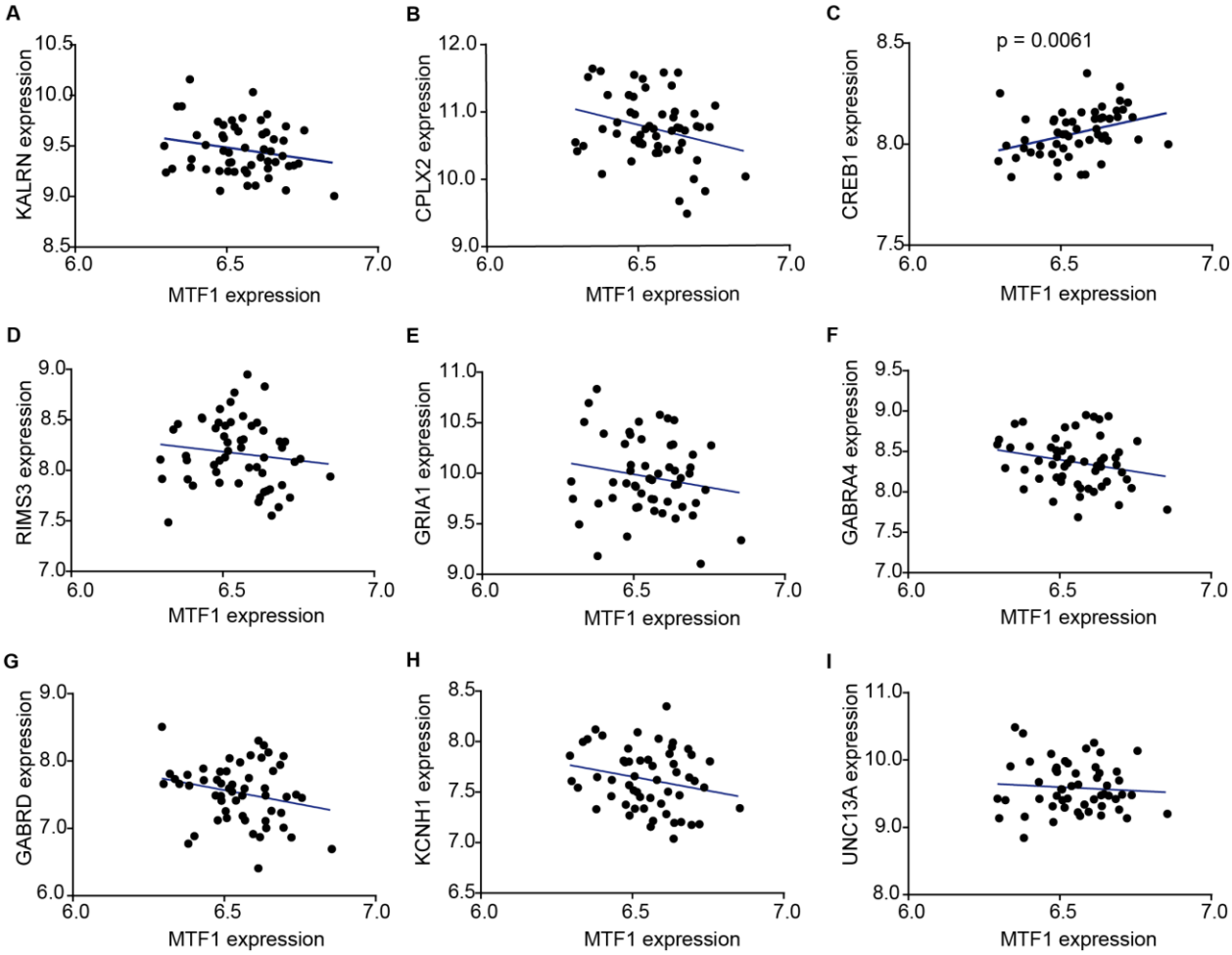

Fig. 14: CREB1 and MTF1 hippocampal expressions correlate in a second human epilepsy cohort. (**A-I**) Regression analyses of MTF1 transcript and KALRN (**A**), CPLX2 (**B**), CREB1 (**C**), RIMS3 (**D**), GRIA1 (**E**), GABRA4 (**F**), GABDRD (**G**), KCNH1 (**H**), UNC13A (**I**) transcript in 55 patients affected by TLE with HS. A positive correlation is observed only for MTF1 and CREB1 (Linear regression, ** P≤ 0.01, N = 55).

3.4.3 Correlation of CREB1 mRNA expression and hippocampal neuronal loss confirms the involvement of CREB1 in human TLE

As our previous results indicated CREB1 as a new potential target of the Zn^{2+}/MTF1 pathway in TLE pathogenesis, we decided to focus on this gene and its correlation with TLE. One of the clear pathological hallmarks of TLE is neuronal loss in the hippocampal region (Peixoto-Santos et al., 2015; Babb et al., 1984). We next investigated whether CREB1 gene expression correlates with hippocampal neuronal loss. Intriguingly, higher CREB1 transcript levels were observed in resected CA1, CA2, CA3 and CA4 hippocampal subregions affected by severe cellular loss (> 50 % of cell loss), compared to subregions less affected by neuronal loss (< 50 % of cell loss). In contrast, no differences in CREB1 levels were observed in resected DG subregions affected by higher or lower neuronal loss (**Fig. 15A**). Another remarkable finding was the significantly higher CREB1 expression in patients that were operated at a younger age (below 25 years) compared to patients that were operated at a later stage (**Fig. 15B**). Altogether these findings support the theory of CREB1 involvement in the development of TLE.

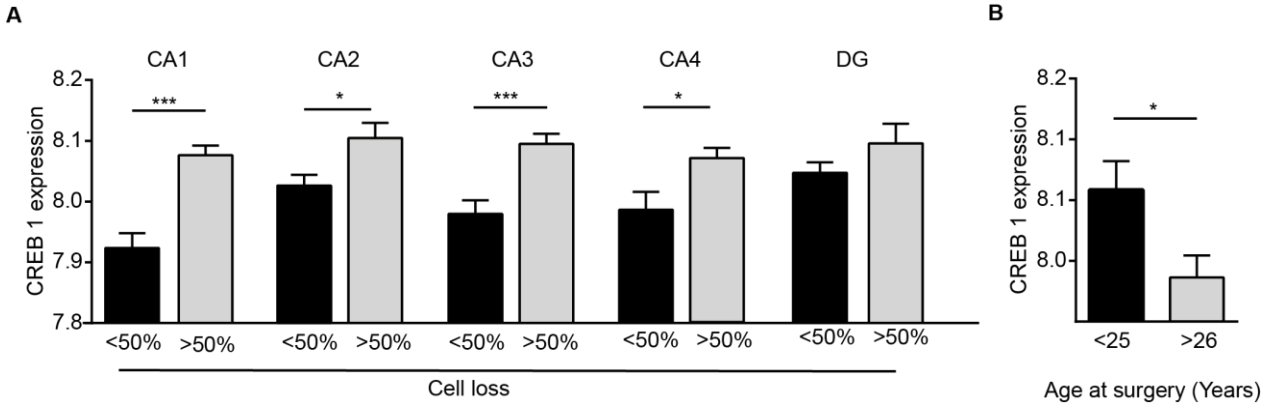

Fig. 15: Correlation between CREB1 mRNA expression and clinical parameters in a human TLE cohort**.** (**A**) CREB1 mRNA levels in CA1, CA2, CA3, CA4 and DG of 55 surgical biopsy specimens associated with lower (< 50 %) or higher (> 50 %) neuronal loss (t-test,* $P \leq 0.05$,*** $P \leq 0.001$; CA1, N = 8 cell loss < 50 %, 36 cell loss > 50 %; CA2, N = 35 cell loss < 50 %, 20 cell loss > 50 %; CA3, N = 18 cell loss < 50 %,37 cell loss > 50 %; CA4, N = 10 cell loss < 50 %,45 cell loss > 50 %; DG, N = 44 cell loss < 50 %,11 cell loss < 50 %).(**B**) CREB1 gene expression in patients who underwent surgery at an age ≤ 25 years vs. patients who had surgery at an age ≥ 26 years (t-test, * $P \leq 0.05$, N = 14 patients ≤ 25 years, 41 patients ≥ 26 years)

3.4.3 Creb1 mRNA increase correlates with Mtf1 mRNA augmentation in the pilocarpine-SE model

As Creb1 resulted to be regulated in a Zn^{2+}/Mtf1-dependent manner *in vitro* and was found to correlate with MTF1 expression in human TLE, we decided to focus on Creb1 in our subsequent experiments. We next investigated whether Creb1 would also be a potential target for the Mtf1-Zn^{2+} cascade in the pilocarpine-induced SE animal model. Previously, we have shown that Mtf1 mRNA is significantly increased early after pilocarpine-induced SE (6 and 12 h after pilocarpine-induced SE) in hippocampal CA1 (**Fig. 16A**, van Loo et al., 2015). If Mtf1 regulates Creb1 transcriptional expression, the mRNA expression of Creb1 should increase after pilocarpine-induced SE, and its changes should follow those of Mtf1 mRNA expression. We therefore analysed the time course of Mtf1 and Creb1 expression in the early phases of epileptogenesis after pilocarpine-induced SE. Mice were pilocarpine-SE or sham treated and were sacrificed 6, 12, 24, 36 and 72 h after SE-induction. Next, hippocampi were micro-dissected (CA1, CA3 and DG subregions) and Mtf1 and Creb1 mRNA expressions levels were measured. Besides the hippocampal CA1 increase 6 and 12 h after SE, we found Mtf1 mRNAs to be increased also in the CA3 subregion, at 6 ($p \leq 0.05$), 12 ($p \leq 0.0001$), 24 ($p \leq 0.001$) and 36 ($p \leq 0.0001$) h after SE (**Fig. 16C**) and in the DG, at 12, 24 and 36 ($p \leq 0.05$) h after SE (**Fig 16E**). Creb1 mRNAs were significantly augmented in hippocampal CA1 at 12, 24 ($p \leq 0.05$) and 72 ($p \leq 0.0001$) h after SE (**Fig. 16B**), in CA3 at 12 ($p \leq 0.0001$), 24 ($p \leq 0.001$), 36 ($p \leq 0.0001$) and 72 ($p \leq 0.05$) h after SE (**Fig. 16D**) and in DG at 36 ($p \leq 0.05$) h after SE (**Fig. 16F**). Interestingly, when comparing the changes of Creb1 mRNA levels to those of Mtf1 mRNA levels, the increase of Mtf1 preceded Creb1 augmentation clearly in CA1 (**Fig. 16A,B**) and CA3 (**Fig. 16C,D**), and for one time point also in the DG subregion (**Fig. 16E,F**). Altogether these data strengthen our hypothesis that Mtf1 could be responsible for the Creb1 augmentation observed after pilocarpine-induced SE.

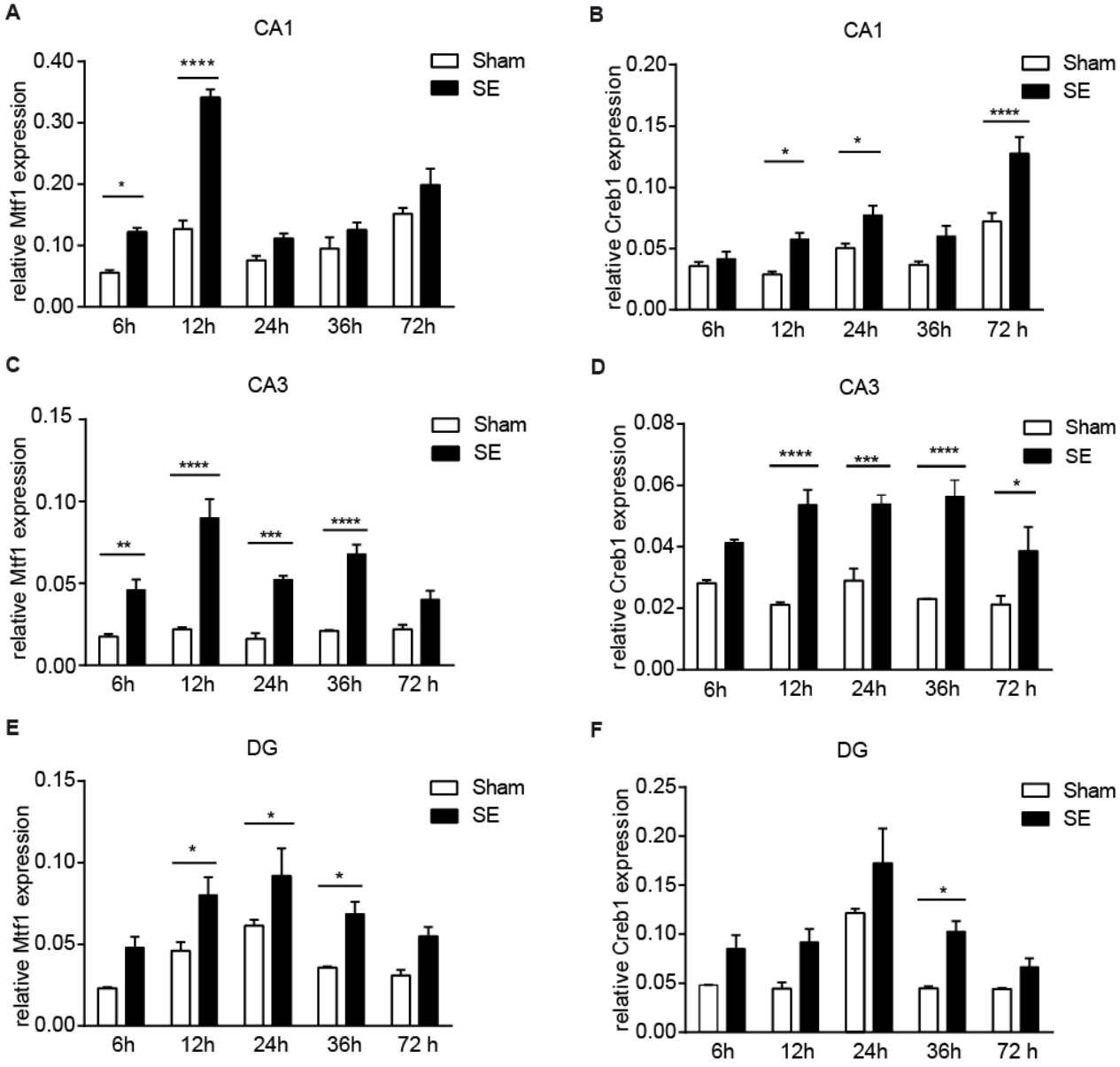

Fig. 16: Mtf1 and Creb1 expression levels in the early phases of epileptogenesis after pilocarpine-induced SE. (**A**) Mtf1 mRNA expression of hippocampal CA1 area at different time points after pilocarpine-induced SE in mice (van Loo et al., 2015). (**B,D,F**) Creb1 mRNA expression of hippocampal CA1 (**B**), CA3 (**D**) and DG (**F**) areas 6, 12, 24, 36 and 72 h after pilocarpine-induced SE in mice. (**C**,**E**) Mtf1 mRNA expression of hippocampal CA3 (**C**) and DG (**E**) subregions 6, 12, 24, 36, 72 h after SE. Quantification was performed with synaptophysin as reference gene. (Two-way ANOVA, *Sidak´s multiple comparisons test*, * $P \leq 0.05$, *** $P \leq 0.001$, **** $P \leq 0.0001$ N ≥ 4 sham, 4 SE)

3.4.4 Zn^{2+}-activated Mtf1 colocalizes with Creb1 and increases Creb1 fluorescence intensity 1 day after pilocarpine-induced SE

To strengthen our hypothesis that Creb1 expression could be regulated by Mtf1, we next questioned whether Mtf1 and Creb1 are expressed in the same neuronal populations. For this, we carried out immunofluorescence staining against Venus (indicator of Mtf1) and Creb1 in hippocampal section slices of mice. Since we specifically wanted to visualize the Zn^{2+}-activated nuclear Mtf1 expression and not cytoplasmic Mtf1, we used the above identified transcriptional reporter unit to label Mtf1-expressing neurons. Adult C57Bl6/N mice were injected with rAAV-MTI-Venus and after 2 weeks they were subjected to sham or pilocarpine-SE treatment. Animals were scarified one day after SE induction. This time point was selected based on the experiment described in paragraph 3.2.3 (**Fig. 10C**) and the time course of Mtf1 and Creb1 mRNAs expression (**Fig. 16**). We observed that Venus, and thereby nuclear Mtf1, colocalizes with Creb1, although Creb1 is expressed in a broader spectrum of cells than Mtf1 (**Fig. 17A**). Nevertheless, if Mtf1 regulates Creb1 expression, Creb1 protein levels should be higher in Mtf1-positive neurons of pilocarpine-SE animals compared to those of Mtf1-negative neurons in pilocarpine-SE animals and to those of sham-treated animals. Therefore, we next quantified the Creb1 fluorescence intensity of Mtf1-positive and Mtf1-negative neurons in sham and pilocarpine-treated animals. Indeed, we found that the Creb1 fluorescence intensity signal in Mtf1-positive expressing neurons of pilocarpine-SE treated animals is stronger than the once of Mtf1-negative neurons and of sham-treated animals (**Fig. 17B**). Altogether these results indicate Creb1 as a new target gene of Mtf1.

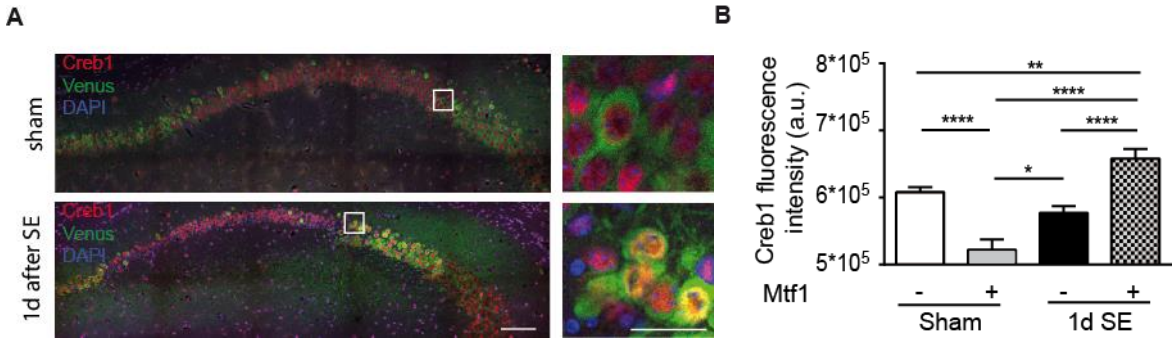

Fig. 17: Mtf1 colocalizes with Creb1 and increases Creb1 fluorescence intensity in pilocarpine-SE treated animals compared to sham-treated animals. (**A**) Representative

image of a sham (upper panel) and a pilocarpine-SE treated (lower panel) mouse hippocampi injected with rAAV-MTI-Venus and stained against Creb1 (red) and Venus (green) 1 day after SE. Scale bar, 100 µm (left images). Right panels show magnification images of white square from the overview images. Scale bar, 25 µm. (**B**) Semiquantitative analysis of Creb1 fluorescence intensity signal in Mtf1-poasitive and Mtf1-negative neurons of sham- and pilocarpine-SE treated animals 1 day after pilocarpine-induced SE. One way-ANOVA, *Tukey's multiple comparison test*, * $P \leq 0.05$, ** $P \leq 0.01$, **** $P \leq 0.0001$; N = 3. Fluorescence intensity was defined in arbitrary units (a.u.).

3.4.5 Transcriptomic spectrum of Mtf1-modulated neuronal populations

3.4.5.1 Establishment of several Mtf1-related RNA-seq libraries

As stated above, in order to identify new downstream targets of the Zn^{2+}/Mtf1 pathway, we carried out two independent approaches. The first one, more "biased", was based on bioinformatic analysis aimed to identify synaptic-genes with MRE binding sites within their promoter regions (**Fig 12**). The second one, an "unbiased" approach, was based on RNA-seq of hippocampi of sham- and pilocarpine-SE treated animals which were intracranially injected either with a control (GFP), or Mtf1 or dnMtf1 virus. More in detail, we analyzed 5 experimental conditions: animals injected with rAAV-hSyn-GFP and subsequently sham or pilocarpine-SE treated (GFP_Sham and GFP_Pilo-SE, respectively), animals injected with rAAV-hSyn-Mtf1-IRES-Venus and sham treated (Mtf1_Sham), and animals injected with rAAV-hSyn-dnMtf1-IRES-Venus and then sham or pilocarpine-SE treated (dnMtf1_Sham and dnMtf1_Pilo-SE, respectively). Three days after induction of SE, mice were sacrificed and hippocampi were isolated.

Quality control and initial bioinformatic analyses of the RNAseq libraries were performed by our collaborator Dr. Ashley van Waardenberg (Queesland, Australia). Principal component analysis (PCA) revealed a clear separation between sham groups (black, green and turquois dots) and pilocarpine-SE treated groups (red and blue dots) (**Fig. 18A**). In addition, within the pilocarpine-SE groups, a separation between the GFP- (blue dots) and the dnMtf1- (red dots) groups was observed. However, for the sham-treated groups (GFP and Mtf1 overexpression), all the samples clustered together (**Fig. 18A**). As a consequence, we asked ourselves whether a good viral transduction efficiency was achieved during the experimental procedure. To this end, we checked the mapped read

counts of Mtf1 and dnMtf1 in each experimental condition. As stated before, dnMtf1 is a truncated variant of Mtf1, missing its transactivation domains and therefore lacking the C-terminal part of Mtf1. When aligning the N-terminal sequence of Mtf1 in our dataset, a higher percentage of mapped reads was observed for the dnMtf1-sham, dnMtf1 pilo-SE and for the Mtf1-sham groups (**Fig. 17B**, left panel). Likewise, when aligning the C-terminal sequence of Mtf1 with the cDNA of our samples, a higher percentage of mapped reads was detected only for the Mtf1-sham group (**Fig. 17B**, right panel). These results indicate that neurons were transduced with a sufficient amount of rAAV particles. We next analyzed the differentially expressed (DE) genes by combining the results obtained from the EdgeR, DESeq2 and voom/limma algorithms. When comparing the transcripts of GFP-injected and sham-treated animals with the expression levels of the transcripts of Mtf1-injected and sham-treated animals, no statistically significant DE genes were detectable (**Fig. 18C**, left panel). When comparing the transcripts of GFP-injected sham- versus pilocarpine-SE treated animals, 5419 genes were significantly differentially expressed (** $P \leq 0.01$, DE = 3831; * $P \leq 0.05$, DE = 1588; **Fig.18C**, middle panel). Finally, when comparing the GFP_Pilo-SE condition with the dnMtf1_Pilo-SE condition, 32 genes were significantly differentially expressed (**Fig. 18C**, right panel). The fact that numerous genes were differentially expressed in the GFP_Sham versus GFP_Pilo-SE condition, whereas none or only a few genes were differentially expressed when comparing the transcriptome of GFP_Sham versus Mtf1_Sham and GFP_Pilo-SE versus dnMtf1_Pilo-SE condition, suggests a minimal effect of Mtf1 overexpression on the transcriptome under these experimental settings.

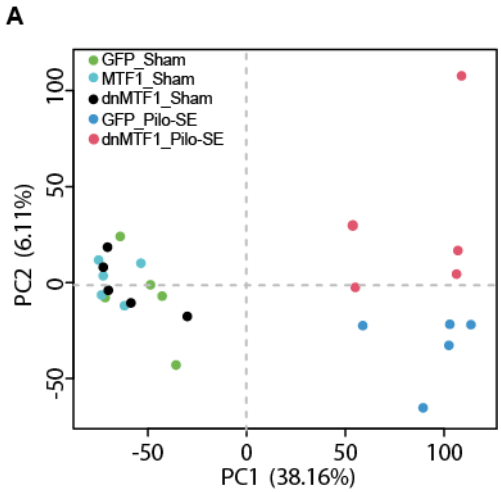

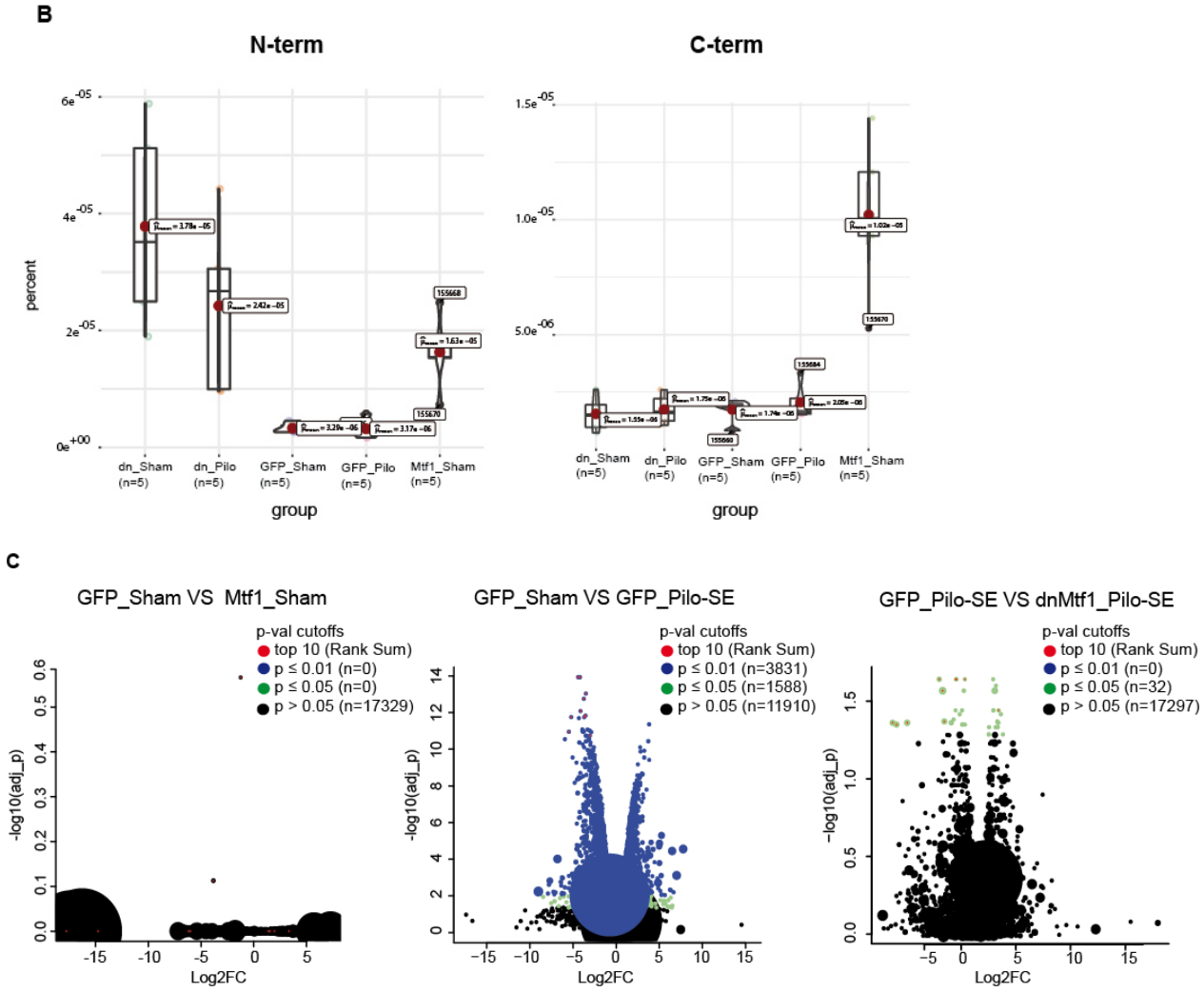

Fig. 18: Quality control of Mtf1 RNA-sequencing library. (**A**) PCA plot of 5 biological replicates/each experimental condition separates sham treated (black, green and turquoise dots) from Pilocarpine-SE treated (blue and red dots) samples and, within the pilocarpine-SE condition, separated the dnMtf1-injected animals (red dots) from the GFP-injected animals (blue dots). (**B**) Assessment of Mtf1 and dnMtf1 viral transduction efficiency. The percentage of mapped read counts of the N-terminal and the C-terminal sequence of Mtf1 in each experimental condition are given (N = 5). (**C**) Volcano plots representing 0 DE genes in GFP_sham samples compared to Mtf1_Sham samples (left panel), 5419 DE genes in GFP_Sham samples compared to GFP_Pilo-SE samples (middle panel) and 32 DE genes in GFP_Pilo-SE samples compared to dnMtf1_Pilo-SE samples (right panel). Each gene is colored based on -log$_{10}$ adjusted *P*-value. (** $P \leq 0.01$: blue dots, * $P \leq 0.05$: green dots, $P > 0.05$: black dots. Size of dots based on variability of Log2FoldChange (Log2FC) estimated by 3 RNA-seq algorithms).

3.4.5.2 Mtf1 is involved in synaptic plasticity-related biological processes

Previously, it has been shown that Mtf1 plays a key role in regulating intracellular Zn^{2+} homeostasis and oxidative stress conditions (Grzywacz et al., 2015). Furthermore, it has been shown how Mtf1 plays a role also in intrinsic plasticity by regulating Cav3.2 expression (van Loo et al., 2015). However, its function with regard to synaptic plasticity processes is still unclear. To get a better insight into the contribution of the Mtf1 pathway in additional biological processes, we performed GO enrichment analysis with a focus on two comparisons of our RNAseq libraries, i.e. the GFP_Sham versus Mtf1_Sham condition and the GFP_Pilo-SE versus dnMtf1_Pilo-SE condition. GO enrichment analysis based on the first 500 DE genes in GFP_Sham versus Mtf1_Sham samples revealed many GO terms associated with immunological terms (**Fig.19)**. Besides the immunological terms, over-represented biological processes were related to cellular responses to Zn^{2+} ions, reflecting the role of Mtf1 in cellular heavy metal homeostasis, to stress responses, to synapse pruning and to serotonin secretion (**Fig. 20**, left panel) (Andrews, 1992; Bahadorani et al, 2010). GO enrichment analysis based on the first 500 DE genes in dnMtf1_Pilo-SE versus GFP_Pilo-SE samples revealed GO terms associated with regulation of trans-synaptic signalling, chemical synaptic transmission modulation, potassium ion import and positive regulation of gamma-aminobutyric acid secretion (**Fig. 20**, right panel). Altogether these terms indicate the involvement of Mtf1 in plasticity-related biological processes, specifically in synapse morphology, neurotransmitters release and ions regulation.

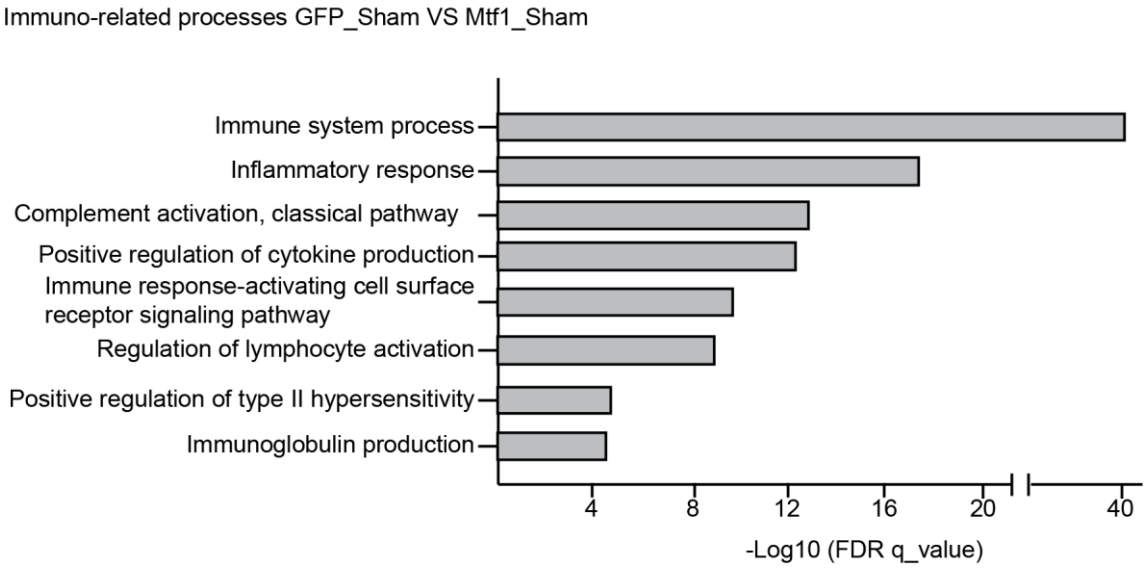

Fig. 19: Mtf1 immuno-related Gene Ontology (GO) terms. Some of the over-represented immune-related terms based on the first 500 DE genes from Mtf1-sham compared to GFP-sham samples.

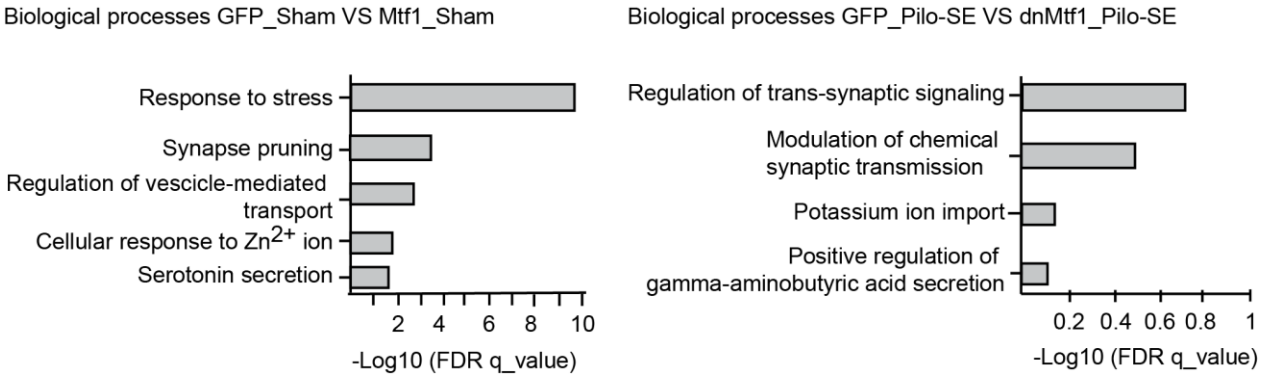

Fig. 20: Mtf1 Gene Ontology (GO) terms. Left panel, over-represented terms based on the first 500 DE genes from Mtf1-sham compared to GFP-sham samples. Right panel, GO biological processes based on first 500 DE genes from dnMtf1_Pilo-SE compared to GFP_Pilo-SE samples.

3.4.5.3 Identification of Mtf1-responsive target genes using RNA-seq libraries

We next investigated whether our Mtf1-associated RNAseq libraries would reveal additional Mtf1-responsive target genes. To this end, we analysed the above described

RNAseq dataset at the single gene level, notifying the changes in read counts of possible genes of interest among the five experimental conditions (**Fig. 18A**). The criteria used to select possible Mtf1 target genes were: 1) they should be statistically differently expressed for at least one algorithm used to normalise the read counts (edgeR_adj_p or DESeq2_adj_p < 0.05. The voom/limma algorithm has not been considered as parameter because it is susceptible to high p-values (low significance) for lower replicates and for lower depth); 2) the mapped read counts of the putative genes should be increased in the Mtf1 overexpression condition compared to the GFP-sham condition; 3) the mapped read counts of the putative genes should be increased in GFP_Pilo-SE condition compared to GFP_sham condition; 4) the mapped read counts of the putative genes should be decreased in dnMTF1_Pilo-SE condition compared to GFP_Pilo-SE condition; 5) finally, if the gene fulfilled the above described criteria 1-4, the gene should harbour MREs within their promoter regions.

Using this strategy, we identified three possible Mtf1-associated target genes: 1) Immunoglobulin Heavy Constant Gamma 1 (*Ighg1*); 2) 5-Hydroxytryptamine Receptor 2A (*htr2a*) and 3) Dopamine Receptor D2 (*drd2*). *Ighg1* expression strongly but not significantly, increases after Mtf1 overexpression (OE) and after pilocarpine-treatment and was significantly decreased after dnMtf1-pilocarpine-SE compared to controls (edger_adj-p = 0.0104, deseq_adj-p = 0.0049). *Htr2a* expression increases, albeit not significantly, after Mtf1-treatment compared to GFP-sham treatment and was significantly decreased after dnMtf1-pilocarpine treatment when compared to GFP-pilocarpine treatment (edger_adj-p= 0.0136, deseq_adj-p= 0.0138). *Drd2* expression slightly increases after Mtf1-OE and GFP-pilocarpine treatment, and was statistically decreased after dnMtf1-pilocarpine treatment (edger_adj-p= 0.0436). (**Tab. 12).**

Tab. 12: Mean read counts of Mtf1-associated target genes identified via RNA-seq in GFP- and Mtf1-sham conditions and GFP- and dnMtf1-pilocarpine SE conditions. *The statistical significance expressed by the Edger_adjust p value and DESeq2_adjust p value refers to the comparison between the dnMtf1- and GFP-pilocarpine-SE treatments.

Gene	GFP-sham	MTF1-sham	GFP_Pilo-SE	dnMTF1_Pilo-SE	Edger-adj-p*	Deseq_adj-p*
Ighg1	1.344	192.3098	28.1047	0.0191	0.0104	0.0048
Htr2a	13.4487	15.8330	6.8661	2.3321	0.0136	0.0133
Drd2	1.2885	3.7351	2.5777	0.1984	0.0436	0.0712

We next checked whether all three genes harbour a predictive Mtf1 binding site within their promoter region. *Ighg1* has an MRE with a cut-off value of 81.3 %, whereas *htr2a* and *drd2* have MREs with a cut-off value of 97.6 % (**Tab. 13**).

Tab. 13: MRE consensus sequences of the Mtf1-target genes identified by RNA-seq.
***** Bold letters represent the core sequences of the Mtf1-binding motive.

Gene	Cut-off %	Sequence*
Ighg1	81.3	TT**TGCACCCT**TCCC
Htr2a	97.6	TG**TGCGCTCG**CCTC
Drd2	97.6	TG**CGCGCGCG**GCGC

.

.

4. Discussion

The severe clinical manifestation of TLE pathogenesis, along with the high percentage of patients that are pharmacoresistant to the current medications, requires a better understanding of the disease with the final goal to develop new pharmacological treatments. Within this study, we investigated the implications of the Mtf1/Zn^{2+} cascade in the process of epileptogenesis using *in vitro* and *in vivo* approaches. To analyse the neuronal changes occurring during the latent phase of TLE, we used the pilocarpine-induced SE animal model. *In vitro* and *in vivo* reporter gene assays allowed the development of a genetic tool which allowed to characterize Mtf1-expressing cells. Through *in vivo* imaging, we demonstrated that Mtf1 is strongly activated immediately after a brain trauma. Using bioinformatic analysis and RNA-sequencing approaches, we identified additional targets of Mtf1 which might contribute to the hyperexcitability of the hippocampal circuit observed in TLE. Although a deeper investigation with regards to electrophysiological consequences of the observed molecular dynamics is needed, we concluded that Mtf1 is involved in different cascades of epileptogenesis and interfering with (part of) this cascade can be a promising target for treating (a subpopulation of) TLE patients.

4.1 The MTI transcriptional unit *in vitro*

Mtf1 is well characterized with regards to its role in heavy metal homeostasis and oxidative stress (Günther et al., 2012). In addition, recent data suggested Mtf1 as a key modulator of intrinsic plasticity in TLE (van Loo et al., 2015). Mtf1-mediated gene regulation occurs via binding to MREs mainly located within the promoter region of genes of interest (Stuart et al., 1984; 1985). Here, we first developed a reporter unit to label Mtf1-expressing neurons in mouse brains by selecting several MREs, specifically MRE-d/c, MRE-3/4, MRE*S 4, MRE-Cav and MRE-MTI. Our data demonstrated that in primary hippocampal neurons, the full-length MTI promoter had the strongest transcriptional activity after Zn^{2+}/Mtf1 challenge, followed by the MRE-d/c transcriptional unit, while MRE-3/4 only showed an increased transcriptional tendency after Zn^{2+}/Mtf1 treatment. Surprisingly, MRE-Cav did not exhibit metal regulatory activity in hippocampal neurons. These results can be explained by looking at the DNA sequence of the

considered transcriptional tools. MTI, MRE-d/c and MRE-3/4 either are natural promoters or fragments of promoters, containing therefore both the core metal regulatory sequence and the flanking regions. In contrast, MRE-Cav is a rearranged minimal promoter, containing only the core sequence 5'-TGCRCNC-3' (R=G and N=C). Although the 5'-TGCRCNC-3' core sequence is necessary for Mtf1 binding, it seems that the binding affinity and the transcriptional activity is influenced by the flanking regions (Wang et al., 2004 a). This hypothesis can be confirmed when looking at the results of the *LacZ* expression under the control of the Cav3.2-1020 promoter *in vivo* (**Fig. 8B**, lower panels). Although for that experiment we used a shorter length of Cav3.2 promoter (Cav3.2-1020), both core consensus sequence and flanking regions were kept and indeed, after pilocarpine-induced SE, an increase in transcriptional activity was observed, confirming the metal inducible transcriptional activity discovered in van Loo et al. (2015). Congruently, Inukai et al. (2017) indicated how not only core consensus sequences but also flanking regions, DNA shape and epigenetic factors influence TFs binding affinity.

The following goal was to track the Zn^{2+}/Mtf1-mediated activation of the MTI transcriptional reporter unit in time by measuring the Venus reporter gene fluorescence intensity in cultured hippocampal neurons. Transcription factor-mediated gene regulation is a dynamic event depending on the TFs concentration, its post-translational activations, and on the binding/dissociating kinetics (Swift and Coruzzi, 2017). We found that already 2 h after Zn^{2+} incubation, Mtf1 was activated by Zn^{2+} and able to bind to the transcriptional tool. The fast activation of Mtf1 also confirmed its fundamental role in cellular metal homeostasis (Grzywacz et al., 2015). The persisting elevated levels of Venus at 7.5 h after Zn^{2+} incubation indicated the consistency of gene expression linked to TF concentration (Swift and Coruzzi, 2017). At 15 h after Zn^{2+} incubation, no further increase of Venus signal was observed. This could be explained by a saturation of the MREs by the overload of Mtf1 TF.

4.2 The MTI transcriptional unit *in vivo*

Eventually, cis-regulatory elements which regulate gene expression in transfected cells in culture, do not redirect gene expression in analogous cells *in vivo*, due to the complexity of biological processes such as external stimuli or compensatory

mechanisms (Kitsis and Leinwand, 1992). Thus, we next evaluated whether the identified transcriptional tool also reflected the Zn^{2+}/Mtf1-dependent gene regulation *in vivo*. The *in vivo* capacity of the MTI transcriptional unit to be regulated in a Zn^{2+}/Mtf1-manner was clearly present when we expressed MTI-*LacZ* in the mouse hippocampus. In this experiment, pilocarpine-SE animals showed a strong increase of *LacZ* signal compared to sham-treated littermates. The same results could be reproduced in animals injected with a combination of Mtf1 and MTI-*LacZ* viruses where an intense *LacZ* staining was observed in comparison to animals injected with a combination of Mtf1- and GFP-viruses. These results suggested that the MTI transcriptional unit is a reliable genetic tool for labelling neurons expressing Mtf1 in a Zn^{2+}-dependent manner and to investigate the Zn^{2+}/Mtf1 pathway in the process of epileptogenesis both *in vitro* and *in vivo*.

Mtf1 emerged relatively recently as a pathogenetically relevant factor involved in the development of TLE. However, its activation during the process of epileptogenesis is still unknown. As the efficiency of therapeutic approaches relies on target validation as well as time of intervention, we used the identified MTI transcriptional unit to monitor Mtf1 activity throughout the process of epileptogenesis by using iRFP *in vivo* imaging. iRFP *in vivo* imaging is a non-invasive, easy and with low cytotoxic technology also used to trace tumor tissue growth, metabolites and gene expression (Filonov et al., 2011). By measuring the iRFP signal under the control of the MTI transcriptional unit in AAV-intracranial infected sham and pilocarpine-induced SE mice, we observed that Mtf1-dependent changes in gene expression occur early after an initial precipitating event. This result is important when considering that the transcriptional regulation of activity-dependent genes could be useful as potential biomarkers for pathology diagnosis as well as for validation of antiepileptogenic interventions (Kaur et al., 2011). Although, to date there are no reliable biomarkers for epileptogenesis yet, growing evidence suggests miRNAs, as well as genes involved in epigenetic DNA modifications as potential biomarkers, along with magnetic resonance imaging and, positron emission tomography to monitor changes in the structure of the brain (Feng et al., 2020; Martinez and Peplow, 2023; Hansen et al., 2014; Berger et al., 2019; Pitkänen and Engel, 2014). Also, different transcription factors such as brain-derived neurotrophic factor (Bdnf), Egr1 and Egr3 are nowadays under investigation for their role in activating different

cascades of signaling events after seizures (Brooks-Kayal, et al., 2009; van Loo et al., 2019). Since hippocampal Mtf1 mRNA is upregulated 12 h after pilocarpine-SE and Mtf1-dependent gene regulation increases immediately after pilocarpine-SE, Mtf1 itself or its gene targets could result in potential biomarkers (van Loo et al., 2015). Furthermore, these results indicate Mtf1 as an early upstream component of different signaling pathways initiated by seizures. Thus, interfering with Mtf1 immediately after a brain trauma might be fundamental to prevent the cellular changes that contribute to the occurrence of TLE.

Besides its involvement in hypoxia and heavy metal homeostasis, recent studies revealed that Mtf1 is involved in a wider spectrum of biological processes, like inflammation by regulating expression of pro- and anti-inflammatory cytokines, or neuronal plasticity by regulating the expression of β-synuclein (Dubé et al., 2011; Günther et al., 2012; Mocchegiani et al., 2004; McHugh et al., 2011). Therefore, we intended to visualize the scale of the hippocampal Mtf1-micronetwork and to understand to which extent it overlaps and contributes to the Cav3.2-micronetwork both in physiological and pathological conditions. Although, we expected that Mtf1 would have been expressed in a broader number of cells than Cav3.2, as the TF plays a role in different physiological pathways, our data displayed that both in physiological and pathological conditions, the Mtf1-micronetwork overlaps with the one of Cav3.2. The strong correlation between Mtf1 and Cav3.2 expression was also observed by Jing et al. (2021), who showed that ventral CA3 hippocampal neurons through Mtf1-mediated activation of Cav3.2 are responsible for social-stress-induced anxiety-like behaviours.

4.3 Challenges in identifying the Mtf1-transcriptome

CA1 PCs show pronounced transcriptional variability along the dorsal-ventral axis, indicating the existence of different classes of neurons (Cembrowski et al., 2016). Such transcriptional differences are reflected in functional heterogeneity and might be an indicator of different microcircuits to which subpopulations of neurons are involved in. In addition, it has been shown that Mtf1 can activate the promoter and corresponding mRNA expression of $Ca_V3.2$ and MTs in a Zn^{2+}-dependent way, but it is still unknown whether Mtf1 regulates a larger set of epilepsy-associated genes. Previously, our research group generated an extensive RNA-sequencing (RNA-seq) dataset from

pilocarpine-SE and control mice at various time points after SE (2, 6, 12, 24, 36 and 72 h after SE; unpublished results). Subsequent bioinformatic analyses revealed that of the 3300 genes that showed a significant upregulation 72 h after SE (the time point of maximal $Ca_V3.2$ mRNA increase after SE (Becker et al., 2008)), 330 genes had more than one predicted binding sites for Mtf1 in their promoter region, indicating that more genes besides $Ca_V3.2$ might be regulated by the Zn^{2+}/Mtf1 cascade during the process of epileptogenesis. Therefore, we intended to uncover the neuronal behavior of Mtf1-expressing cells, both under physiological and epileptic conditions by performing FACS sorting of Mtf1-positive and Mtf1-negative cells under sham and pilocarpine-SE conditions for subsequent RNA-seq approaches. Our data proved that in the early latent phase of TLE there is an activation and an increase of a hippocampal subpopulation expressing Mtf1, indicating the activation of a specific microcircuit. However, we unfortunately did not succeed in revealing the transcriptome of this subpopulation of cells. In order to perform successful RNA-seq approaches, the ribonucleic acid has to be intact, corresponding to a RIN^e value above 7. In our hands, we unfortunately did not reach this requirement. We adapted several parameters (e.g. different sorting buffers, sorting set-ups, different processes to extract RNA), however we managed to obtain a good RIN^e value only occasionally, and only specifically for the cells not expressing Mtf1 under sham conditions. Our results suggested that the isolated pyramidal neurons, given their shape, are not suitable for the experiment set-up we used: the mechanical pressure coming from the FACS sorting could provoke the rupture of pyramidal branches which is fatal for the neurons. Furthermore, it has to be kept in mind that the neurons experienced virus transduction making the neurons more prone to neuronal death. Therefore, we carried out two other independent strategies, which will be discussed below, in order to identify the Mtf1-downstream targets, which may play a role in converting the hippocampal network hyperexcitable following SE.

4.4 Mtf1 regulates the cAMP responsive element binding protein 1 (Creb1)

To better understand the role of the Mtf1/Zn^{2+} cascade in epileptic network formation, we investigated putative downstream Mtf1-target genes, which were selected based on their specificity to harbor Mtf1-binding sites within their promoter region and their role in synaptic plasticity. *Kalrn*, encoding for the kalirin protein, was selected for its

involvement in a series of synaptic plasticity processes such as dendritic arborization and spine formation, and glutamate receptors activity (Yan et al., 2015; Penzes et al., 2001; Lemtiri-Chlieh et al., 2011; Kiraly et al., 2011). Furthermore, Kalirin mRNA was found to be upregulated early after kainate-induced SE (Sharma et al., 2009). *Cplx2,* which encodes for the complexin-2 protein*,* was selected for its role in controlling synaptic vesicles fusion by interacting with the SNARE complex (Chen et al., 2002; Xue et al., 2008). *Cacna1b*, encoding for the α1B pore-forming subunit of the N-type voltage dependent calcium channel, was selected for its contribution in neurotransmitter release at hippocampal excitatory neurons (Bunda et al., 2019; Wheeler et al., 1994). *Creb1,* encoding for the CAMP Responsive Element binding protein 1, was selected based on its involvement in neuronal excitability modulation (Zhou et al., 2009; Dong et al., 2006). Furthermore, Lopez de Armentia et al. (2007) showed that Creb1-mediated gene expression increases CA1 pyramidal neuron intrinsic excitability. *Git1*, encoding for the ARF GTPase-activating protein GIT1, was selected according to its known role in synapse formation and dendritic spine morphogenesis (Zhang et al., 2003; 2005). *Ntrk2,* encoding for the neurotrophic tyrosine receptor kinase 2, as all the other members of the tyrosine kinase members, plays an important role in cell signaling, growth and central nervous system development (Chao, 2003). In particular, Ntrk2 is implicated in hippocampal long-term potentiation (LTP) and hippocampal synaptogenesis (Sakuragi et al., 2013; Sonoyama et al., 2020). Moreover, there are different reports claiming a correlation between Ntrk2 and the development of epileptic encephalopathy (Yoganathan et al., 2021). *Rims3* encodes for the γ isoform of the Rab3 interacting molecules (RIMs). Although RIM3 is less investigated compared to RIM1α, it is believed to be located as for the other isoforms, at the active zone of the presynaptic terminals and to regulate neurotransmitters release (Schoch and Gundelfinger, 2006). *Gria1*, encoding for the glutamate ionotropic receptor AMPA type subunit 1, was considered for its physiological role of being a subunit of the excitatory neurotransmitter receptor, its implications are found in LTP maintenance, long-term depression (LTD) and homeostasis scaling (Kessels and Malinow, 2009; Jiang et al., 2021; Diering and Huganir, 2018). Another glutamate ionotropic receptor was considered: *Grin2b*, which has been already investigated for its correlation with intellectual disability with focal epilepsy (Lemke et al., 2014; Platzer and Lemke, 1993; Hu et al., 2016). Different

$GABA_A$ receptor subunits were considered, specifically *Gabra4, Gabrb3, Gabrd* genes which encode respectively for the $GABA_A$ receptor subunit α4, β3 and δ. Those subunits are involved in the trafficking-mediated plasticity at the inhibitory synapses (Luscher et al., 2011). *Kcnh1,* encoding for the potassium voltage-gated channel, subfamily H member 1, was considered due to its reported participation in different cases of epilepsy (von Wrede et al., 2021). Concerning *Kctd13,* which encodes for potassium channel tetramerization domain containing 13, its physiological role is still unclear, however, deletion of this gene results in a reduced synaptic transmission (Escamilla et al., 2017). The leucine-rich repeat transmembrane neuronal 2 gene (*Lrrtn2*) encodes for synaptic cell adhesion molecules which induced excitatory synapses assembly, it interacts with PSD-95 and regulates surface expression of AMPA receptors and plays a role in the TLP by interacting with the neurexin family protein (de Wit et al., 2009; Soler-Llavina et al., 2013). For this reason, we also selected *Nrxn3*, encoding for the neurexin 3 protein (Konopka et al., 2012). *Ptrprs* is a gene encoding for the protein tyrosine phosphatase receptor type S which plays a role in synapses formation and in strengthening TLP (Horn et al., 2012). Finally, *Unc13a*, also known as *Munc13a*, is fundamental for priming synaptic vesicles for fusion (Augustin et al., 1999). From our *in vitro* screening, we identified *Creb1, Rims3, Gabra4, Gabrd and Unc13a* as possible Mtf1-target genes, as their expression was upregulated after Mtf1/Zn^{2+} treatment. In particular, *Creb1*, *Gabra4* and *Unc13a* resulted to be significantly upregulated after Mtf1 treatment, and significantly returned back to normal levels when treated with dnMtf1. While for *Creb1* and *Unc13a* the upstream activators are not known so far, for *Gabra4* it is believed that the augmented mRNA and protein expression observed during epileptogenesis might be correlated with high levels of Egr3 and Bdnf (Grabenstatter et al., 2014). This implies that the regulation of our genes of interest are not limited to Mtf1. Concerning the other genes, which do not show an increased transcriptional activity after Mtf1 treatment, it must be kept in mind that the Jaspar transcription binding site sequences are predicted sequences, based on the position frequency matrix and TF flexible model across six different taxonomic groups. This system, as well as all the probabilistic models of TF binding sites, still faces challenges in its computational prediction (Ambrosini et al., 2020; Keilwagen and Grau, 2015). We next tested whether the selected synaptic plasticity related genes represent a phenomenon also in human TLE by analysing the

mRNA levels of those genes in correlation with MTF1 mRNA levels in 2 human cohorts. Interestingly, our analysis showed that patients with elevated MTF1 transcripts also carried augmented CREB1 transcripts. This correlation is specific for patients affected by TLE with HS, as the MTF1-CREB1 correlation was not observed in patients affected by TLE associated with brain lesions. CREB1 is a transcription factor belonging to the family of leucine zipper motif transcription factors. It is activated by different external stimuli, such as oxidative stress or hormones and covers a fundamental role in immune response, cell proliferation, cell cycle and apoptosis as well as memory consolidation (Pregi et al., 2017; Viguerie et al., 2004; Wen et al., 2010; Niu et al., 2022; Ortega-Martínez, 2015). The activation of the CREB1 signal in epileptic disorders is an established event and our results are in line with the work of Park et al. (2003), where it has been shown that the expression levels of CREB1 and activated CREB1 (phosphorylated CREB1 - pCREB1) are significantly increased in hippocampi of MTLE patients compared to healthy controls (Beaumont et al., 2012; Rakhade et al., 2005). In animal models of TLE, it has been seen that reducing Creb1 expression shortens SE and the frequency of spontaneous seizures in the chronic phase (Zhu et al., 2012, 2015). Therefore, if Mtf1 is the upstream regulator of Creb1, modulating Mtf1 activity could truly prevent the activation of different pathways of epileptogenesis. In addition, in case that inhibiting or decreasing Mtf1 activity as therapeutic approach leads to toxicity or fatality, reducing Creb1 activity could serve as a secondary therapeutic approach (Wang et al., 2004 b; Li et al., 2016). Our data also showed that high levels of CREB1 were correlated with neuronal loss in the hippocampal CA1, CA2 and CA3 subregions, but not in the DG. In addition, an increase of CREB1 expression was found in patients younger than 25 years of age. Although activated-CREB1 promotes cell survival (Lee et al., 2009; Bonni et al., 1999; Niu et al., 2022), it must be kept in mind that at the time of human tissue resection, the pathology is already at an advanced state. Therefore, the high levels of Creb1 expression could be an initial compensatory mechanism, which is not enough to preserve the cells' survival against the progress of the disease. In addition, CA neurons seem to be more prone to SE-induced cell death compared to DG neurons (Hansen et al., 2014). Nevertheless, the observed positive correlation between CREB1 levels and the anagraphic data suggests CREB1 expression as a biomarker for a specific subgroup of patients affected by TLE. In Alzheimer’s patients, a positive

correlation between elevated expression of pCREB1 in the post-mortem brain and in the peripheral blood mononuclear cells (PBMC) has been observed (Bartolotti and Lazarov, 2019). This indicates that for CREB1 a pathological crosstalk between brain and blood exists, and that pCREB1 expression in PBMC can be used as a biomarker for cognitive dysfunction in patients affected by Alzheimer's disease. It would therefore be highly interesting to monitor peripheral CREB1 signals in patients affected by TLE in order to discover whether CREB1 expression can be used as a biomarker to detect the early stages of the disease. Given the Zn^{2+}/Mtf1-dependent upregulation of Creb1 *in vitro* and the positive correlation of MTF1 and CREB1 transcripts in human resected brain tissues, we intended to see whether the correlation between the two transcription factors was also present in the pilocarpine-SE animal model of TLE. Our data showed that both Mtf1 and Creb1 mRNA are upregulated in tissue derived from pilocarpine-SE animals compared to their sham-treated controls, reproducing the MTF1-CREB1 correlation seen in the human cohorts. In particular, our data showed that the Creb1 upregulation consistently follows the Mtf1 expression in all the subregions of the hippocampus. From our experiment, where we virally transduced the CA1 hippocampal region with the mRuby3 protein under control of the MTI transcriptional unit, we saw that even one day after SE, the mRuby3 expression was higher in pilocarpine-SE treated animals compared to the sham-littermates (**Fig.10C**). This means that within 24 h after SE, the upregulated Mtf1 RNA is translated into protein, activated and able to regulate the expression of its downstream genes. Interestingly, based on the Mtf1-Creb1 pilocarpine-SE timeline experiment (**Fig. 16**), Mtf1 is translated and activated even before 24 h after SE, binds to the MREs within the promoter region of Creb1 and gives rise to its upregulation even within 12 h after the transient brain insult. To further prove that Creb1 upregulation in TLE is Mtf1-dependent, we visualized the subpopulations of cells expressing the two TFs by immunostaining. Our stainings displayed a colocalization of Mtf1- and Creb1-expressing cells. However, Creb1 distribution turned out to be broader and more homogeneously expressed then Mtf1. In principle, this is not surprising when considering the physiological role of Creb1 as a mediator of inflammation, glucose metabolism and memory, which are all processes that underlie the wider expression throughout the brain (Wen et al., 2010; Jin et al., 2013; Barco et al., 2003; Kim et al., 2013; Ortega-Martínez, 2015). Furthermore, Creb1 activity is also present in glial cells.

For example, after SE, a CRE-mediated expression occurs also in astrocytes and microglia, persisting for up to 20 days (Lee et al., 2007).

The involvement of Creb1 in TLE is well documented. Creb1 and pCreb1 expression is increased both in human brain tissue of patients affected by TLE and animal models (Park et al., 2003; Conte et al., 2020; Hansen et al., 2014). Decreasing Creb1-activity in animal models of TLE shortens SE and reduces the severity of seizures in the chronic phase of the disease (Zhu et al., 2012; 2015). In addition, Creb1-mediated gene expression is responsible for increasing intrinsic bursting in pyramidal neurons (Lopez de Armentia et al., 2007). In order to further validate the Mtf1/Zn^{2+}-Creb1 cascade, it would be interesting to analyze transcript and protein levels of pCreb1 and some downstream targets of Creb1-signalling in hippocampal neurons after Mtf1/Zn^{2+} treatment. As alternative, it would be interesting to investigate whether Mtf1 or dnMt1-treatment influences Creb1-mediated gene expression. In terms of alterations at the network level, organotypic slice cultures could be recorded after Mtf1/Zn^{2+}-incubation and Creb1/pCreb1 levels and its downstream targets could be measured thereafter. In addition, organotypic network activity could be recorded after Mtf1-inhibition (e.g. by using the Mtf1 inhibitor LOR-253 (https://www.adooq.com/lor-253.html)) and analyze whether the Creb1 expression is reduced. Another alternative could be to interfere with a Creb1 inhibitor, such as 666-15 (https://www.medchemexpress.com/666-15.html?utm_source=google&utm_medium=CPC&utm_campaign=Europe&utm_term=HY-101120&utm_content=666-15&gclid=Cj0KCQiA5NSdBhDfARIsALzs2EAFlaoO7jra0B31AX886z_wb0xVqTv1OIlKLhyLXH-9B0MKgwdrF4gaAgrrEALw_wcB) and to analyze whether both molecular and physiological data would reflect the data obtained from pharmacological interference with Mtf1. To prove unequivocally that Creb1 is a target of the Mtf1/Zn^{2+} cascade, Chromatin-immunoprecipitation (ChIP) experiments will reveal whether Mtf1 can bind to the Creb1 promoter region. Initial ChIP-seq experiments using an antibody against Mtf1 on hippocampal homogenates of sham and pilocarpine-SE mice were performed, however samples unfortunately were not successful. To date, Mtf1 Chip-sequencing experiments confirmed the interaction of Mtf1 with the *Cacna1h* and *MT-I* promoter, and revealed the involvement of Mtf1 in the regulation of genes associated with myogenesis

(Jing et al., 2021; Daniels and Andrews, 2003; Tavera-Montañez et al., 2019). Thus, indicating this approach as a reliable way to find new Mtf1-targets.

4.5 Mtf1 and synaptic plasticity biological processes

SE triggers changes in neuronal excitability, synaptic reorganization and cellular morphology which are consequences of altered plasticity-related pathways, cell death and neuroprotective events (Hansen et al., 2014). Many of these processes are the result of a marked alteration of transcriptional activity which occurs during the process of epileptogenesis (Lösing et al., 2017; Sun et al., 2022). To gain a deeper insight into the MTF1-mediated transcriptome, we performed RNA-sequencing. Our data revealed none or only a few differentially expressed genes when comparing the transcriptional profiles of GFP_Sham versus Mtf1_Sham and GFP_Pilo-SE versus dnMtf1_Pilo-SE conditions, indicating a minimal Mtf1-transcriptional activity on the pilocarpine-SE transcriptome. This result can be explained taking in consideration that Mtf1 is expressed in only a subpopulation of neurons, while the current analyses were performed on whole hippocampus homogenates. The RNA-seq dataset came thus from a heterogeneous cell population and this has led to a dilution of the Mtf1 viral transduction effect. Congruently, different studies demonstrated how transcriptome variability is cell-type and time-dependent (Henkel et al., 2021; Hansen et al., 2014). Therefore, a deeper insight into Mtf1-transcriptome could be given by single-cell RNA-sequencing. Moreover, the dilution effect hypothesis is in line with the absence of significant changes in C*acna1h* expression both in the Mtf1- and dnMtf1-overexpression conditions compared to the respective controls, which is known to occur at the selected time point (Becker et al., 2008).

A more detailed analysis of the RNAseq data revealed several immunological-associated processes to be associated with Mtf1 expression, i.e. type II ‘hypersensibility’ and immunoglobulin and cytokine production processes. The contribution of Mtf1 to inflammatory processes has already been shown in previous studies. For example, Mtf1 has been described as a regulator of cytokine production via a crosstalk with nuclear factor-kB (Nf-κB) and has been proved to mediate neuropathic pain in dorsal horn neurons (Schuster et al., 2019; Hao et al., 2022). Furthermore, it must be noted that dysregulation of Zn^{2+} homeostasis is linked to impaired regulation of innate immune

responses and a reduced production of cytokines (Gao et al., 2018; Haase and Rink, 2007). In line with the study of Grzywacz et al. (2015), Zn^{2+} has been reported to be indispensable for Nf-κB-signaling activation (Haase et al., 2008). This proposes Mtf1 as a mediator of Zn^{2+}-mediated immunological responses. Besides the inflammatory and immunological pathways mentioned above, our data revealed that Mtf1 is implicated in responses to stress and cellular responses to Zn^{2+}, congruently with the physiological role of Mtf1. In addition, Mtf1 resulted to be involved also in a series of processes like synapse pruning, regulation of vesicle-mediated transport, serotonin and GABA secretion, potassium import, regulation of trans-synaptic signal and modulation of synaptic transmission, thus taking part in synaptic plasticity-associated processes. Of special interest is the association of Mtf1 with the positive secretion of GABA processes. To date, still little is known about the role of Mtf1 with regard to synaptic or intrinsic plasticity. Although free Zn^{2+} mainly localizes at presynaptic glutamatergic synapses, it has been shown that free Zn^{2+} is also present in GABA-containing neurons (Suh et al., 2001; Franco-Pons et al., 2000; Wang et al. 2001). Here, this triggers concentration-dependent and cell-specific biphasic effects (Blakemore and Trombley, 2017; Vergnano et al., 2014). Takeda et al. (2004), demonstrated that Zn^{2+} release in the synaptic cleft of CA3 hippocampal neurons augments GABA release, while Vergnano et al. (2014), showed that neuronal activity mainly triggers Zn^{2+} and glutamate corelease at the Schaffer collateral-CA1 and Mossy fiber-CA3 synapses. These data suggest that Mtf1, as Zn^{2+}-dependent effector, can play different functions according to cell-type specificity and Zn^{2+} concentration. At the single gene level, we identified three genes harboring MREs within their promoter region with altered transcripts when Mtf1 activity was potentiated by Mtf1 overexpression or reduced by dnMtf1 overexpression after pilocarpine-induced SE: *Ighg1, Htr2a* and *Drd2. Ighg1* encodes for the constant region of the heavy chain of immunoglobulin G. Although alterations of immunoglobulins has been suggested as a consequence of anti-epileptic treatments, patients affected by TLE often show changes of immunoglobulin levels already before starting the therapy (Aarli, 1976; Fontana et al., 1976; Callenbach et al., 2003; Sorrell and Forbes, 1975). Interestingly, IgGs have been noted as Zn^{2+}-binding proteins (Babaeva et al., 2006). Therefore, the Mtf1-dependent changes in the heavy chain of IgG expression could be an initial compensatory mechanism to repristinate the physiological levels of Zn^{2+} after

seizures. *Htr2a* encodes for the serotonin 5-HT-2A receptor which is a member of the $G_{q/11}$-coupled receptor. Although around 25 % of the proteins of this receptor colocalize with glutamate decarboxylase-containing neurons, its main role consists in mediating glutamate excitatory postsynaptic currents in pyramidal neurons (Santana et al., 2004; Aghajanian and Marek, 1997; 1999). The involvement of 5-HT-2A in epilepsy is far from being completely understood. Several studies claimed that potentiating the serotonin system or activating 5-HT-2A produces an anticonvulsant effect (Favale et al., 2003; Guiard and Di Giovanni, 2015; Van Oekelen et al., 2003). Other studies however, showed pro-epileptic effects when activating 5-HT-2A. In fact, pharmacological administration of 5-HT-2A antagonists have been proved to delay the development of seizures or to inhibit seizures in a dose-dependent manner (Wada et al., 1992; Ritz and George, 1997). Furthermore, in favor of the latter results, functional genetic mutation of *htr2a* has been shown to be responsible for early onset seizures in patients with TLE (Manna et al., 2012). In this regard, further studies will be necessary in order to clarify the role of *htr2a* in the process of epileptogenesis. A gene with intriguing functional implications to be differentially expressed in a Mtf1-dependent manner was *Drd2.* This gene encodes for the dopamine receptor D2 which is a G-protein coupled receptor. As all the family members of the dopamine receptors, the Drd2 is putatively involved in the regulation of motor activity as well as neurological diseases like Parkinson's disease, Alzheimer's disease and hyperactivity/schizophrenic disorders (Mishra et al., 2018). Dopamine receptor 2 belongs to the D2-like subclass of dopamine G-coupled receptor (D2-D4) (Missale et al., 1998) and its activation is generally associated with reduced dopaminergic tone and inhibitory processes (Ford, 2014; Chen et al., 2006; Stoof and Kebabian, 1984). With regard to epilepsy, stimulation of D2-like receptors exhibits anti-convulsant effects (Bozzi and Borrelli, 2013). Mice lacking the Drd2 have a lower threshold to seizure-susceptibility and neurotoxicity following administration of pilocarpine and kainic acid (Bozzi et al., 2000; Bozzi and Borrelli, 2013; Brodovskaya et al., 2021). However, it must also be kept in mind that D2 receptors are terminal autoreceptors, meaning that they are susceptible to a negative feedback regulation. This implies that following elevated levels of dopamine, they can reduce dopamine synthesis and packaging and inhibit dopamine release with reduction of its inhibitory activity (Onali et al., 1988).

As a perspective, on the genetic level, further investigation is required in order to confirm whether and how in detail Mtf1 regulates the transcripts of the above-mentioned genes and also determines their precise involvement in the process of epileptogenesis. It would be highly interesting to see whether the Mtf1-dependent changes of gene expression are reproducible also in other systems, including the same experimental setup as has been done for *Creb1,* by incubating neurons with Mtf1/dnMtf1-Zn^{2+}following transcripts measurement via qPCR. In addition, it would be interesting to learn whether also the protein concentration increases after Mtf1/Zn^{2+} challenge, using western Blot or Elisa/MSD assays. Finally, also the correlation between Mtf1 and the newly identified target genes, i.e. *Ighg1, Htr2a* and *Drd2* could be investigated in human TLE cohorts.

4.6 Conclusion

The early activation of Mtf1 after a transient brain trauma triggers abnormal transcriptional regulation of its target genes. In this study we provide evidence that, besides *Canca1h*, the Mtf1/Zn^{2+} cascade may regulate additional target genes, including *Creb1, Ighg1, Htr2a* and *Drd2,* genes involved in synaptic plasticity, thus, promoting hippocampal network hyperexcitability and seizures development. In conclusion, pharmacologically interfering with the Mtf1/Zn^{2+}-pathway or with one of its downstream targets, could be a strategy to arrest or delay the development of epileptogenesis.

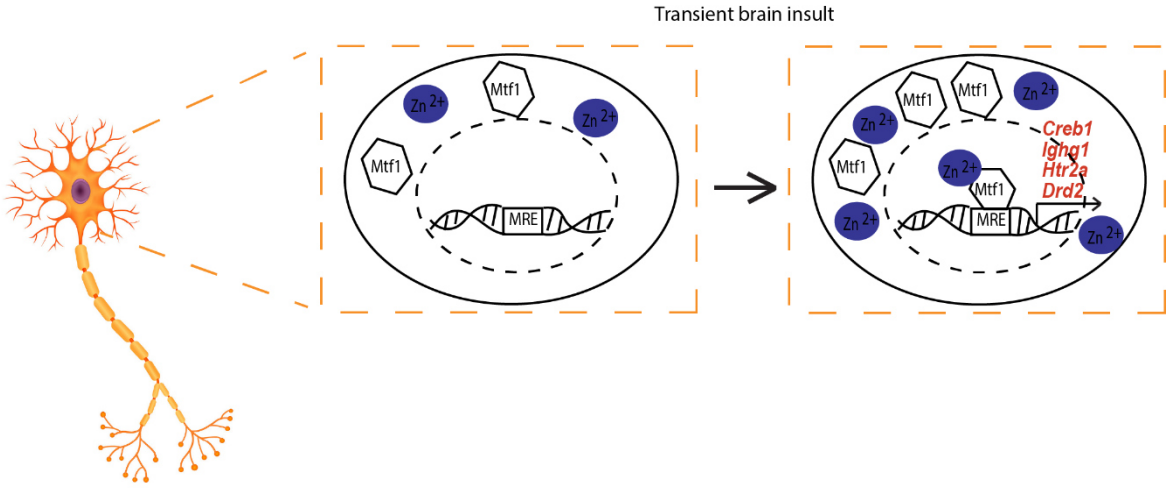

Fig. 21: The Zn^{2+}/Mtf1-cascades of epileptogenesis. The early activation of Mtf1 after a transient brain insult triggers abnormal transcriptional regulation of its target genes. Besides *Canca1h*, the Mtf1/Zn^{2+} cascade may regulate additional target genes, including *Creb1, Ighg1, Htr2a* and *Drd2,* genes involved in synaptic plasticity, thus, promoting hippocampal network hyperexcitability and seizures development.

5. Abstract

Temporal lobe epilepsy (TLE) is the most common form of focal epilepsy. It usually occurs after a transient brain insult, including status epilepticus (SE), which triggers a latent period of epileptogenesis prior to the occurrence of spontaneous seizures. In an experimental animal model, the Metal-regulatory Transcription Factor 1 (Mtf1) mediates the Zn^{2+}-induced upregulation of the T-type Ca^{2+} channel $Ca_V3.2$, leading to an increase in intrinsic excitability of hippocampal neurons. However, Mtf1 emerged relatively recently as a pathogenetically relevant factor involved in the development of TLE and still little is known about its involvement in the process of epileptogenesis. Therefore, in this study we aim to achieve novel insights about Mtf1 with regard to its spatio-temporal location and activation during epileptogenesis, and to identify new Mtf1-downstream targets. Here, we provide evidence that Mtf1 is activated immediately after SE, and that it regulates several genes associated with synaptic plasticity processes. A transcriptional unit was successfully developed which allowed the identification of Mtf1-expressing neurons *in vivo* and the monitoring of Mtf1 activation during epileptogenesis. Adeno-associated virus (rAAV) transfer of Mtf1 and a dominant-negative form of Mtf1 (dnMtf1) in hippocampal neurons resulted in an increase of cAMP responsive element binding protein 1 (Creb1) mRNA expression. The kinetics of Creb1 expression followed the expression levels of Mtf1 in the hippocampal subregions of pilocarpine-SE animals. Immunofluorescence of murine slices showed a stronger Creb1 protein expression in neurons containing nuclear-activated Mtf1. Data from resected hippocampi of pharmacoresistant patients affected by TLE associated with hippocampal sclerosis support the Zn^{2+}-Mtf1-Creb1 pathway. Finally, RNA-sequencing from dissected murine hippocampi transduced with Mtf1 and dnMtf1 revealed the Immunoglobulin Heavy Constant Gamma 1 (*Ighg1*), Serotonin 5-HT-2A Receptor (*Htr2a*) and the Dopamine Receptor D2 (*Drd2*) as downstream target genes of Mtf1. This work uncovered a novel transcription factor regulated transcript module in the process of epileptogenesis and provides new prospects for preventing and treating TLE.

6. List of Figures

7. List of Tables

8. References

Aarli JA 1976. “Changes in Serum Immunoglobulin Levels during Phenytoin Treatment of Epilepsy.” *Acta Neurologica Scandinavica* 54 (5): 423–430

Afrin LB 2010. “Fatal Copper Deficiency from Excessive Use of Zinc-Based Denture Adhesive.” *The American Journal of the Medical Sciences* 340 (2): 164–168

Aghajanian GK, Marek GJ. 1997. “Serotonin Induces Excitatory Postsynaptic Potentials in Apical Dendrites of Neocortical Pyramidal Cells.” *Neuropharmacology* 36 (4–5): 589–599

Aghajanian GK, Marek GJ. 1999. “Serotonin, via 5-HT2A Receptors, Increases EPSCs in Layer V Pyramidal Cells of Prefrontal Cortex by an Asynchronous Mode of Glutamate Release.” *Brain Research* 825 (1–2): 161–171

Agoston A, Kunz L, Krieger A, Mayerhofer A. 2004. “Two Types of Calcium Channels in Human Ovarian Endocrine Cells: Involvement in Steroidogenesis.” *The Journal of Clinical Endocrinology and Metabolism* 89 (9): 4503–4512

Ahmed Juvale II, Che Has AT. 2020. “The Evolution of the Pilocarpine Animal Model of Status Epilepticus.” *Heliyon* 6 (7): e04557.

Alexander SP, Mathie A, Peters JA. 2011. “Guide to Receptors and Channels (GRAC), 5th Edition.” *British Journal of Pharmacology* 164 Suppl 1 (Suppl 1): S1-324.

Altman J, Bayer SA. 1990. “Migration and Distribution of Two Populations of Hippocampal Granule Cell Precursors during the Perinatal and Postnatal Periods.” *The Journal of Comparative Neurology* 301 (3): 365–381

Ambrosini G, Vorontsov I, Penzar D, Groux R, Fornes O, Nikolaeva DD, Ballester B, Grau J, Grosse I, Makeev V., Kulakovskiy I, Bucher P. 2020. “Insights Gained from a Comprehensive All-against-All Transcription Factor Binding Motif Benchmarking Study.” *Genome Biology* 21 (1): 114. https://doi.org/10.1186/s13059-020-01996-3.

Andrews RC. 1992. “Diabetes and Schizophrenia: Genes or Zinc Deficiency?” *Lancet (London, England)* 340 (8828): 1160

Arnold EC, McMurray C, Gray R, Johnston D. 2019. “Epilepsy-Induced Reduction in HCN Channel Expression Contributes to an Increased Excitability in Dorsal, But Not Ventral, Hippocampal CA1 Neurons.” *ENeuro* 6 (2): ENEURO.0036-19.2019

Astori S, Wimmer RD, Prosser HM, Corti C, Corsi M, Liaudet N, Volterra A, Franken P, Adelman JP, Lüthi A. 2011. “The Ca(V)3.3 Calcium Channel Is the Major Sleep Spindle Pacemaker in Thalamus.” *Proceedings of the National Academy of Sciences of the United States of America* 108 (33): 13823–13828

Atlas D. 2013. “The Voltage-Gated Calcium Channel Functions as the Molecular Switch of Synaptic Transmission.” *Annual Review of Biochemistry* 82: 607–635

Augustin I, Rosenmund C, Südhof TC, Brose N. 1999. “Munc13-1 Is Essential for Fusion Competence of Glutamatergic Synaptic Vesicles.” *Nature* 400 (6743): 457–461

Babaeva EE, Vorobyova UA, Denisova EA, Medvedeva DA, Cheknev SB. 2006. “Binding of Zinc Cations to Human Serum Gamma-Globulin.” *Bulletin of Experimental Biology and Medicine* 141 (5): 602–605

Babb TL, Brown WJ, Pretorius J, Davenport C, Lieb JP, Crandall PH. 1984. “Temporal Lobe Volumetric Cell Densities in Temporal Lobe Epilepsy.” *Epilepsia* 25 (6): 729–740

Bahadorani S, Mukai S, Egli D, Hilliker AJ. 2010. “Overexpression of Metal-Responsive Transcription Factor (MTF-1) in Drosophila Melanogaster Ameliorates Life-Span Reductions Associated with Oxidative Stress and Metal Toxicity.” *Neurobiology of Aging* 31 (7): 1215–1226

Barco A, Pittenger C, Kandel ER. 2003. “CREB, Memory Enhancement and the Treatment of Memory Disorders: Promises, Pitfalls and Prospects.” *Expert Opinion on Therapeutic Targets* 7 (1): 101–114

Bartolotti N, Lazarov O. 2019. “CREB Signals as PBMC-Based Biomarkers of Cognitive Dysfunction: A Novel Perspective of the Brain-Immune Axis.” *Brain, Behavior, and Immunity* 78 (May): 9–20

Beaumont TL, Yao B, Shah A, Kapatos G, Loeb JA. 2012. “Layer-Specific CREB Target Gene Induction in Human Neocortical Epilepsy.” *The Journal of Neuroscience: The Official Journal of the Society for Neuroscience* 32 (41): 14389–14401

Beck H, Steffens R, Elger CE, Heinemann U. 1998. “Voltage-Dependent Ca2+ Currents in Epilepsy.” *Epilepsy Research* 32 (1–2): 321–332

Beck H, Yaari Y. 2008. “Plasticity of Intrinsic Neuronal Properties in CNS Disorders.” *Nature Reviews. Neuroscience* 9 (5): 357–369

Becker AJ, Pitsch J, Sochivko D, Opitz T, Staniek M, Chen CC, Campbell KP, Schoch S, Yaari Y, Beck H. 2008. “Transcriptional Upregulation of Cav3.2 Mediates Epileptogenesis in the Pilocarpine Model of Epilepsy.” *The Journal of Neuroscience: The Official Journal of the Society for Neuroscience* 28 (49): 13341–13353

Bellingham SA, Coleman LA, Masters CL, Camakaris J, Hill AF. 2009. “Regulation of Prion Gene Expression by Transcription Factors SP1 and Metal Transcription Factor-1.” *The Journal of Biological Chemistry* 284 (2): 1291–1301

Berg AT, Berkovic SF, Brodie MJ, Buchhalter J, Cross JH, van Emde Boas W, Engel J, French J, Glauser TA, Mathern GW, Moshé SL, Nordli D, Plouin P, Scheffer IE 2010. “Revised Terminology and Concepts for Organization of Seizures and Epilepsies: Report of the ILAE Commission on Classification and Terminology, 2005-2009.” *Epilepsia* 51 (4): 676–685

Berger TC, Vigeland MD, Hjorthaug HS, Etholm L, Nome CG, Taubøll E, Heuser K, Selmer KK. 2019. “Neuronal and Glial DNA Methylation and Gene Expression Changes in Early Epileptogenesis.” *PloS One* 14 (12): e0226575

Bernard C, Anderson A, Becker AJ, Poolos NP, Beck H, Johnston D. 2004. “Acquired Dendritic Channelopathy in Temporal Lobe Epilepsy.” *Science (New York, N.Y.)* 305 (5683): 532–535

Bien CG, Urbach H, Schramm J, Soeder BM, Becker AJ, Voltz R, Vincent A, Elger CE. 2007. “Limbic Encephalitis as a Precipitating Event in Adult-Onset Temporal Lobe Epilepsy.” *Neurology* 69 (12): 1236–1244

Bien CG, Elger CE. 2007. “Limbic Encephalitis: A Cause of Temporal Lobe Epilepsy with Onset in Adult Life.” *Epilepsy & Behavior: E&B* 10 (4): 529–538

Black MM. 1998. “Zinc Deficiency and Child Development.” *The American Journal of Clinical Nutrition* 68 (2 Suppl): 464S-469S

Blakemore LJ, Trombley PQ. 2017. “Zinc as a Neuromodulator in the Central Nervous System with a Focus on the Olfactory Bulb.” *Frontiers in Cellular Neuroscience* 11: 297

Blümcke I, Beck H, Lie AA, Wiestler OD. 1999. “Molecular Neuropathology of Human Mesial Temporal Lobe Epilepsy.” *Epilepsy Research* 36 (2–3): 205–223

Blümcke I, Becker AJ, Klein C, Scheiwe C, Lie AA, Beck H, Waha A, Friedl MG, Kuhn R, Emson P, Elger C, Wiestler OD. 2000. “Temporal Lobe Epilepsy Associated Up-Regulation of Metabotropic Glutamate Receptors: Correlated Changes in MGluR1 MRNA and Protein Expression in Experimental Animals and Human Patients.” *Journal of Neuropathology and Experimental Neurology* 59 (1): 1–10

Bonni A, Brunet A, West AE, Datta SR, Takasu MA, Greenberg ME. 1999. “Cell Survival Promoted by the Ras-MAPK Signaling Pathway by Transcription-Dependent and -Independent Mechanisms.” *Science (New York, N.Y.)* 286 (5443): 1358–1362

Bouilleret V, Loup F, Kiener T, Marescaux C, Fritschy JM. 2000. “Early Loss of Interneurons and Delayed Subunit-Specific Changes in GABA(A)-Receptor Expression in a Mouse Model of Mesial Temporal Lobe Epilepsy.” *Hippocampus* 10 (3): 305–324

Bourinet E, Alloui A, Monteil A, Barrère C, Couette B, Poirot O, Pages A, McRory J, Snutch TP, Eschalier A, Nargeot J. 2005. “Silencing of the Cav3.2 T-Type Calcium Channel Gene in Sensory Neurons Demonstrates Its Major Role in Nociception.” *The EMBO Journal* 24 (2): 315–324

Bozzi Y, Vallone D, Borrelli E. 2000. “Neuroprotective Role of Dopamine against Hippocampal Cell Death.” *The Journal of Neuroscience: The Official Journal of the Society for Neuroscience* 20 (22): 8643–8649

Bozzi Y, Borrelli E. 2013. “The Role of Dopamine Signaling in Epileptogenesis.” *Frontiers in Cellular Neuroscience* 7 (September): 157

Brodovskaya A, Shiono S, Kapur J. 2021. “Activation of the Basal Ganglia and Indirect Pathway Neurons during Frontal Lobe Seizures.” *Brain: A Journal of Neurology* 144 (7): 2074–2091

Brooks-Kayal AR. 2005. “Rearranging Receptors.” *Epilepsia* 46 Suppl 7: 29–38

Brooks-Kayal AR, Raol YH, Russek SJ. 2009. “Alteration of Epileptogenesis Genes.” *Neurotherapeutics: The Journal of the American Society for Experimental NeuroTherapeutics* 6 (2): 312–318

Brugnera E, Georgiev O, Radtke F, Heuchel R, Baker E, Sutherland GR, Schaffner W. 1994. “Cloning, Chromosomal Mapping and Characterization of the Human Metal-Regulatory Transcription Factor MTF-1.” *Nucleic Acids Research* 22 (15): 3167–3173

Bunda A, LaCarubba B, Bertolino M, Akiki M, Bath K, Lopez-Soto J, Lipscombe D, Andrade A. 2019. “Cacna1b Alternative Splicing Impacts Excitatory Neurotransmission and Is Linked to Behavioral Responses to Aversive Stimuli.” *Molecular Brain* 12 (1): 81

Büsselberg D, Michael D, Evans ML, Carpenter DO, Haas HL. 1992. “Zinc (Zn2+) Blocks Voltage Gated Calcium Channels in Cultured Rat Dorsal Root Ganglion Cells.” *Brain Research* 593 (1): 77–81

Cain SM, Snutch TP. 2010. “Contributions of T-Type Calcium Channel Isoforms to Neuronal Firing.” *Channels (Austin, Tex.)* 4 (6): 475–82

Cajal SR. 1913. “Estudios Sobre La Degeneración y Regeneración Del Sistema Nervioso,” 1914 1913, London: Oxford University Press, 1928. edition.

Callenbach PMC, Jol-Van Der Zijde CM, Geerts AT, Arts WFM, Van Donselaar CA, Peters ACB, Stroink H, Brouwer OF, Van Tol MJD; Dutch Study of Epilepsy in Childhood. 2003. “Immunoglobulins in Children with Epilepsy: The Dutch Study of Epilepsy in Childhood.” *Clinical and Experimental Immunology* 132 (1): 144–151

Catalanotto C, Cogoni C, Zardo G. 2016. “MicroRNA in Control of Gene Expression: An Overview of Nuclear Functions.” *International Journal of Molecular Sciences* 17 (10): 1712

Catterall WA. 2000. “Structure and Regulation of Voltage-Gated Ca2+ Channels.” *Annual Review of Cell and Developmental Biology* 16: 521–555.

Catterall WA. 2011. “Voltage-Gated Calcium Channels.” *Cold Spring Harbor Perspectives in Biology* 3 (8): a003947

Cembrowski MS, Bachman JL, Wang L, Sugino K, Shields BC, Spruston N. 2016. “Spatial Gene-Expression Gradients Underlie Prominent Heterogeneity of CA1 Pyramidal Neurons.” *Neuron* 89 (2): 351–368

Chang KY, Park YG, Park HY, Homanics GE, Kim J, Kim D. 2011. “Lack of CaV3.1 Channels Causes Severe Motor Coordination Defects and an Age-Dependent Cerebellar Atrophy in a Genetic Model of Essential Tremor.” *Biochemical and Biophysical Research Communications* 410 (1): 19–23

Chao MV. 2003. “Neurotrophins and Their Receptors: A Convergence Point for Many Signalling Pathways.” *Nature Reviews. Neuroscience* 4 (4): 299–309

Chemin J, Monteil A, Perez-Reyes E, Nargeot J, Lory P. 2001. “Direct Inhibition of T-Type Calcium Channels by the Endogenous Cannabinoid Anandamide.” *The EMBO Journal* 20 (24): 7033–7040

Chemin J, Cazade M, Lory P. 2014. “Modulation of T-Type Calcium Channels by Bioactive Lipids.” *Pflugers Archiv: European Journal of Physiology* 466 (4): 689–700

Chemin J, Nargeot J, Lory P. 2007. “Chemical Determinants Involved in Anandamide-Induced Inhibition of T-Type Calcium Channels.” *The Journal of Biological Chemistry* 282 (4): 2314–2323

Chemin J, Siquier-Pernet K, Nicouleau M, Barcia G, Ahmad A, Medina-Cano D, Hanein S, Altin N, Hubert L, Bole-Feysot C, Fourage C, Nitschké P, Thevenon J, Rio M, Blanc P, Vidal C, Bahi-Buisson N, Desguerre I, Munnich A, Lyonnet S, Boddaert N, Fassi E, Shinawi M, Zimmerman H, Amiel J, Faivre L, Colleaux L, Lory P,

Cantagrel V. 2018. “De Novo Mutation Screening in Childhood-Onset Cerebellar Atrophy Identifies Gain-of-Function Mutations in the CACNA1G Calcium Channel Gene.” *Brain: A Journal of Neurology* 141 (7): 1998–2013

Chemin J, Stamenic TT, Cazade M, Llinares J, Blesneac I, Todorovic SM, Lory P. 2019. “A Novel Phospho-Modulatory Mechanism Contributes to the Calcium-Dependent Regulation of T-Type Ca2+ Channels.” *Scientific Reports* 9 (1): 15642

Chen CC, Shen JW, Chung NC, Min MY, Cheng SJ, Liu IY. 2012. “Retrieval of Context-Associated Memory Is Dependent on the Ca(v)3.2 T-Type Calcium Channel.” *PloS One* 7 (1): e29384

Chen G, Kittler JT, Moss SJ, Yan Z. 2006. “Dopamine D3 Receptors Regulate GABAA Receptor Function through a Phospho-Dependent Endocytosis Mechanism in Nucleus Accumbens.” *The Journal of Neuroscience: The Official Journal of the Society for Neuroscience* 26 (9): 2513–2521

Chen X L, Bayliss DA, Fern RJ, Barrett PQ. 1999. “A Role for T-Type Ca2+ Channels in the Synergistic Control of Aldosterone Production by ANG II and K+.” *The American Journal of Physiology* 276 (5): F674-683

Chen X, Tomchick DR, Kovrigin E, Araç D, Machius M, Südhof TC, Rizo J. 2002. “Three-Dimensional Structure of the Complexin/SNARE Complex.” *Neuron* 33 (3): 397–409

Choi S, Na HS, Kim J, Lee J, Lee S, Kim D, Park J, Chen CC, Campbell KP, Shin HS. 2007. “Attenuated Pain Responses in Mice Lacking Ca(V)3.2 T-Type Channels.” *Genes, Brain, and Behavior* 6 (5): 425–431

Choi S, Bird AJ. 2014. “Zinc’ing Sensibly: Controlling Zinc Homeostasis at the Transcriptional Level.” *Metallomics: Integrated Biometal Science* 6 (7): 1198–1215

Clusmann H, Kral T, Fackeldey E, Blümcke I, Helmstaedter C, von Oertzen J, Urbach H, Schramm J. 2004. “Lesional Mesial Temporal Lobe Epilepsy and Limited Resections: Prognostic Factors and Outcome.” *Journal of Neurology, Neurosurgery, and Psychiatry* 75 (11): 1589–1596

Conte G, Parras A, Alves M, Ollà I, De Diego-Garcia L, Beamer E, Alalqam R, Ocampo A, Mendez R, Henshall DC, Lucas JJ, Engel T. 2020. “High Concordance between Hippocampal Transcriptome of the Mouse Intra-Amygdala Kainic Acid Model and Human Temporal Lobe Epilepsy.” *Epilepsia* 61 (12): 2795–2810

Coutelier M, Blesneac I, Monteil A, Monin ML, Ando K, Mundwiller E, Brusco A, Le Ber I, Anheim M, Castrioto A, Duyckaerts C, Brice A, Durr A, Lory P, Stevanin G. 2015. “A Recurrent Mutation in CACNA1G Alters Cav3.1 T-Type Calcium-Channel Conduction and Causes Autosomal-Dominant Cerebellar Ataxia.” *American Journal of Human Genetics* 97 (5): 726–737

Cribbs LL, Lee JH, Yang J, Satin J, Zhang Y, Daud A, Barclay J, Williamson MP, Fox M, Rees M, Perez-Reyes E. 1998. “Cloning and Characterization of Alpha1H from Human Heart, a Member of the T-Type Ca2+ Channel Gene Family.” *Circulation Research* 83 (1): 103–109

Daniels PJ, Andrews GK. 2003. “Dynamics of the Metal-Dependent Transcription Factor Complex in Vivo at the Mouse Metallothionein-I Promoter.” *Nucleic Acids Research* 31 (23): 6710–6721

De Deyn PP, D'Hooge R, Marescau B, Pei YQ. 1992. “Chemical Models of Epilepsy with Some Reference to Their Applicability in the Development of Anticonvulsants.” *Epilepsy Research* 12 (2): 87–110

Dhir A. 2012. “Pentylenetetrazol (PTZ) Kindling Model of Epilepsy.” *Current Protocols in Neuroscience* Chapter 9: Unit9.37

Diering GH, Huganir RL. 2018. “The AMPA Receptor Code of Synaptic Plasticity.” *Neuron* 100 (2): 314–329

Dong Y, Green T, Saal D, Marie H, Neve R, Nestler EJ, Malenka RC. 2006. “CREB Modulates Excitability of Nucleus Accumbens Neurons.” *Nature Neuroscience* 9 (4): 475–477

Dong ZF, Tang LJ, Deng GF, Zeng T, Liu SJ, Wan RP, Liu T, Zhao QH, Yi YH, Liao WP, Long YS. 2014. “Transcription of the Human Sodium Channel SCN1A Gene Is

Repressed by a Scaffolding Protein RACK1." *Molecular Neurobiology* 50 (2): 438–448

Du F, Whetsell WO Jr, Abou-Khalil B, Blumenkopf B, Lothman EW, Schwarcz R. 1993. "Preferential Neuronal Loss in Layer III of the Entorhinal Cortex in Patients with Temporal Lobe Epilepsy." *Epilepsy Research* 16 (3): 223–233

Dubé A, Harrisson JF, Saint-Gelais G, Séguin C. 2011. "Hypoxia Acts through Multiple Signaling Pathways to Induce Metallothionein Transactivation by the Metal-Responsive Transcription Factor-1 (MTF-1)." *Biochemistry and Cell Biology = Biochimie Et Biologie Cellulaire* 89 (6): 562–577

Duclot F, Kabbaj M. 2017. "The Role of Early Growth Response 1 (EGR1) in Brain Plasticity and Neuropsychiatric Disorders." *Frontiers in Behavioral Neuroscience* 11: 35

Durnam DM, Palmiter RD. 1981. "Transcriptional Regulation of the Mouse Metallothionein-I Gene by Heavy Metals." *The Journal of Biological Chemistry* 256 (11): 5712–5716.

El Ghaleb Y, Schneeberger PE, Fernández-Quintero ML, Geisler SM, Pelizzari S, Polstra AM, van Hagen JM, Denecke J, Campiglio M, Liedl KR, Stevens CA, Person RE, Rentas S, Marsh ED, Conlin LK, Tuluc P, Kutsche K, Flucher BE. 2021. "CACNA1I Gain-of-Function Mutations Differentially Affect Channel Gating and Cause Neurodevelopmental Disorders." *Brain: A Journal of Neurology* 144 (7): 2092–2106

Elliott RC, Miles MF, Lowenstein DH. 2003. "Overlapping Microarray Profiles of Dentate Gyrus Gene Expression during Development- and Epilepsy-Associated Neurogenesis and Axon Outgrowth." *The Journal of Neuroscience: The Official Journal of the Society for Neuroscience* 23 (6): 2218–2227

Engel J. 1993. "Appendix II: Presurgical Evaluation Protocols." In *Surgical Treatment of the Epilepsies*, 2nd ed., 707–50. New York: Raven Press.

Engel J. 1996. "Introduction to Temporal Lobe Epilepsy." *Epilepsy Research* 26 (1): 141–150

Engel J. 2003. “A Greater Role for Surgical Treatment of Epilepsy: Why and When?” *Epilepsy Currents* 3 (2): 37–40

Ernst WL, Zhang Y, Yoo JW, Ernst SJ, Noebels JL. 2009. “Genetic Enhancement of Thalamocortical Network Activity by Elevating Alpha 1g-Mediated Low-Voltage-Activated Calcium Current Induces Pure Absence Epilepsy.” *The Journal of Neuroscience: The Official Journal of the Society for Neuroscience* 29 (6): 1615–1625

Escamilla CO, Filonova I, Walker AK, Xuan ZX, Holehonnur R, Espinosa F, Liu S, Thyme SB, López-García IA, Mendoza DB, Usui N, Ellegood J, Eisch AJ, Konopka G, Lerch JP, Schier AF, Speed HE, Powell CM. 2017. “Kctd13 Deletion Reduces Synaptic Transmission via Increased RhoA.” *Nature* 551 (7679): 227–231

Favale E, Audenino D, Cocito L, Albano C. 2003. “The Anticonvulsant Effect of Citalopram as an Indirect Evidence of Serotonergic Impairment in Human Epileptogenesis.” *Seizure* 12 (5): 316–318

Feng Y, Yang H, Yue Y, Tian F. 2020. “MicroRNAs and Target Genes in Epileptogenesis.” *Epilepsia* 61 (10): 2086–2096

Filonov GS, Piatkevich KD, Ting LM, Zhang J, Kim K, Verkhusha VV. 2011. “Bright and Stable Near-Infrared Fluorescent Protein for in Vivo Imaging.” *Nature Biotechnology* 29 (8): 757–761

Fisher RS, Cross JH, French JA, Higurashi N, Hirsch E, Jansen FE, Lagae L, Moshé SL, Peltola J, Roulet Perez E, Scheffer IE, Zuberi SM. 2017. “Operational Classification of Seizure Types by the International League Against Epilepsy: Position Paper of the ILAE Commission for Classification and Terminology.” *Epilepsia* 58 (4): 522–530

Földy C, Darmanis S, Aoto J, Malenka RC, Quake SR, Südhof TC. 2016. “Single-Cell RNAseq Reveals Cell Adhesion Molecule Profiles in Electrophysiologically Defined Neurons.” *Proceedings of the National Academy of Sciences of the United States of America* 113 (35): E5222-5231

Fontana A, Grob PJ, Sauter R, Joller H. 1976. “IgA Deficiency, Epilepsy, and Hydantoin Medication.” *Lancet (London, England)* 2 (7979): 228–231

Ford CP. 2014. “The Role of D2-Autoreceptors in Regulating Dopamine Neuron Activity and Transmission.” *Neuroscience* 282 (December): 13–22

Franco-Pons N, Casanovas-Aguilar C, Arroyo S, Rumià J, Pérez-Clausell J, Danscher G 2000. “Zinc-Rich Synaptic Boutons in Human Temporal Cortex Biopsies.” *Neuroscience* 98 (3): 429–435

Friedman LK, Pellegrini-Giampietro DE, Sperber EF, Bennett MV, Moshé SL, Zukin RS. 1994. “Kainate-Induced Status Epilepticus Alters Glutamate and GABAA Receptor Gene Expression in Adult Rat Hippocampus: An in Situ Hybridization Study.” *The Journal of Neuroscience: The Official Journal of the Society for Neuroscience* 14 (5 Pt 1): 2697–2707

Fritsch B, Stott JJ, Joelle Donofrio J, Rogawski MA. 2010. “Treatment of Early and Late Kainic Acid-Induced Status Epilepticus with the Noncompetitive AMPA Receptor Antagonist GYKI 52466.” *Epilepsia* 51 (1): 108–117

Gao H, Dai W, Zhao L, Min J, Wang F. 2018. “The Role of Zinc and Zinc Homeostasis in Macrophage Function.” *Journal of Immunology Research* 2018: 6872621

García-Caballero A, Gadotti VM, Stemkowski P, Weiss N, Souza IA, Hodgkinson V, Bladen C, Chen L, Hamid J, Pizzoccaro A, Deage M, François A, Bourinet E, Zamponi GW. 2014. “The Deubiquitinating Enzyme USP5 Modulates Neuropathic and Inflammatory Pain by Enhancing Cav3.2 Channel Activity.” *Neuron* 83 (5): 1144–1158

Gloor P, Olivier A, Quesney LF, Andermann F, Horowitz S. 1982. “The Role of the Limbic System in Experiential Phenomena of Temporal Lobe Epilepsy.” *Annals of Neurology* 12 (2): 129–144

Grabenstatter HL, Cogswell M, Cruz Del Angel Y, Carlsen J, Gonzalez MI, Raol YH, Russek SJ, Brooks-Kayal AR. 2014. “Effect of Spontaneous Seizures on GABAA Receptor A4 Subunit Expression in an Animal Model of Temporal Lobe Epilepsy.” *Epilepsia* 55 (11): 1826–1833

Graef JD, Godwin DW. 2010. “Intrinsic Plasticity in Acquired Epilepsy: Too Much of a Good Thing?” *The Neuroscientist: A Review Journal Bringing Neurobiology, Neurology and Psychiatry* 16 (5): 487–495

Grazzini E, Durroux T, Payet MD, Bilodeau L, Gallo-Payet N, Guillon G. 1996. “Membrane-Delimited G Protein-Mediated Coupling between V1a Vasopressin Receptor and Dihydropyridine Binding Sites in Rat Glomerulosa Cells.” *Molecular Pharmacology* 50 (5): 1273–1283

Gross C, Yao X, Engel T, Tiwari D, Xing L, Rowley S, Danielson SW, Thomas KT, Jimenez-Mateos EM, Schroeder LM, Pun RYK, Danzer SC, Henshall DC, Bassell GJ. 2016. “MicroRNA-Mediated Downregulation of the Potassium Channel Kv4.2 Contributes to Seizure Onset.” *Cell Reports* 17 (1): 37–45

Grzywacz A, Gdula-Argasińska J, Muszyńska B, Tyszka-Czochara M, Librowski T, Opoka W. 2015. “Metal Responsive Transcription Factor 1 (MTF-1) Regulates Zinc Dependent Cellular Processes at the Molecular Level.” *Acta Biochimica Polonica* 62 (3): 491–498

Guiard BP, Di Giovanni G. 2015. “Central Serotonin-2A (5-HT2A) Receptor Dysfunction in Depression and Epilepsy: The Missing Link?” *Frontiers in Pharmacology* 6: 46

Gulsuner S, Walsh T, Watts AC, Lee MK, Thornton AM, Casadei S, Rippey C, Shahin H; Consortium on the Genetics of Schizophrenia (COGS); PAARTNERS Study Group; Nimgaonkar VL, Go RC, Savage RM, Swerdlow NR, Gur RE, Braff DL, King MC, McClellan JM. 2013. “Spatial and Temporal Mapping of de Novo Mutations in Schizophrenia to a Fetal Prefrontal Cortical Network.” *Cell* 154 (3): 518–529

Günes C, Heuchel R, Georgiev O, Müller KH, Lichtlen P, Blüthmann H, Marino S, Aguzzi A, Schaffner W. 1998. “Embryonic Lethality and Liver Degeneration in Mice Lacking the Metal-Responsive Transcriptional Activator MTF-1.” *The EMBO Journal* 17 (10): 2846–2854

Günther V, Lindert U, Schaffner W. 2012. “The Taste of Heavy Metals: Gene Regulation by MTF-1.” *Biochimica Et Biophysica Acta* 1823 (9): 1416–1425

Guo L, Lichten LA, Ryu MS, Liuzzi JP, Wang F, Cousins RJ. 2010. “STAT5-Glucocorticoid Receptor Interaction and MTF-1 Regulate the Expression of ZnT2 (Slc30a2) in Pancreatic Acinar Cells.” *Proceedings of the National Academy of Sciences of the United States of America* 107 (7): 2818–2823

Haase H, Ober-Blöbaum JL, Engelhardt G, Hebel S, Heit A, Heine H, Rink L. 2008. “Zinc Signals Are Essential for Lipopolysaccharide-Induced Signal Transduction in Monocytes.” *Journal of Immunology (Baltimore, Md.: 1950)* 181 (9): 6491–6502

Haase H, Rink L. 2007. “Signal Transduction in Monocytes: The Role of Zinc Ions.” *Biometals: An International Journal on the Role of Metal Ions in Biology, Biochemistry, and Medicine* 20 (3–4): 579–585

Hansen KF, Sakamoto K, Pelz C, Impey S, Obrietan K. 2014. “Profiling Status Epilepticus-Induced Changes in Hippocampal RNA Expression Using High-Throughput RNA Sequencing.” *Scientific Reports* 4 (November): 6930

Hansen SL, Sperling BB, Sánchez C. 2004. “Anticonvulsant and Antiepileptogenic Effects of GABAA Receptor Ligands in Pentylenetetrazole-Kindled Mice.” *Progress in Neuro-Psychopharmacology & Biological Psychiatry* 28 (1): 105–113

Hao LY, Zhang M, Tao Y, Xu H, Liu Q, Yang K, Wei R, Zhou H, Jin T, Liu XD, Xue Z, Shen W, Cao JL, Pan Z. 2022. “MiRNA-22 Upregulates Mtf1 in Dorsal Horn Neurons and Is Essential for Inflammatory Pain.” *Oxidative Medicine and Cellular Longevity* 2022: 8622388

Hedera P, Peltier A, Fink JK, Wilcock S, London Z, Brewer GJ. 2009. “Myelopolyneuropathy and Pancytopenia Due to Copper Deficiency and High Zinc Levels of Unknown Origin II. The Denture Cream Is a Primary Source of Excessive Zinc.” *Neurotoxicology* 30 (6): 996–999

Henkel ND, Smail MA, Wu X, Enright HA, Fischer NO, Eby HM, McCullumsmith RE, Shukla R. McCullumsmith, and Rammohan Shukla. 2021. “Cellular, Molecular, and Therapeutic Characterization of Pilocarpine-Induced Temporal Lobe Epilepsy.” *Scientific Reports* 11 (1): 19102

Heuchel R, Radtke F, Georgiev O, Stark G, Aguet M, Schaffner W. 1994. “The Transcription Factor MTF-1 Is Essential for Basal and Heavy Metal-Induced Metallothionein Gene Expression.” *The EMBO Journal* 13 (12): 2870–2875

Horn KE, Xu B, Gobert D, Hamam BN, Thompson KM, Wu CL, Bouchard JF, Uetani N, Racine RJ, Tremblay ML, Ruthazer ES, Chapman CA, Kennedy TE 2012. “Receptor Protein Tyrosine Phosphatase Sigma Regulates Synapse Structure, Function and Plasticity.” *Journal of Neurochemistry* 122 (1): 147–161

Hu C, Depuy SD, Yao J, McIntire WE, Barrett PQ. 2009. “Protein Kinase A Activity Controls the Regulation of T-Type CaV3.2 Channels by Gbetagamma Dimers.” *The Journal of Biological Chemistry* 284 (12): 7465–7473

Hu C, Chen W, Myers SJ, Yuan H, Traynelis SF. 2016. “Human GRIN2B Variants in Neurodevelopmental Disorders.” *Journal of Pharmacological Sciences* 132 (2): 115–121

Inukai S, Kock KH, Bulyk ML. 2017. “Transcription Factor-DNA Binding: Beyond Binding Site Motifs.” *Current Opinion in Genetics & Development* 43 (April): 110–119

Jeong SW, Park BG, Park JY, Lee JW, Lee JH. 2003. “Divalent Metals Differentially Block Cloned T-Type Calcium Channels.” *Neuroreport* 14 (11): 1537–1540

Jiang CH, Wei M, Zhang C, Shi YS. 2021. “The Amino-Terminal Domain of GluA1 Mediates LTP Maintenance via Interaction with Neuroplastin-65.” *Proceedings of the National Academy of Sciences of the United States of America* 118 (9): e2019194118

Jin N, Qian W, Yin X, Zhang L, Iqbal K, Grundke-Iqbal I, Gong CX, Liu F. 2013. “CREB Regulates the Expression of Neuronal Glucose Transporter 3: A Possible Mechanism Related to Impaired Brain Glucose Uptake in Alzheimer’s Disease.” *Nucleic Acids Research* 41 (5): 3240–3256

Jing W, Zhang T, Liu J, Huang X, Yu Q, Yu H, Zhang Q, Li H, Deng M, Zhu LQ, Du H, Lu Y. 2021. “A Circuit of COCH Neurons Encodes Social-Stress-Induced Anxiety via MTF1 Activation of Cacna1h.” *Cell Reports* 37 (13): 110177

Kagi JH, Valee BL. 1960. “Metallothionein: A Cadmium- and Zinc-Containing Protein from Equine Renal Cortex.” *The Journal of Biological Chemistry* 235 (December): 3460–3465

Kale R. 1997. “Bringing Epilepsy out of the Shadows.” *BMJ (Clinical Research Ed.)* 315 (7099): 2–3

Kaler P, Prasad R. 2007. “Molecular Cloning and Functional Characterization of Novel Zinc Transporter RZip10 (Slc39a10) Involved in Zinc Uptake across Rat Renal Brush-Border Membrane.” *American Journal of Physiology. Renal Physiology* 292 (1): F217-229

Karin M, Haslinger A, Heguy A, Dietlin T, Cooke T. 1987. “Metal-Responsive Elements Act as Positive Modulators of Human Metallothionein-IIA Enhancer Activity.” *Molecular and Cellular Biology* 7 (2): 606–613

Kaur M, MacPherson CR, Schmeier S, Narasimhan K, Choolani M, Bajic VB. 2011. “In Silico Discovery of Transcription Factors as Potential Diagnostic Biomarkers of Ovarian Cancer.” *BMC Systems Biology* 5 (September): 144

Keilwagen J, Grau J. 2015. “Varying Levels of Complexity in Transcription Factor Binding Motifs.” *Nucleic Acids Research* 43 (18): e119

Kessels HW, Malinow R. 2009. “Synaptic AMPA Receptor Plasticity and Behavior.” *Neuron* 61 (3): 340–350

Kim CH. 2015. “Cav3.1 T-Type Calcium Channel Modulates the Epileptogenicity of Hippocampal Seizures in the Kainic Acid-Induced Temporal Lobe Epilepsy Model.” *Brain Research* 1622 (October): 204–216

Kim DY, Carey BW, Wang H, Ingano LA, Binshtok AM, Wertz MH, Pettingell WH, He P, Lee VM, Woolf CJ, Kovacs DM 2007. “BACE1 Regulates Voltage-Gated Sodium Channels and Neuronal Activity.” *Nature Cell Biology* 9 (7): 755–764

Kim JH, Guimaraes PO, Shen MY, Masukawa LM, Spencer DD. 1990. “Hippocampal Neuronal Density in Temporal Lobe Epilepsy with and without Gliomas.” *Acta Neuropathologica* 80 (1): 41–45

Kim J, Kwon JT, Kim HS, Han JH. 2013. “CREB and Neuronal Selection for Memory Trace.” *Frontiers in Neural Circuits* 7: 44

Kiraly DD, Lemtiri-Chlieh F, Levine ES, Mains RE, Eipper BA. 2011. “Kalirin Binds the NR2B Subunit of the NMDA Receptor, Altering Its Synaptic Localization and Function.” *The Journal of Neuroscience: The Official Journal of the Society for Neuroscience* 31 (35): 12554–12565

Kitsis RN, Leinwand LA. 1992. “Discordance between Gene Regulation in Vitro and in Vivo.” *Gene Expression* 2 (4): 313–318

Konopka G, Wexler E, Rosen E, Mukamel Z, Osborn GE, Chen L, Lu D, Gao F, Gao K, Lowe JK, Geschwind DH. 2012. “Modeling the Functional Genomics of Autism Using Human Neurons.” *Molecular Psychiatry* 17 (2): 202–214

Kotagal P, Lüders HO, Williams G, Nichols TR, McPherson J. 1995. “Psychomotor Seizures of Temporal Lobe Onset: Analysis of Symptom Clusters and Sequences.” *Epilepsy Research* 20 (1): 49–67

Krahe R, Gabbiani F. 2004. “Burst Firing in Sensory Systems.” *Nature Reviews. Neuroscience* 5 (1): 13–23

Kral T, Clusmann H, Urbach J, Schramm J, Elger CE, Kurthen M, Grunwald T. 2002. “Preoperative Evaluation for Epilepsy Surgery (Bonn Algorithm).” *Zentralblatt Fur Neurochirurgie* 63 (3): 106–110

Kuhn HG, Dickinson-Anson H, Gage FH. 1996. “Neurogenesis in the Dentate Gyrus of the Adult Rat: Age-Related Decrease of Neuronal Progenitor Proliferation.” *The Journal of Neuroscience: The Official Journal of the Society for Neuroscience* 16 (6): 2027–2033

Kulbida R, Wang Y, Mandelkow EM, Schoch S, Becker AJ, van Loo KM. 2015. “Molecular Imaging Reveals Epileptogenic Ca2+-Channel Promoter Activation in Hippocampi of Living Mice.” *Brain Structure & Function* 220 (5): 3067–3073

Kwan P, Sander JW. 2004. “The Natural History of Epilepsy: An Epidemiological View.” *Journal of Neurology, Neurosurgery, and Psychiatry* 75 (10): 1376–1381

Laity JH, Lee BM, Wright PE. 2001. “Zinc Finger Proteins: New Insights into Structural and Functional Diversity.” *Current Opinion in Structural Biology* 11 (1): 39–46

Langmade SJ, Ravindra R, Daniels PJ, Andrews GK. 2000. “The Transcription Factor MTF-1 Mediates Metal Regulation of the Mouse ZnT1 Gene.” *The Journal of Biological Chemistry* 275 (44): 34803–34809

LaRochelle O, Labbé S, Harrisson JF, Simard C, Tremblay V, St-Gelais G, Govindan MV, Séguin C: 2008. “Nuclear Factor-1 and Metal Transcription Factor-1 Synergistically Activate the Mouse Metallothionein-1 Gene in Response to Metal Ions.” *The Journal of Biological Chemistry* 283 (13): 8190–8201

Law CW, Chen Y, Shi W, Smyth GK. 2014. “Voom: Precision Weights Unlock Linear Model Analysis Tools for RNA-Seq Read Counts.” *Genome Biology* 15 (2): R29

Lee B, Cao R, Choi YS, Cho HY, Rhee AD, Hah CK, Hoyt KR, Obrietan K. 2009. “The CREB/CRE Transcriptional Pathway: Protection against Oxidative Stress-Mediated Neuronal Cell Death.” *Journal of Neurochemistry* 108 (5): 1251–1265

Lee B, Dziema H, Lee KH, Choi YS, Obrietan K. 2007. “CRE-Mediated Transcription and COX-2 Expression in the Pilocarpine Model of Status Epilepticus.” *Neurobiology of Disease* 25 (1): 80–91

Lee JH, Daud AN, Cribbs LL, Lacerda AE, Pereverzev A, Klöckner U, Schneider T, Perez-Reyes E. 1999. “Cloning and Expression of a Novel Member of the Low Voltage-Activated T-Type Calcium Channel Family.” *The Journal of Neuroscience: The Official Journal of the Society for Neuroscience* 19 (6): 1912–1921

Lee, J. H., J. C. Gomora, L. L. Cribbs, and E. Perez-Reyes. 1999. “Nickel Block of Three Cloned T-Type Calcium Channels: Low Concentrations Selectively Block Alpha1H.” *Biophysical Journal* 77 (6): 3034–3042

Lemke JR, Hendrickx R, Geider K, Laube B, Schwake M, Harvey RJ, James VM, Pepler A, Steiner I, Hörtnagel K, Neidhardt J, Ruf S, Wolff M, Bartholdi D, Caraballo R, Platzer K, Suls A, De Jonghe P, Biskup S, Weckhuysen S. 2014. “GRIN2B

Mutations in West Syndrome and Intellectual Disability with Focal Epilepsy." *Annals of Neurology* 75 (1): 147–154

Lemtiri-Chlieh F, Zhao L, Kiraly DD, Eipper BA, Mains RE, Levine ES. 2011. "Kalirin-7 Is Necessary for Normal NMDA Receptor-Dependent Synaptic Plasticity." *BMC Neuroscience* 12 (December): 126

Lerche H, Shah M, Beck H, Noebels J, Johnston D, Vincent A. 2013. "Ion Channels in Genetic and Acquired Forms of Epilepsy." *The Journal of Physiology* 591 (4): 753–764

Lévesque M, Avoli M, Bernard C. 2016. "Animal Models of Temporal Lobe Epilepsy Following Systemic Chemoconvulsant Administration." *Journal of Neuroscience Methods* 260 (February): 45–52

Li BX, Gardner R, Xue C, Qian DZ, Xie F, Thomas G, Kazmierczak SC, Habecker BA, Xiao X.. 2016. "Systemic Inhibition of CREB Is Well-Tolerated in Vivo." *Scientific Reports* 6 (October): 34513

Li Y, Kimura T, Huyck RW, Laity JH, Andrews GK. 2008. "Zinc-Induced Formation of a Coactivator Complex Containing the Zinc-Sensing Transcription Factor MTF-1, P300/CBP, and Sp1." *Molecular and Cellular Biology* 28 (13): 4275–4284

Lichten LA, Ryu MS, Guo L, Embury J, Cousins RJ. 2011. "MTF-1-Mediated Repression of the Zinc Transporter Zip10 Is Alleviated by Zinc Restriction." *PloS One* 6 (6): e21526

Lindert U, Cramer M, Meuli M, Georgiev O, Schaffner W. 2009. "Metal-Responsive Transcription Factor 1 (MTF-1) Activity Is Regulated by a Nonconventional Nuclear Localization Signal and a Metal-Responsive Transactivation Domain." *Molecular and Cellular Biology* 29 (23): 6283–6293

Liu B, Hill SJ, Khan RN. 2005. "Oxytocin Inhibits T-Type Calcium Current of Human Decidual Stromal Cells." *The Journal of Clinical Endocrinology and Metabolism* 90 (7): 4191–4197

Liu S, Yu W, Lü Y. 2016. "The Causes of New-Onset Epilepsy and Seizures in the Elderly." *Neuropsychiatric Disease and Treatment* 12: 1425–1434

Lledo PM, Israel JM, Vincent JD. 1990a. “A Guanine Nucleotide-Binding Protein Mediates the Inhibition of Voltage-Dependent Calcium Currents by Dopamine in Rat Lactotrophs.” *Brain Research* 528 (1): 143–147

Lledo PM, Legendre P, Israel JM, Vincent JD.. 1990b. “Dopamine Inhibits Two Characterized Voltage-Dependent Calcium Currents in Identified Rat Lactotroph Cells.” *Endocrinology* 127 (3): 990–1001

van Loo KMJ, Rummel CK, Pitsch J, Müller JA, Bikbaev AF, Martinez-Chavez E, Blaess S, Dietrich D, Heine M, Becker AJ, Schoch S. 2019. “Calcium Channel Subunit A2δ4 Is Regulated by Early Growth Response 1 and Facilitates Epileptogenesis.” *The Journal of Neuroscience: The Official Journal of the Society for Neuroscience* 39 (17): 3175–3187

van Loo KM, Schaub C, Pernhorst K, Yaari Y, Beck H, Schoch S, Becker AJ. 2012. “Transcriptional Regulation of T-Type Calcium Channel CaV3.2: Bi-Directionality by Early Growth Response 1 (Egr1) and Repressor Element 1 (RE-1) Protein-Silencing Transcription Factor (REST).” *The Journal of Biological Chemistry* 287 (19): 15489–14501

van Loo KM, Schaub C, Pitsch J, Kulbida R, Opitz T, Ekstein D, Dalal A, Urbach H, Beck H, Yaari Y, Schoch S, Becker AJ. 2015. “Zinc Regulates a Key Transcriptional Pathway for Epileptogenesis via Metal-Regulatory Transcription Factor 1.” *Nature Communications* 6 (October): 8688.

Lopez de Armentia M, Jancic D, Olivares R, Alarcon JM, Kandel ER, Barco A. 2007. “CAMP Response Element-Binding Protein-Mediated Gene Expression Increases the Intrinsic Excitability of CA1 Pyramidal Neurons.” *The Journal of Neuroscience: The Official Journal of the Society for Neuroscience* 27 (50): 13909–13918

Lory P, Nicole S, Monteil A. 2020. “Neuronal Cav3 Channelopathies: Recent Progress and Perspectives.” *Pflugers Archiv: European Journal of Physiology* 472 (7): 831–844

Löscher W. 2017. “Animal Models of Seizures and Epilepsy: Past, Present, and Future Role for the Discovery of Antiseizure Drugs.” *Neurochemical Research* 42 (7): 1873–1888

Lösing P, Niturad CE, Harrer M, Reckendorf CMZ, Schatz T, Sinske D, Lerche H, Maljevic S, Knöll B. 2017. “SRF Modulates Seizure Occurrence, Activity Induced Gene Transcription and Hippocampal Circuit Reorganization in the Mouse Pilocarpine Epilepsy Model.” *Molecular Brain* 10 (1): 30

Love, MI, Huber W, Anders S. 2014. “Moderated Estimation of Fold Change and Dispersion for RNA-Seq Data with DESeq2.” *Genome Biology* 15 (12): 550

Lowenstein DH, Bleck T, Macdonald RL. 1999. “It’s Time to Revise the Definition of Status Epilepticus.” *Epilepsia* 40 (1): 120–122

Luscher B, Fuchs T, Kilpatrick CL. 2011. “GABAA Receptor Trafficking-Mediated Plasticity of Inhibitory Synapses.” *Neuron* 70 (3): 385–409

Majores M, Schoch S, Lie A, Becker AJ. 2007. “Molecular Neuropathology of Temporal Lobe Epilepsy: Complementary Approaches in Animal Models and Human Disease Tissue.” *Epilepsia* 48 Suppl 2: 4–12

Mangoni ME, Couette B, Marger L, Bourinet E, Striessnig J, Nargeot J. 2006. “Voltage-Dependent Calcium Channels and Cardiac Pacemaker Activity: From Ionic Currents to Genes.” *Progress in Biophysics and Molecular Biology* 90 (1–3): 38–63

Mangoni ME, Traboulsie A, Leoni AL, Couette B, Marger L, Le Quang K, Kupfer E, Cohen-Solal A, Vilar J, Shin HS, Escande D, Charpentier F, Nargeot J, Lory P. 2006. “Bradycardia and Slowing of the Atrioventricular Conduction in Mice Lacking CaV3.1/Alpha1G T-Type Calcium Channels.” *Circulation Research* 98 (11): 1422–1430

Manna I, Labate A, Mumoli L, Palamara G, Ferlazzo E, Aguglia U, Quattrone A, Gambardella A. 2012. “A Functional Genetic Variation of the 5-HTR2A Receptor Affects Age at Onset in Patients with Temporal Lobe Epilepsy.” *Annals of Human Genetics* 76 (4): 277–282

Martin S, Nishimune A, Mellor JR, Henley JM. 2007. “SUMOylation Regulates Kainate-Receptor-Mediated Synaptic Transmission.” *Nature* 447 (7142): 321–325

Martinez B, Peplow PV. 2023. “MicroRNAs as Potential Biomarkers in Temporal Lobe Epilepsy and Mesial Temporal Lobe Epilepsy.” *Neural Regeneration Research* 18 (4): 716–726

McGivern JG. 2006. “Pharmacology and Drug Discovery for T-Type Calcium Channels.” *CNS & Neurological Disorders Drug Targets* 5 (6): 587–603

McHugh, PC, Wright JA, Brown DR. 2011. “Transcriptional Regulation of the Beta-Synuclein 5’-Promoter Metal Response Element by Metal Transcription Factor-1.” *PloS One* 6 (2): e17354

McNamara, JO. 1999. “Emerging Insights into the Genesis of Epilepsy.” *Nature* 399 (6738 Suppl): A15-22

Miller LA, McLachlan RS, Bouwer MS, Hudson LP, Munoz DG. 1994. “Amygdalar Sclerosis: Preoperative Indicators and Outcome after Temporal Lobectomy.” *Journal of Neurology, Neurosurgery, and Psychiatry* 57 (9): 1099–1105

Mishra A, Singh S, Shukla S. 2018. “Physiological and Functional Basis of Dopamine Receptors and Their Role in Neurogenesis: Possible Implication for Parkinson’s Disease.” *Journal of Experimental Neuroscience* 12: 1179069518779829

Misonou H, Mohapatra DP, Park EW, Leung V, Zhen D, Misonou K, Anderson AE, Trimmer JS. 2004. “Regulation of Ion Channel Localization and Phosphorylation by Neuronal Activity.” *Nature Neuroscience* 7 (7): 711–718

Missale C, Nash SR, Robinson SW, Jaber M, Caron MG. 1998. “Dopamine Receptors: From Structure to Function.” *Physiological Reviews* 78 (1): 189–225

Mocchegiani E, Giacconi R, Cipriano C, Gasparini N, Bernardini G, Malavolta M, Menegazzi M, Cavalieri E, Muzzioli M, Ciampa AR, Suzuki H. “The Variations during the Circadian Cycle of Liver CD1d-Unrestricted NK1.1+TCR Gamma/Delta+ Cells Lead to Successful Ageing. Role of Metallothionein/IL-6/Gp130/PARP-1 Interplay in Very Old Mice.” *Experimental Gerontology* 39 (5): 775–788

Monaghan MM, Menegola M, Vacher H, Rhodes KJ, Trimmer JS. 2008. “Altered Expression and Localization of Hippocampal A-Type Potassium Channel Subunits in the Pilocarpine-Induced Model of Temporal Lobe Epilepsy.” *Neuroscience* 156 (3): 550–562

Murray CJ, Lopez AD, Jamison DT. 1994. “The Global Burden of Disease in 1990: Summary Results, Sensitivity Analysis and Future Directions.” *Bulletin of the World Health Organization* 72 (3): 495–509.

Ngugi AK, Bottomley C, Kleinschmidt I, Sander JW, Newton CR. 2010. “Estimation of the Burden of Active and Life-Time Epilepsy: A Meta-Analytic Approach.” *Epilepsia* 51 (5): 883–890

Nguyen KT, Holloway MP, Altura RA. 2012. “The CRM1 Nuclear Export Protein in Normal Development and Disease.” *International Journal of Biochemistry and Molecular Biology* 3 (2): 137–151.

Nilius B, Hess P, Lansman JB, Tsien RW. 1985. “A Novel Type of Cardiac Calcium Channel in Ventricular Cells.” *Nature* 316 (6027): 443–446

Niu RZ, Wang LQ, Yang W, Sun LZ, Tao J, Sun H, Mei S, Wang WJ, Feng KX, Qian DL, Bai XF. 2022. “MicroRNA-582-5p Targeting Creb1 Modulates Apoptosis in Cardiomyocytes Hypoxia/Reperfusion-Induced Injury.” *Immunity, Inflammation and Disease* 10 (11): e708

Nowycky MC, Fox AP, Tsien RW. 1985. “Three Types of Neuronal Calcium Channel with Different Calcium Agonist Sensitivity.” *Nature* 316 (6027): 440–443

Okazaki MM, Evenson DA, Nadler JV. 1995. “Hippocampal Mossy Fiber Sprouting and Synapse Formation after Status Epilepticus in Rats: Visualization after Retrograde Transport of Biocytin.” *The Journal of Comparative Neurology* 352 (4): 515–534

Okumura F, Li Y, Itoh N, Nakanishi T, Isobe M, Andrews GK, Kimura T. 2011. “The Zinc-Sensing Transcription Factor MTF-1 Mediates Zinc-Induced Epigenetic Changes in Chromatin of the Mouse Metallothionein-I Promoter.” *Biochimica Et Biophysica Acta* 1809 (1): 56–62

Onali P, Olianas MC, Bunse B. 1988. “Evidence That Adenosine A2 and Dopamine Autoreceptors Antagonistically Regulate Tyrosine Hydroxylase Activity in Rat Striatal Synaptosomes.” *Brain Research* 456 (2): 302–309

Ortega-Martínez S. 2015. “A New Perspective on the Role of the CREB Family of Transcription Factors in Memory Consolidation via Adult Hippocampal Neurogenesis.” *Frontiers in Molecular Neuroscience* 8: 46

Palmiter RD, Findley SD. 1995. “Cloning and Functional Characterization of a Mammalian Zinc Transporter That Confers Resistance to Zinc.” *The EMBO Journal* 14 (4): 639–649

Parent JM, Yu TW, Leibowitz RT, Geschwind DH, Sloviter RS, Lowenstein DH. 1997. “Dentate Granule Cell Neurogenesis Is Increased by Seizures and Contributes to Aberrant Network Reorganization in the Adult Rat Hippocampus.” *The Journal of Neuroscience: The Official Journal of the Society for Neuroscience* 17 (10): 3727–3738

Park SA, Kim TS, Choi KS, Park HJ, Heo K, Lee BI. 2003. “Chronic Activation of CREB and P90RSK in Human Epileptic Hippocampus.” *Experimental & Molecular Medicine* 35 (5): 365–370

Peixoto-Santos JE, Velasco TR, Galvis-Alonso OY, Araujo D, Kandratavicius L, Assirati JA, Carlotti CG, Scandiuzzi RC, Santos AC, Leite JP. 2015. “Temporal Lobe Epilepsy Patients with Severe Hippocampal Neuron Loss but Normal Hippocampal Volume: Extracellular Matrix Molecules Are Important for the Maintenance of Hippocampal Volume.” *Epilepsia* 56 (10): 1562–1570

Peng Z, Huang CS, Stell BM, Mody I, Houser CR . 2004. “Altered Expression of the Delta Subunit of the GABAA Receptor in a Mouse Model of Temporal Lobe Epilepsy.” *The Journal of Neuroscience: The Official Journal of the Society for Neuroscience* 24 (39): 8629–8639

Penzes P, Johnson RC, Sattler R, Zhang X, Huganir RL, Kambampati V, Mains RE, Eipper BA. 2001. “The Neuronal Rho-GEF Kalirin-7 Interacts with PDZ Domain-

Containing Proteins and Regulates Dendritic Morphogenesis." *Neuron* 29 (1): 229–242

Perez-Reyes E, Cribbs LL, Daud A, Lacerda AE, Barclay J, Williamson MP, Fox M, Rees M, Lee JH. 1998. "Molecular Characterization of a Neuronal Low-Voltage-Activated T-Type Calcium Channel." *Nature* 391 (6670): 896–900

Pernhorst K, Herms S, Hoffmann P, Cichon S, Schulz H, Sander T, Schoch S, Becker AJ, Grote A. 2013. "TLR4, ATF-3 and IL8 Inflammation Mediator Expression Correlates with Seizure Frequency in Human Epileptic Brain Tissue." *Seizure* 22 (8): 675–678

Pfeiffer-Linn C, Lasater EM. 1993. "Dopamine Modulates in a Differential Fashion T- and L-Type Calcium Currents in Bass Retinal Horizontal Cells." *The Journal of General Physiology* 102 (2): 277–294

Pitkänen A, Tuunanen J, Kälviäinen R, Partanen K, Salmenperä T. 1998. "Amygdala Damage in Experimental and Human Temporal Lobe Epilepsy." *Epilepsy Research* 32 (1–2): 233–253

Pitkänen A, Engel J. 2014. "Past and Present Definitions of Epileptogenesis and Its Biomarkers." *Neurotherapeutics: The Journal of the American Society for Experimental NeuroTherapeutics* 11 (2): 231–241

Pitkänen A, Roivainen R, Lukasiuk K. 2016. "Development of Epilepsy after Ischaemic Stroke." *The Lancet. Neurology* 15 (2): 185–197

Pitsch J, Schoch S, Gueler N, Flor PJ, van der Putten H, Becker AJ. 2007. "Functional Role of MGluR1 and MGluR4 in Pilocarpine-Induced Temporal Lobe Epilepsy." *Neurobiology of Disease* 26 (3): 623–633

Platano D, Magli MC, Ferraretti AP, Gianaroli L, Aicardi G. 2005. "L- and T-Type Voltage-Gated Ca2+ Channels in Human Granulosa Cells: Functional Characterization and Cholinergic Regulation." *The Journal of Clinical Endocrinology and Metabolism* 90 (4): 2192–2197

Platzer K, Lemke JR. 1993. "GRIN2B-Related Neurodevelopmental Disorder." In *GeneReviews*®, edited by Margaret P. Adam, Ghayda M. Mirzaa, Roberta A.

Pagon, Stephanie E. Wallace, Lora JH Bean, Karen W. Gripp, and Anne Amemiya. Seattle (WA): University of Washington, Seattle

Pollard H, Héron A, Moreau J, Ben-Ari Y, Khrestchatisky M. 1993. “Alterations of the GluR-B AMPA Receptor Subunit Flip/Flop Expression in Kainate-Induced Epilepsy and Ischemia.” *Neuroscience* 57 (3): 545–554

Pregi N, Belluscio LM, Berardino BG, Castillo DS, Cánepa ET. 2017. “Oxidative Stress-Induced CREB Upregulation Promotes DNA Damage Repair Prior to Neuronal Cell Death Protection.” *Molecular and Cellular Biochemistry* 425 (1–2): 9–24

Radtke F, Georgiev O, Müller HP, Brugnera E, Schaffner W. 1995. “Functional Domains of the Heavy Metal-Responsive Transcription Regulator MTF-1.” *Nucleic Acids Research* 23 (12): 2277–2286

Radtke F, Heuchel R, Georgiev O, Hergersberg M, Gariglio M, Dembic Z, Schaffner W. 1993. “Cloned Transcription Factor MTF-1 Activates the Mouse Metallothionein I Promoter.” *The EMBO Journal* 12 (4): 1355–1362

Rakhade SN, Yao B, Ahmed S, Asano E, Beaumont TL, Shah AK, Draghici S, Krauss R, Chugani HT, Sood S, Loeb JA. 2005. “A Common Pattern of Persistent Gene Activation in Human Neocortical Epileptic Foci.” *Annals of Neurology* 58 (5): 736–747

Ransom CB, Blumenfeld H. 2007. “Acquired Epilepsy: Cellular and Molecular Mechanisms.,” no. Molecular neurology: 347–370.

Reid CA, Berkovic SF, Petrou S. 2009. “Mechanisms of Human Inherited Epilepsies.” *Progress in Neurobiology* 87 (1): 41–57

Remondelli P, Moltedo O, Leone A. 1997. “Regulation of ZiRF1 and Basal SP1 Transcription Factor MRE-Binding Activity by Transition Metals.” *FEBS Letters* 416 (3): 254–258

Represa A, Jorquera I, Le Gal La Salle G, Ben-Ari Y. 1993. “Epilepsy Induced Collateral Sprouting of Hippocampal Mossy Fibers: Does It Induce the Development of Ectopic Synapses with Granule Cell Dendrites?” *Hippocampus* 3 (3): 257–268

Ritchie ME, Phipson B, Wu D, Hu Y, Law CW, Shi W, Smyth GK. 2015. “Limma Powers Differential Expression Analyses for RNA-Sequencing and Microarray Studies.” *Nucleic Acids Research* 43 (7): e47

Ritz MC, George FR. 1997. “Cocaine-Induced Convulsions: Pharmacological Antagonism at Serotonergic, Muscarinic and Sigma Receptors.” *Psychopharmacology* 129 (4): 299–310

Robinson MD, McCarthy DJ, Smyth GK. 2010. “EdgeR: A Bioconductor Package for Differential Expression Analysis of Digital Gene Expression Data.” *Bioinformatics (Oxford, England)* 26 (1): 139–140

Sakkaki S, Gangarossa G, Lerat B, Françon D, Forichon L, Chemin J, Valjent E, Lerner-Natoli M, Lory P. 2016. “Blockade of T-Type Calcium Channels Prevents Tonic-Clonic Seizures in a Maximal Electroshock Seizure Model.” *Neuropharmacology* 101 (February): 320–329

Sakuragi S, Tominaga-Yoshino K, Ogura A. 2013. “Involvement of TrkB- and P75(NTR)-Signaling Pathways in Two Contrasting Forms of Long-Lasting Synaptic Plasticity.” *Scientific Reports* 3 (November): 3185

Sanabria ER, Su H, Yaari Y. 2001. “Initiation of Network Bursts by Ca2+-Dependent Intrinsic Bursting in the Rat Pilocarpine Model of Temporal Lobe Epilepsy.” *The Journal of Physiology* 532 (Pt 1): 205–216

Sandelin A, Alkema W, Engström P, Wasserman WW, Lenhard B. 2004. “JASPAR: An Open-Access Database for Eukaryotic Transcription Factor Binding Profiles.” *Nucleic Acids Research* 32 (Database issue): D91-94

Sands Z, Grottesi A, Sansom MSP. 2005. “Voltage-Gated Ion Channels.” *Current Biology: CB* 15 (2): R44-47

Santana N, Bortolozzi A, Serrats J, Mengod G, Artigas F. 2004. “Expression of Serotonin1A and Serotonin2A Receptors in Pyramidal and GABAergic Neurons of the Rat Prefrontal Cortex.” *Cerebral Cortex (New York, N.Y.: 1991)* 14 (10): 1100–1109

Saydam N, Georgiev O, Nakano MY, Greber UF, Schaffner W. 2001. “Nucleo-Cytoplasmic Trafficking of Metal-Regulatory Transcription Factor 1 Is Regulated by Diverse Stress Signals.” *The Journal of Biological Chemistry* 276 (27): 25487–25495

Scheffer IE, Berkovic S, Capovilla G, Connolly MB, French J, Guilhoto L, Hirsch E, Jain S, Mathern GW, Moshé SL, Nordli DR, Perucca E, Tomson T, Wiebe S, Zhang YH, Zuberi SM. 2017. “ILAE Classification of the Epilepsies: Position Paper of the ILAE Commission for Classification and Terminology.” *Epilepsia* 58 (4): 512–521

Schindelin J, Arganda-Carreras I, Frise E, Kaynig V, Longair M, Pietzsch T, Preibisch S, Rueden C, Saalfeld S, Schmid B, Tinevez JY, White DJ, Hartenstein V, Eliceiri K, Tomancak P, Cardona A. 2012. “Fiji: An Open-Source Platform for Biological-Image Analysis.” *Nature Methods* 9 (7): 676–682

Schizophrenia Working Group of the Psychiatric Genomics Consortium. 2014. “Biological Insights from 108 Schizophrenia-Associated Genetic Loci.” *Nature* 511 (7510): 421–427

Schmitt H, Meves H. 1995. “Model Experiments on Squid Axons and NG108-15 Mouse Neuroblastoma x Rat Glioma Hybrid Cells.” *Journal of Physiology, Paris* 89 (4–6): 181–193

Schoch S , Gundelfinger ED. 2006. “Molecular Organization of the Presynaptic Active Zone.” *Cell and Tissue Research* 326 (2): 379–391

Schuster J, Laan L, Klar J, Jin Z, Huss M, Korol S, Noraddin FH, Sobol M, Birnir B, Dahl N. 2019. “Transcriptomes of Dravet Syndrome IPSC Derived GABAergic Cells Reveal Dysregulated Pathways for Chromatin Remodeling and Neurodevelopment.” *Neurobiology of Disease* 132 (December): 104583

Scott RC. 2014. “What Are the Effects of Prolonged Seizures in the Brain?” *Epileptic Disorders: International Epilepsy Journal with Videotape* 16 Spec No 1 (Spec No 1): S6-11

Seipel K, Georgiev O, Schaffner W. 1992. “Different Activation Domains Stimulate Transcription from Remote ('enhancer’) and Proximal ('promoter’) Positions.” *The EMBO Journal* 11 (13): 4961–4968

Sharma AK, Reams RY, Jordan WH, Miller MA, Thacker HL, Snyder PW. 2007. “Mesial Temporal Lobe Epilepsy: Pathogenesis, Induced Rodent Models and Lesions.” *Toxicologic Pathology* 35 (7): 984–999

Sharma AK, Searfoss GH, Reams RY, Jordan WH, Snyder PW, Chiang AY, Jolly RA, Ryan TP. 2009. “Kainic Acid-Induced F-344 Rat Model of Mesial Temporal Lobe Epilepsy: Gene Expression and Canonical Pathways.” *Toxicologic Pathology* 37 (6): 776–789

Shorvon, SD. 2011. “The Etiologic Classification of Epilepsy.” *Epilepsia* 52 (6): 1052–1057

Sloviter RS, Kudrimoti HS, Laxer KD, Barbaro NM, Chan S, Hirsch LJ, Goodman RR, Pedley TA. 2004. “‘Tectonic’ Hippocampal Malformations in Patients with Temporal Lobe Epilepsy.” *Epilepsy Research* 59 (2–3): 123–153

Soler-Llavina GJ, Arstikaitis P, Morishita W, Ahmad M, Südhof TC, Malenka RC. 2013. “Leucine-Rich Repeat Transmembrane Proteins Are Essential for Maintenance of Long-Term Potentiation.” *Neuron* 79 (3): 439–446

Sonoyama T, Stadler LKJ, Zhu M, Keogh JM, Henning E, Hisama F, Kirwan P, Jura M, Blaszczyk BK, DeWitt DC, Brouwers B, Hyvönen M, Barroso I, Merkle FT, Appleyard SM, Wayman GA, Farooqi IS. 2020. “Human BDNF/TrkB Variants Impair Hippocampal Synaptogenesis and Associate with Neurobehavioural Abnormalities.” *Scientific Reports* 10 (1): 9028

Sorrell TC, Forbes IJ. 1975. “Depression of Immune Competence by Phenytoin and Carbamazepine. Studies in Vivo and in Vitro.” *Clinical and Experimental Immunology* 20 (2): 273–285

Sosanya NM, Huang PP, Cacheaux LP, Chen CJ, Nguyen K, Perrone-Bizzozero NI, Raab-Graham KF. 2013. “Degradation of High Affinity HuD Targets Releases

Kv1.1 MRNA from MiR-129 Repression by MTORC1." *The Journal of Cell Biology* 202 (1): 53–69

Speca DJ, Ogata G, Mandikian D, Bishop HI, Wiler SW, Eum K, Wenzel HJ, Doisy ET, Matt L, Campi KL, Golub MS, Nerbonne JM, Hell JW, Trainor BC, Sack JT, Schwartzkroin PA, Trimmer JS. 2014. "Deletion of the Kv2.1 Delayed Rectifier Potassium Channel Leads to Neuronal and Behavioral Hyperexcitability." *Genes, Brain, and Behavior* 13 (4): 394–408

Stoof JC, Kebabian JW. 1984. "Two Dopamine Receptors: Biochemistry, Physiology and Pharmacology." *Life Sciences* 35 (23): 2281–2296

Stuart GW, Searle PF, Chen HY, Brinster RL, Palmiter RD. 1984. "A 12-Base-Pair DNA Motif That Is Repeated Several Times in Metallothionein Gene Promoters Confers Metal Regulation to a Heterologous Gene." *Proceedings of the National Academy of Sciences of the United States of America* 81 (23): 7318–7322

Stuart GW, Searle PF, Palmiter RD. 1985. "Identification of Multiple Metal Regulatory Elements in Mouse Metallothionein-I Promoter by Assaying Synthetic Sequences." *Nature* 317 (6040): 828–831

Su H, Sochivko D, Becker A, Chen J, Jiang Y, Yaari Y, Beck H. 2002. "Upregulation of a T-Type Ca2+ Channel Causes a Long-Lasting Modification of Neuronal Firing Mode after Status Epilepticus." *The Journal of Neuroscience: The Official Journal of the Society for Neuroscience* 22 (9): 3645–3655

Suh SW, Thompson RB, Frederickson CJ. 2001. "Loss of Vesicular Zinc and Appearance of Perikaryal Zinc after Seizures Induced by Pilocarpine." *Neuroreport* 12 (7): 1523–1525

Sun Q, Xu W, Piao J, Su J, Ge T, Cui R, Yang W, Li B. 2022. "Transcription Factors Are Potential Therapeutic Targets in Epilepsy." *Journal of Cellular and Molecular Medicine* 26 (19): 4875–4885

Sutula T, He XX, Cavazos J, Scott G. 1988. "Synaptic Reorganization in the Hippocampus Induced by Abnormal Functional Activity." *Science (New York, N.Y.)* 239 (4844): 1147–1150

Swandulla D, Armstrong CM. 1989. “Calcium Channel Block by Cadmium in Chicken Sensory Neurons.” *Proceedings of the National Academy of Sciences of the United States of America* 86 (5): 1736–1740

Swift J, and Coruzzi GM. 2017. “A Matter of Time - How Transient Transcription Factor Interactions Create Dynamic Gene Regulatory Networks.” *Biochimica Et Biophysica Acta. Gene Regulatory Mechanisms* 1860 (1): 75–83

Takeda A, Minami A, Seki Y, Oku N. 2004. “Differential Effects of Zinc on Glutamatergic and GABAergic Neurotransmitter Systems in the Hippocampus.” *Journal of Neuroscience Research* 75 (2): 225–229

Talavera K, Staes M, Janssens A, Droogmans G, Nilius B. 2004. “Mechanism of Arachidonic Acid Modulation of the T-Type Ca2+ Channel Alpha1G.” *The Journal of General Physiology* 124 (3): 225–238

Talley EM, Cribbs LL, Lee JH, Daud A, Perez-Reyes E, Bayliss DA. 1999. “Differential Distribution of Three Members of a Gene Family Encoding Low Voltage-Activated (T-Type) Calcium Channels.” *The Journal of Neuroscience: The Official Journal of the Society for Neuroscience* 19 (6): 1895–1911

Tan NN, Tang HL, Lin GW, Chen YH, Lu P, Li HJ, Gao MM, Zhao QH, Yi YH, Liao WP, Long YS. 2017. “Epigenetic Downregulation of Scn3a Expression by Valproate: A Possible Role in Its Anticonvulsant Activity.” *Molecular Neurobiology* 54 (4): 2831–2842

Tavera-Montañez C, Hainer SJ, Cangussu D, Gordon SJV, Xiao Y, Reyes-Gutierrez P, Imbalzano AN, Navea JG, Fazzio TG, Padilla-Benavides T. 2019. “The Classic Metal-Sensing Transcription Factor MTF1 Promotes Myogenesis in Response to Copper.” *FASEB Journal: Official Publication of the Federation of American Societies for Experimental Biology* 33 (12): 14556–14574

Téllez-Zenteno JF, Hernández-Ronquillo L. 2012. “A Review of the Epidemiology of Temporal Lobe Epilepsy.” *Epilepsy Research and Treatment* 2012: 630853

Todorovic SM, Meyenburg A, Jevtovic-Todorovic V. 2002. “Mechanical and Thermal Antinociception in Rats Following Systemic Administration of Mibefradil, a T-Type Calcium Channel Blocker.” *Brain Research* 951 (2): 336–340

Traboulsie A, Chemin J, Chevalier M, Quignard JF, Nargeot J, Lory P. 2007. “Subunit-Specific Modulation of T-Type Calcium Channels by Zinc.” *The Journal of Physiology* 578 (Pt 1): 159–171

Uebele VN, Gotter AL, Nuss CE, Kraus RL, Doran SM, Garson SL, Reiss DR, Li Y, Barrow JC, Reger TS, Yang ZQ, Ballard JE, Tang C, Metzger JM, Wang SP, Koblan KS, Renger JJ. 2009. “Antagonism of T-Type Calcium Channels Inhibits High-Fat Diet-Induced Weight Gain in Mice.” *The Journal of Clinical Investigation* 119 (6): 1659–1667

Vallee BL, Auld DS. 1990. “Zinc Coordination, Function, and Structure of Zinc Enzymes and Other Proteins.” *Biochemistry* 29 (24): 5647–5659

Van Oekelen D, Megens A, Meert T, Luyten WH, Leysen JE. 2003. “Functional Study of Rat 5-HT2A Receptors Using Antisense Oligonucleotides.” *Journal of Neurochemistry* 85 (5): 1087–1100

Vergnano AM, Rebola N, Savtchenko LP, Pinheiro PS, Casado M, Kieffer BL, Rusakov DA, Mulle C, Paoletti P. 2014. “Zinc Dynamics and Action at Excitatory Synapses.” *Neuron* 82 (5): 1101–1114

Vezzani A, Fujinami RS, White HS, Preux PM, Blümcke I, Sander JW, Löscher W. 2016. “Infections, Inflammation and Epilepsy.” *Acta Neuropathologica* 131 (2): 211–234

Viguerie N, Clement K, Barbe P, Courtine M, Benis A, Larrouy D, Hanczar B, Pelloux V, Poitou C, Khalfallah Y, Barsh GS, Thalamas C, Zucker JD, Langin D. 2004. “In Vivo Epinephrine-Mediated Regulation of Gene Expression in Human Skeletal Muscle.” *The Journal of Clinical Endocrinology and Metabolism* 89 (5): 2000–2014

Wada Y, Nakamura M, Hasegawa H, Yamaguchi N. 1992. “Role of Serotonin Receptor Subtype in Seizures Kindled from the Feline Hippocampus.” *Neuroscience Letters* 141 (1): 21–24

Wallace RH, Wang DW, Singh R, Scheffer IE, George AL Jr, Phillips HA, Saar K, Reis A, Johnson EW, Sutherland GR, Berkovic SF, Mulley JC. 1998. “Febrile Seizures and Generalized Epilepsy Associated with a Mutation in the Na+-Channel Beta1 Subunit Gene SCN1B.” *Nature Genetics* 19 (4): 366–370

Wang J, Lin ZJ, Liu L, Xu HQ, Shi YW, Yi YH, He N, Liao WP. 2017. “Epilepsy-Associated Genes.” *Seizure* 44 (January): 11–20

Wang Y, Lorenzi I, Georgiev O, Schaffner W. 2004a. “Metal-Responsive Transcription Factor-1 (MTF-1) Selects Different Types of Metal Response Elements at Low vs. High Zinc Concentration.” *Biological Chemistry* 385 (7): 623–632

Wang Y, Wimmer U, Lichtlen P, Inderbitzin D, Stieger B, Meier PJ, Hunziker L, Stallmach T, Forrer R, Rülicke T, Georgiev O, Schaffner W. 2004b. “Metal-Responsive Transcription Factor-1 (MTF-1) Is Essential for Embryonic Liver Development and Heavy Metal Detoxification in the Adult Liver.” *FASEB Journal: Official Publication of the Federation of American Societies for Experimental Biology* 18 (10): 1071–1079

Wang Z, Li JY, Dahlström A, Danscher G. 2001. “Zinc-Enriched GABAergic Terminals in Mouse Spinal Cord.” *Brain Research* 921 (1–2): 165–172

Wei F, Yan LM, Su T, He N, Lin ZJ, Wang J, Shi YW, Yi YH, Liao WP. 2017. “Ion Channel Genes and Epilepsy: Functional Alteration, Pathogenic Potential, and Mechanism of Epilepsy.” *Neuroscience Bulletin* 33 (4): 455–477

Weiss N, Black SA, Bladen C, Chen L, Zamponi GW. 2013. “Surface Expression and Function of Cav3.2 T-Type Calcium Channels Are Controlled by Asparagine-Linked Glycosylation.” *Pflugers Archiv: European Journal of Physiology* 465 (8): 1159–1170

Wen AY, Sakamoto KM, Miller LS. 2010. “The Role of the Transcription Factor CREB in Immune Function.” *Journal of Immunology (Baltimore, Md.: 1950)* 185 (11): 6413–6419

Wheeler DB, Randall A, Tsien RW. 1994. “Roles of N-Type and Q-Type Ca2+ Channels in Supporting Hippocampal Synaptic Transmission.” *Science (New York, N.Y.)* 264 (5155): 107–111

Wiebe S, Blume WT, Girvin JP, Eliasziw M; Effectiveness and Efficiency of Surgery for Temporal Lobe Epilepsy Study Group. 2001. “A Randomized, Controlled Trial of Surgery for Temporal-Lobe Epilepsy.” *The New England Journal of Medicine* 345 (5): 311–318

Williamson PD, Engel JJ, Munari C. 1997. “Anatomic Classification of Localization-Related Epilepsies.” *Epilepsy: A Comprehensive Textbook.*, 1997.

Wimmer U, Wang Y, Georgiev O, Schaffner W. 2005. “Two Major Branches of Anti-Cadmium Defense in the Mouse: MTF-1/Metallothioneins and Glutathione.” *Nucleic Acids Research* 33 (18): 5715–5727

de Wit J, Sylwestrak E, O'Sullivan ML, Otto S, Tiglio K, Savas JN, Yates JR 3rd, Comoletti D, Taylor P, Ghosh A. 2009. “LRRTM2 Interacts with Neurexin1 and Regulates Excitatory Synapse Formation.” *Neuron* 64 (6): 799–806

von Wrede R, Jeub M, Ariöz I, Elger CE, von Voss H, Klein HG, Becker AJ, Schoch S, Surges R, Kunz WS. 2021. “Novel KCNH1 Mutations Associated with Epilepsy: Broadening the Phenotypic Spectrum of KCNH1-Associated Diseases.” *Genes* 12 (2): 132

Xue M, Stradomska A, Chen H, Brose N, Zhang W, Rosenmund C, Reim K. 2008. “Complexins Facilitate Neurotransmitter Release at Excitatory and Inhibitory Synapses in Mammalian Central Nervous System.” *Proceedings of the National Academy of Sciences of the United States of America* 105 (22): 7875–7880

Yan Y, Eipper BA, Mains RE. 2015. “Kalirin-9 and Kalirin-12 Play Essential Roles in Dendritic Outgrowth and Branching.” *Cerebral Cortex (New York, N.Y.: 1991)* 25 (10): 3487–3501

Yao JJ, Zhao QR, Liu DD, Chow CW, Mei YA. 2016. “Neuritin Up-Regulates Kv4.2 α-Subunit of Potassium Channel Expression and Affects Neuronal Excitability by

Regulating the Calcium-Calcineurin-NFATc4 Signaling Pathway.” *The Journal of Biological Chemistry* 291 (33): 17369–17381

Yoganathan S, Arunachal G, Gowda VK, Vinayan KP, Thomas M, Whitney R, Jain P.. 2021. “NTRK2-Related Developmental and Epileptic Encephalopathy: Report of 5 New Cases.” *Seizure* 92 (November): 52–55

Young CC, Stegen M, Bernard R, Müller M, Bischofberger J, Veh RW, Haas CA, Wolfart J. 2009. “Upregulation of Inward Rectifier K+ (Kir2) Channels in Dentate Gyrus Granule Cells in Temporal Lobe Epilepsy.” *The Journal of Physiology* 587 (Pt 17): 4213–4233

Yunker AM, Sharp AH, Sundarraj S, Ranganathan V, Copeland TD, McEnery MW. 2003. “Immunological Characterization of T-Type Voltage-Dependent Calcium Channel CaV3.1 (Alpha 1G) and CaV3.3 (Alpha 1I) Isoforms Reveal Differences in Their Localization, Expression, and Neural Development.” *Neuroscience* 117 (2): 321–335

Zamponi GW, Striessnig J, Koschak A, Dolphin AC. 2015. “The Physiology, Pathology, and Pharmacology of Voltage-Gated Calcium Channels and Their Future Therapeutic Potential.” *Pharmacological Reviews* 67 (4): 821–870

Zhang H, Webb DJ, Asmussen H, Horwitz AF. 2003. “Synapse Formation Is Regulated by the Signaling Adaptor GIT1.” *The Journal of Cell Biology* 161 (1): 131–142

Zhang H, Webb DJ, Asmussen H, Niu S, Horwitz AF.. 2005. “A GIT1/PIX/Rac/PAK Signaling Module Regulates Spine Morphogenesis and Synapse Formation through MLC.” *The Journal of Neuroscience: The Official Journal of the Society for Neuroscience* 25 (13): 3379–3388

Zhang SP, Zhang M, Tao H, Luo Y, He T, Wang CH, Li XC, Chen L, Zhang LN, Sun T, Hu QK. 2018. “Dimethylation of Histone 3 Lysine 9 Is Sensitive to the Epileptic Activity, and Affects the Transcriptional Regulation of the Potassium Channel Kcnj10 Gene in Epileptic Rats.” *Molecular Medicine Reports* 17 (1): 1368–1374

Zhang Y, Cribbs LL, Satin J. 2000. “Arachidonic Acid Modulation of Alpha1H, a Cloned Human T-Type Calcium Channel.” *American Journal of Physiology. Heart and Circulatory Physiology* 278 (1): H184-193.

Zhou Y, Won J, Karlsson MG, Zhou M, Rogerson T, Balaji J, Neve R, Poirazi P, Silva AJ. . 2009. “CREB Regulates Excitability and the Allocation of Memory to Subsets of Neurons in the Amygdala.” *Nature Neuroscience* 12 (11): 1438–1443

Zhu X, Dubey D, Bermudez C, Porter BE. 2015. “Suppressing CAMP Response Element-Binding Protein Transcription Shortens the Duration of Status Epilepticus and Decreases the Number of Spontaneous Seizures in the Pilocarpine Model of Epilepsy.” *Epilepsia* 56 (12): 1870–1878

Zhu X, Han X, Blendy JA, Porter BE.. 2012. “Decreased CREB Levels Suppress Epilepsy.” *Neurobiology of Disease* 45 (1): 253–263

9. Acknowledgements

With this work, I would like to thank at first my supervisor, Dr. Karen van Loo, for giving me the opportunity to work on this project, for her availability to discuss data and logistics, her structured way of working, and her help during these years.

I would like to thank Prof. Dr. Albert Becker for correcting the thesis and giving financial support to this project in my last year of doctoral studies, without which I probably would not have been able to obtain the data presented in this work.

Prof. Dr. Susanne Schoch for her involvement and suggestions in the project, her ideas and expertise have been fundamental for the development of some experiments.

Dr. Julika Pitsch for all the bureaucratic work and help with the animal permission. But mostly, I would like to thank her for recognizing all the efforts behind the FACS experiment and showing awareness about it.

I would like to thank Dr. Philippe Lory and Prof. Dr. Florian Mormann for accepting to be part of my PhD committee and for reading this thesis.

A big thanks to Pia Trebing and Sabine Opitz for their dedication, commitment, efficiency and professionality, the lab would be lost without you and your hard work.

I would like to express a huge gratitude to my officemates who easily turned out to be friends. Annika, Idil and Despina, who experienced and shared the rollercoaster of emotions that the PhD brings. Thanks for all of your support. Annika, Idil, I will always thank you for helping me in inducing the SE on Sundays when time was running out. Although not officemate, definitely a friend who show support and good ears in these years, Silvia. Thank you for your energy and positivism.

I would like to thank also my current and old lab friends, Daniel, Anne, Shayne, Jorge, Maksim, Delara, Eva, Marie, Alex, Moritz, Philipp, Aya, Sanja and Nesrine for the nice moments that I will always bring with me, shared in and outside the lab.

I thank my friends Aleix, Alex and Philipp for all the amazing memories that I have in Bonn.

A special thanks to my parents for teaching me the importance of making sacrifices and determination, and for their unconditional love and support. Particularly my mum, for always checking on me although living many km´s apart, making sure that I was fine and happy.

Finally, thank you Neil, for always being by myside, for making me feel at home, whenever we are, for recognizing when I need your help and for your respect.